5-4-2018

Computing Local Fractal Dimension Using Geographical Weighting Scheme

Shuowei Zhang
University of Connecticut - Storrs, shuowei.zhang@uconn.edu

Computing Local Fractal Dimension Using Geographical Weighting Scheme

Shuowei Zhang, Ph.D.

University of Connecticut, 2018

The fractal dimension (D) of a surface can be viewed as a summary or average statistic for characterizing the geometric complexity of that surface. The D values are useful for measuring the geometric complexity of various land cover types. Existing fractal methods only calculate a single D value for representing the whole surface. However, the geometric complexity of a surface varies across patches and a single D value is insufficient to capture these detailed variations. Previous studies have calculated local D values using a moving window technique. The main purpose of this study is to compute local D values using an alternative way by incorporating the geographical weighting scheme within the original global fractal methods. Three original fractal methods are selected in this study: the Triangular Prism method, the Differential Box Counting method and the Fourier Power Spectral Density method. A Gaussian density kernel function is used for the local adaption purpose and various bandwidths are tested. The first part of this dissertation research explores and compares both of the global and local D values of these three methods using test images. The D value is computed for every single pixel across the image to show the surface complexity variation. In the second part of the dissertation, the main goal is to study two major U.S. cities located in two regions. New York City and Houston are compared using D values for both of spatial and temporal comparison. The results show that the geographical weighting scheme is suitable for calculating local D values but very sensitive to small bandwidths. New York City and Houston show similar global D results for both year of 2000 and 2016 indicating there were not much land cover changes during the study period.

Computing Local Fractal Dimension Using Geographical Weighting Scheme

Shuowei Zhang

B.S., China Agriculture University, 2010

M.S., State University of New York at Buffalo, 2013

A Dissertation

Submitted in Partial Fulfillment of the

Requirements for the Degree of

Doctor of Philosophy

at the

University of Connecticut

2018

APPROVAL PAGE

Doctor of Philosophy Dissertation

Computing Local Fractal Dimension Using Geographical Weighting Scheme

Presented by

Shuowei Zhang, B.S., M.S.

Major Advisor ____
Robert G. Cromley

Associate Advisor ____
Dean M. Hanink

Associate Advisor ____
Chuanrong Zhang

Associate Advisor ____
Thomas H. Meyer

University of Connecticut
2018

ACKNOWLEDGEMENTS

First, I would like to thank my major advisor, Dr. Robert Cromley, for his inspiration of this dissertation research. His idea expands my view and understanding of my study field. I feel so grateful for his detailed guidance throughout the research process. In addition, his patience and encouragement motivates me to make progress. Without his comprehensive help, this dissertation would not have been possible. I also would like to thank other committee members, Dr. Thomas Meyer, Dr. Chuanrong Zhang and Dr. Dean Hanink for their kindly help and suggestions on my dissertation. I would like to express my special gratitude to Dr. Thomas Meyer for his valuable insights on this research topic.

Second, I would like to thank the geography department at UConn for providing me with great research environment. I also would like to thank our department head, Dr. Kenneth Foote, for his books on this topic. I also want to thank Dr. Daniel Civco for his help during the beginning of this research and for recommendation of Dr. Thomas Meyer. My thanks also go to Richard Mrozinski, who guided me with my graduate duty while I am at this department. Our department assistant, Stephanie Beron, who has been so helpful. Without her organization, I would not have such a great atmosphere to finish my dissertation.

Finally, I must show my respect to my parents who have always been supportive to me during the entire research process. They always listen to me when I have difficulties and they never wanted to interrupt me even though they really wanted to talk to me. I also need to show my appreciation to my colleagues and friends who has been so helpful to me and we had such a wonderful time. I wish them to be very successful in their study and career.

TABLE OF CONTENTS

LIST OF TABLES

LIST OF FIGURES

Chapter One

Introduction

1.1 Introduction

Mandelbrot’s fractal concept first appeared in his highly cited article, *How Long Is the Coast of Britain,* in 1967. This paper introduced the concepts and theories of how to interpret irregular objects in nature. Other than the classical geometry features, our world is filled up with irregular and rough features. The measurement of their geometric sizes seems impossible. On the other hand, understanding the structure of the natural phenomena can help us perceive the world in a more realistic and precise way. Mandelbrot (1967) stated the geometric characteristics and mathematical foundation for interpreting the fragmented shape of the west coast of Britain (Figure. 1.1). Mandelbrot termed this highly involved shape as a *fractal* and use refer to any natural objects for which the Hausdorff-Besicovich dimension exceeds the standard dimensions (e.g., 0 for points; 1 for lines; 2 for planes) (Goodchild 1987). This classical example of fractals possesses some of the best characteristics of fractals and sparks wide examinations on how to explain the size of these non-regular phenomena. The idea of fractal geometry is possibly the most appropriate approach to describe the shape of the physical forms (Mandelbrot 1977, 1983), and this rises dimension as a powerful tool to capture natural fractals. A quantity D is termed the *fractal dimension* and commonly used to describe the geometric complexity of the fractals. The fractal dimension could be any values between 0 and 1 for a point feature, between 1 and 2 for a linear feature, and between 2 and 3 for a surface feature. For the west coast of Britain using Richardson's (1961) data, Mandelbrot (1967) assigned a fractal dimension of D=1.25. The more complex the fractals are, the higher the value of the fractal dimension would be within the corresponding boundaries of the topographical dimension. The fractal dimension can be considered as an infinite continuous value and this had led researchers to develop various methods for estimating fractal dimensions.

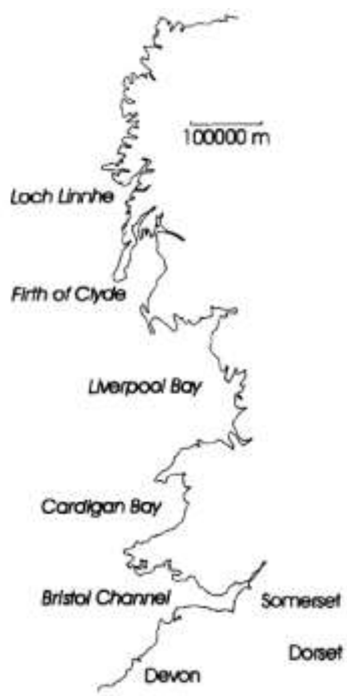

Figure 1.1 West Coast of Britain (Andrle 1996)

Self-similarity is a key characteristic of fractals and it is commonly used to distinguish fractals from other non-fractal phenomena. The definition of self-similarity could be described as natural objects in a whole, the subset parts are indistinguishable from the whole when any parts of it are suitably enlarged to the whole (Mandelbrot 1977, Goodchild 1987). This property has led researchers to another closely related issue of fractal analysis, *scale*. In other words, self-similarity should remain true at all measuring scales, which is also known as strictly self-similar property (Goodchild 1987, Andrle 1996, Lam 2002). We assume that the fractal dimension is a constant throughout any given scales. However, many studies have concluded that the fractal dimension varies over a range of scales. Benguigui (2000) used city landscape as an example to illustrate when and where a city is a true fractal. Not only the spatial aspect of the city has been studied but Benguigui also examined temporal change of city landscape using fractal analysis and concluded that city is not always a fractal both over spatial and temporal changes. Objects with strict self-similarity (Figure. 1.2) exists in stochastic and constructed objects, which are generated using computer simulation process. Therefore, natural phenomena are not “pure” fractals and the fractal dimension D should be analyzed in a different way. Instead of using strict self-similarity to describe fractals, statistical self-similarity is a better term to characterize the nature of fractals (Mandelbrot 1967). The variations of the fractal dimension provide researchers with another promising perspective on fractal analysis by employing fractal dimension methods. Researchers could use these methods to study what the optimal scales are for certain applications such as environmental assessment, landscape ecology, etc. would be.

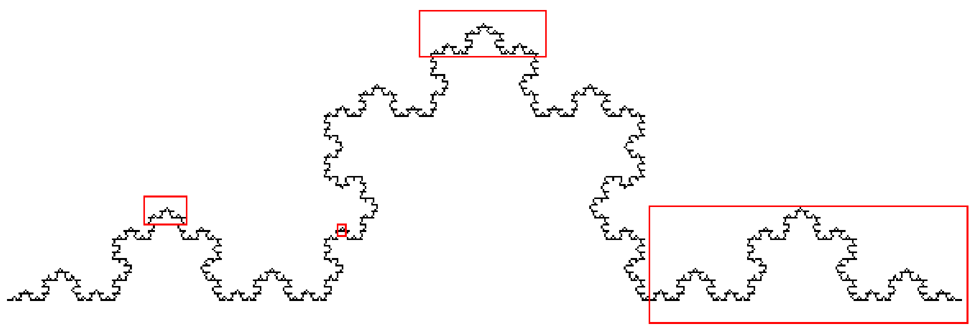

Figure 1.2 Simulated Object with Strictly Self-Similar Property
Source: Google Images

The fractal nature of geographic features has drawn much attention to geographers and spatial statisticians since Goodchild and Mark (1987) reviewed the importance of the fractal ideas in geographic field. Their work has given fractal analysis a geographic and spatial perspective, not surprisingly, spatial phenomena also exhibits fractal nature and has direct relation to applications of fractal analysis methods. Moreover, the statistically self-similar trait of fractals tends to link the fractal analysis methods with the spatial statistics techniques and this connection has potentially caused researchers to expand fractal theories in a non-stationary way.

City morphology is especially appealing to geographers as well as to city planners because of its intrinsic complexity and variability. Different from linear features, city landscape displays heterogeneous land covers such as built-up area and grass, which have contrasting geometric shapes. Batty and Longley's book (1994), *Fractal Cities: A Geometry of Form and Function*, introduced how fractal geometry helps explain the physical forms of cities. Remotely sensed imagery provides a convenient and accessible way for not only fractal analyst but also remote sensing researchers to study various landscapes. Remotely sensed images have an advantage for mapping a large extent of land surface area and it is relatively ideal to study and understand the changing landscape with the information of wide ranging variations. Remotely sensed images are complex in space, spectrum, time and exhibit self-similarity within certain spatial scales, or spatial resolutions (Sun 2006). This characteristic makes the fractal approach a promising tool to understand image landscape pattern. Combining spatial information into the fractal analysis of remotely sensed image has been the focus in recent years and it can help reveal the heterogeneity of city fractals and improve identifying clusters of local neighbors with extreme fractal dimensions.

There is a huge body of interdisciplinary literatures analyzing improved methods of fractal models and the remote sensing applications. Fractal analysis rely heavily on the estimation of fractal dimension. The general research of fractal analysis including the estimation of fractal dimension on coastlines and land boundaries as a line feature (Richardson 1961, Mandelbrot 1967, Goodchild 1987). South Africa's coast exhibits the smoothest shape with a D of 1.03 and West Britain Coast has the largest D value of 1.25 among all the empirical findings from Richardson (1961). The most common and intuitive application of fractal analysis based on remotely sensed images is the estimation of the textural complexity of the entire image, for example, the urban structures have been studied extensively by using fractal analysis methods to estimate a single fractal dimension (Benguigui 2000, Herold 2002, Myint 2003, Liang 2013). Coastal and rural areas were also studied in comparison with the urban landscape. The comparison of various fractal analysis methods revealed that different methods do not yield constant fractal dimension for the same imagery (Lam 1990, 2002). Several research (Emerson 1999, Myint 2003, Luan 2012) have identified that fractal dimension is an effective landscape metric to describe the land cover structure but it alone cannot fully and accurately accomplish this. Fractal dimension has been employed to study the temporal change effect, for example, some of the temporal change studies cover air pollutant, city landscape structure and population density distribution (Benguigui 2000, Lee 2003, Chen 2009). However, aside from the previous article focused on the estimation of a lumped fractal dimension, there has been little research on developing the local fractal dimension.

1.2 Dissertation Objective

The main objective of this dissertation is to incorporate perspective of spatial statistics into the fractal analysis methods. Spatial statistics is one of the most common methods for analyzing geographic issues. Local models haven been used widely to provide an alternative perspective to examine the spatial distribution of the geographic data. Combining fractal analysis methods with local models is a new and meaningful research direction, and this is the main approach for this dissertation.

Another objective of this dissertation is to study the urban landscape of the major U. S. cities by using fractal analysis and fractal dimension. Fractal dimension are estimated for multiple time series of the cities to analyze the temporal change of the D value. In addition, geographical weighted scheme are employed to show the spatial distribution of the fractal dimension across the cities. Moreover, various fractal analysis methods are compared to examine their advantage and limitations. All of these objectives lead to the following research questions.

1.3 Research Questions:

(1) How the estimation results of fractal dimension differ within the selected methods?

(2) Can geographical weighting scheme be applied to local adaption of fractal analysis?

(3) How significant is the spatial resolution in affecting the fractal dimension?

(4) What are the fractal dimension implications of the selected major U.S. cities?

1.4 Research Hypotheses

The above research questions reflect the following research hypotheses:

(1) Various fractal analysis methods will result in different global fractal dimensions.

(2) Landscape neighborhoods (i.e., parking lots, lake body) with low complexity will have small fractal dimension; high complexity landscape (i.e., building concourse) will have large fractal dimension.

(3) The temporal change of the selected major U.S. cities will have little impact on the fractal dimension values.

(4) Geographic weighting scheme can be incorporated into original fractal methods.

The above research questions serves as the guidance for this dissertation. This research dissertation is mainly a quantitative study that it primarily targets on the methods exploration and comparison. The research hypotheses are examined based on the results of the application and some future directions will be pointed out.

1.5 Structure of the Dissertation

In order to address these questions and test the hypotheses, this dissertation is constructed as follows: Chapter Two provides the detailed background regarding the fractal concepts, fractal development and its significant influence. Chapter Three consists of a review of the interdisciplinary literature focusing on current fractal methods, fractal applications in science. Specifically, the review will focus on the fractal application on urban area using remotely sensed images. Chapter Four presents the theoretical framework and the methods of fractal analysis. This chapter first explains the theoretical background of the fractal methods in general, discusses the difference between the current methods. The methods will be focusing on the surface features and three commonly used methods are selected. The algorithm of the three selected methods are listed as well as the geographical weighting scheme. Then all of these fractal methods are localized for generating local fractal dimension using geographically weighted scheme. This expanded approach based on the principle of spatial non-stationarity. Chapter Five is the result of the triangular prism and differential box counting methods. This chapter compares the global and local D values using test images. Chapter Six focuses on the results of the Fourier power spectral density method. Chapter Seven focuses on an empirical analysis of the New York City and Houston for both of spatial and temporal considerations. Finally, Chapter Eight discusses the results and contributions of this research, draws some shortcomings, and outlines the future research directions.

Chapter Two

Background on Fractals and Urban Sustainable Development

2.1 Introduction

Natural fractals can be seen almost everywhere on earth. These real world phenomena have rough shape and appearance, which are difficult to study. The traditional geometry such as point, line and plane failed to capture the intrinsic characteristics of the natural objects. Because of this, it is significant to develop an appropriate way, which is capable of dealing with the natural phenomenon. Fractal concept was first introduced to mathematics field and then distributed to other study fields including geography. Clark and Schweizer in their 1991's book mentioned that fractal geometry is considered one of the four most significant concepts in science of the 20th century. In fact, the natural objects surrounding us have clear fractal nature as well as the artificial architecture (Figure. 2.1).

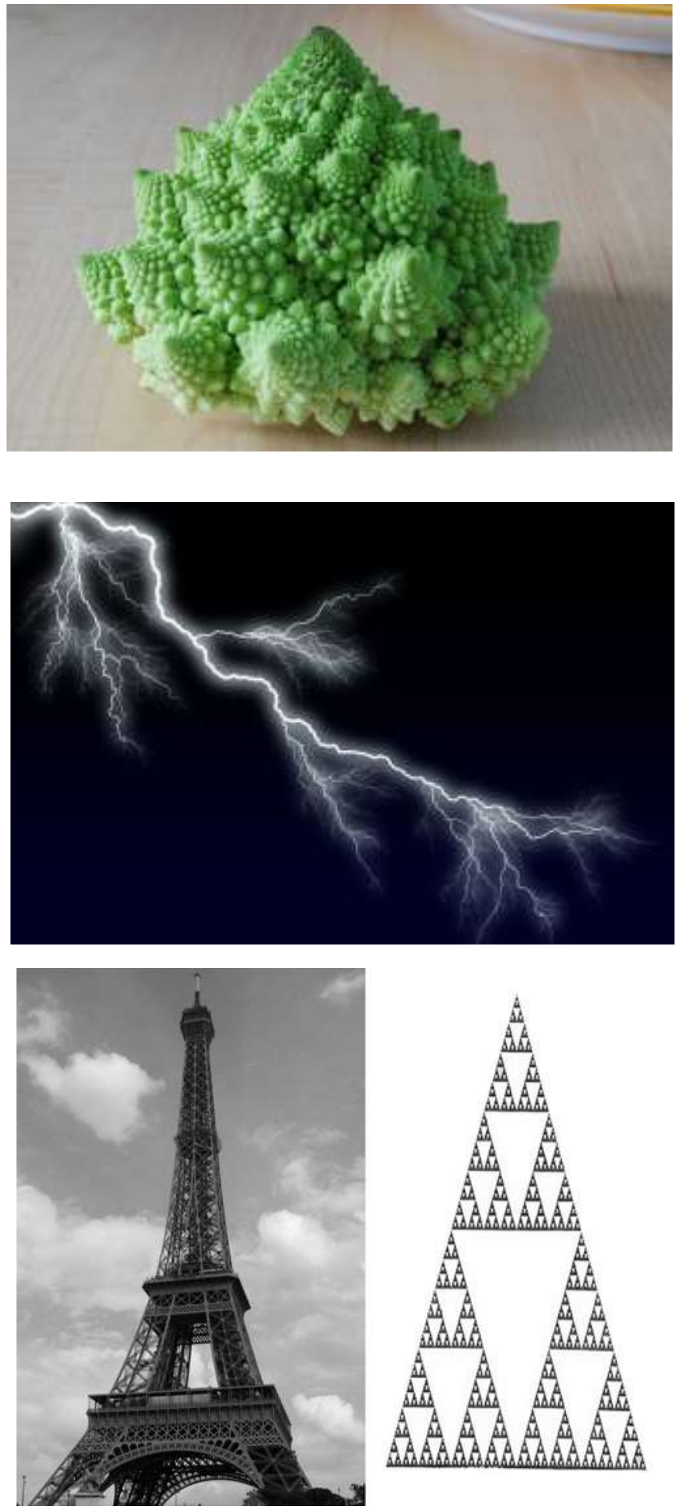

Figure 2.1 Fractal Nature of Geographic Phenomena (Above: Cauliflower; Middle: Thunder; Below: Eiffel Tower)
Source: Google Images

We see fractal geometry in many of our surrounding substances. From cauliflower growing on the ground to the thunder which happens in the sky. It is the most natural and efficient way that the phenomena exist on earth and universe. Human being mimic the fractal idea from the natural phenomenon and create artificial architecture where fractal concepts can be seen embedded in. Eiffel Tower is one of the examples, which uses limited labor and construction materials but turns out to be a very strong man-made construction. Using few materials/occupy limited space and convey optimum function is the core principle of fractal concept.

The fractal concepts indicate a significant meaning that fractals occupy the space in an optimum way (Chen 2009). This unique advantage of fractal can be related to urban sustainable development issue. In fact, city is a suitable candidate of fractals and yields some of the best aspects of fractals (Batty and Longley 1994). A number of studies have focused on applying fractal concepts on urban morphology and city development research. A fractal city somehow exhibits irregular transportation system, which looks like one main road with several branches (Figure. 2.2). On the other hand, a city with a regular road system usually is not considered as a fractal city (Figure. 2.3). Rome is an ancient city in Europe and it indeed demonstrates some of the fractal characteristics. In general, a fractal city means it has the same or similar structures at different scale levels. It has chaotic physical structure, but tens to grow on a way of absorbing the small units into larger unit (Fractal Applications 2003). One of the recognizable traits is the road system in Rome, and it looks irregular and extends to haphazard directions. A diagonal road is 70% shorter than the two rectangle roads to the same destination and this makes a fractal city functions efficiently.

Figure 2.2 Physical Structure of Rome, Italy
Source: Fractal Applications 2003 (Website)

Figure 2.3 Physical Structure of Phoenix, Arizona
Source: Fractal Applications 2003 (Website)

Many of the fractal traits can be seen in the ancient cities in Western world. The form of the ancient city is a process of long history and citizen's decisions from individuals. Fractal city development is slow but organic and can maximize its functionality and sustainability. Unlike the ancient city, a modern city in Figure 2.3 shows a different physical structure, which is in a complete ordered way. This modern city is considered to be an aesthetic one but not in an efficient form. The road system is formed into several squares. The advantage if this formation is that it is simple for drivers to explore the city, however, not surprising then, this is not a sustainable way and limited the city functions as discussed above. Fractal city has been recognized as the fractal foundation and it is meaningful to carry out a direct research on this issue.

This dissertation does not target on the origin of a city, but focuses on the quantitative analysis of the fractal cities. For a complete and detailed discussion about the fractal theory and applications on city, readers are directed to a book *Fractal Cities* edited by Batty and Long (1994). The literatures on the topic of fractal cities are quite countless, some of the text (Batty and Longley 1986, Benguigui et al. 2000, Chen 2010, Herold et al. 2002, Liang et al. 2013) provided an exemplary discussion. The case study in Chapter Seven of this dissertation is focused on the fractal application on the U.S. major cities. The following sections will review the related research.

2.2 Fractal Characteristics of Geographic Phenomena

Before getting into the discussion of the fractal cities, it is necessary to outline some of the key characteristics of the true fractals as well as the relevance to natural geography field. It is evident that fractals demonstrate highly complex shape and form and they possess the unique elements, which are critical for understanding the fractal ideas and real world applications. The properties of fractals are the fundamental issues and very abstract to grasp. In recent years, attentions have been diverted to the field of geographic and spatial phenomena. Goodchild and Mark (1987) state that geographic phenomena hold three characteristics relating to fractals and it is an innovative way to examine the spatial data and phenomena. Fractals are not themselves unless they are applied to the cartography and spatial data analysis (Goodchild and Mark 1987). These key elements of fractals provide a new standard to model the spatial phenomena with more dynamics and reality. In this section, the goal is to briefly outline the most important characteristics of fractals and their relationship to the geographic phenomena.

Scale Measure

Lam (2004) states that, in general, scale has four meanings: (1) overall spatial extent of the study area; (2) data/image (e.g. vector and raster) resolution; (3) bandwidth of a spatial process; and (4) relation scale of the focal point. These four meanings of scale is shown in Figure 2.4 for illustration. One of the most crucial aspects of spatial analysis is scale. Scale affects the geometric measurement (e.g. length, area) of a geographic object. Scale directly influences the size of the symbols (e.g. road, building and river) on the map. GIS data analysis is dramatically affected by changing the scale and the results are quite different. Increasing the scale of a vector data can enlarge the size of the map elements. For example, studies on Connecticut and the U.S. will use two different scale levels. Scale also plays an essential role on raster data. Scale is also referred as *spatial resolution* when dealing with remotely sensed image. Scale change will change the pixel size of an image and it is usually carried out from finest to roughest resolution. Fine resolution image has more pixels and shows more details (e.g. roads, parking lots, neighborhoods). Scale change is a fundamental issue that can help decide the suitable research extent for certain environmental monitoring and assessments.

Fractals are not affected by scale change, in other words, real fractals present an identical structure in response to the changing of scale. It is a rigorous way of fractals to be formed by mathematical equations and each step is constructed based on the same formula. No matter enlarge or shorten, the fractal geometry has the same detail and cannot be distinguishable at all scales. Thus, observers may not be able to estimate the size as this irregular object continue growing infinitely. Geographic phenomena have the characteristic of scale response but are not equal to true fractals. Take a coastline in Figure 1.1 for example, as scale increases, more details can be recognized of a coastline and the total length will increase. The image can be distinguishable when it is not suitably enlarged (e.g.

exceeds the acceptable scale levels). A good indicator of fractals in terms of scale effect is the value of D as discussed in Chapter One. For the natural objects in the geographic domain, D is dependent with the measure of scale and responses in a direct way. For calculating D, using fractal method is also known as a scale-based method (Lam 2004). For fractals, the D value tends to be the same number across the scale change. However, this is not always the case for real world phenomena. This characteristic is explained in the following part.

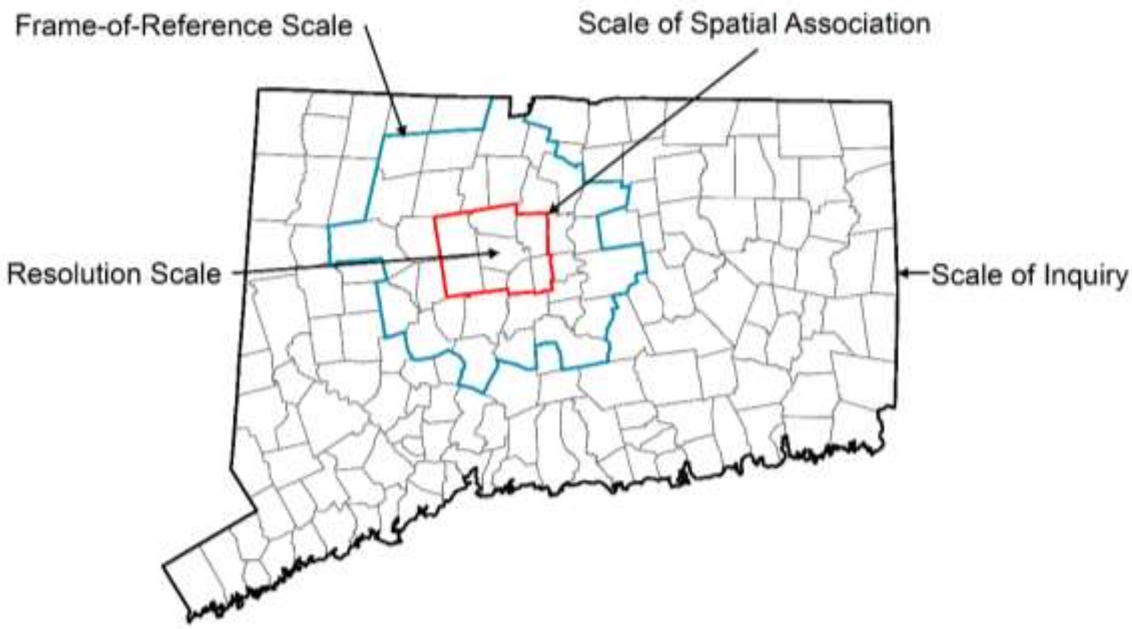

Figure 2.4 Four Meanings of Scale

<u>Self-similarity</u>

Self-similarity is the core characteristic of fractals. Many studies have indicated that self-similarity is a unique and exclusive trait to differ fractals from other forms (Mandelbrot 1967, Goodchild and Mark 1987, Andrle 1996, Benguigui 2000, Sun et al. 2006, Chen 2010). As discussed in Chapter One, self-similarity means that an object is identical to each stage when the scale changes. This directly relates to the scale measure characteristic of fractals from the first part. There are two different interpretations of self-similarity. In the first part above, it discusses the scale measure and its effect on the structure geometry. Here, the goal is to further explain the self-similarity for both fractals and geographic phenomena. Fractals exhibit a property of strict self-similarity that the structure shows no differences in detail across all scale levels (refer to Figure 1.2). Every stage the formation of a fractal is repeated and continues to infinity. Strict self-similarity is a unique property belongs to fractals that it demonstrates and connects the mathematics, geometry, science and even arts. A common and straightforward procedure to generate surface based on fractals is *Fractal Brownian motion* (fBm) and it also has a known D value (Mandelbrot 1983, 247). It is computer-based generating method with a parameter of H, which controls the roughness of the generated surface. The surfaces generated by fBm are not strictly self-similar fractals. In fact, they are irregular and self-similar surfaces possess limited self-similarity. Surfaces of fBm serves as norms for understanding strictly self-similar fractals and other geographic analysis (Goodchild and Mark 1987). Moreover, the generated landscape can also be treated as basis to test various fractal methods to compare the estimated D with the known D value. The methods are limited to surface complexity since the fBm only generates surface features.

On the other hand, geographic phenomena are not mathematically formed objects and they only exhibit self-similarity within certain scale range (Lam 2004, Sun et al. 2006). Similar but different to strict self-similarity, this characteristic is termed statistical self-similarity, an object is self-similar in a statistical sense and the structural differences happen by chances (Goodchild and Mark 1987, Sun et al. 2006). Figure 1.1 and 2.3 both serve as geographic phenomena examples for illustrating the self-similarity property in a statistical manner. In statistical analysis, a hypothesis test is commonly used to decide whether a null hypothesis is rejected or not. For geographic phenomena, the test can be used to examine whether a coastline or urban surface landscape is a fractal. The structure and fractal dimension value will change for natural phenomena and if the test value is within the statistical distribution range, the null hypothesis keeps true that the tested feature is a fractal. Statistical self-similarity makes it possible to relate to spatial statistics and local models for fractal analysis. Moreover, for earth's surface features, self-similarity also relates to a characteristic of randomness that the resemblance of the geographic phenomena is not the same over different scales and it is statistical and happens by chance (Weng 2003).

Filling Space Using Recursive Subdivision

Recursive process directly relates to self-similarity property. Fractals are formed in a recursive way to fill up a space. Irregular lines with self-similarity property can be constructed in several stages based on the same manner. Figure 2.5 illustrates a process of a fractal line using recursive subdivision fashion. At the first stage, a curve starts with a letter N in a 2D space. Then the process repeats that each line segment is replaced by a letter N and are connected to each other. As the process continues, this N letter shape curves will fill up the space and continues to infinite stages. This example is also called the *Morton Sequence* or *N-tree*. In this case, the curve is a fractal with strict self-similarity property. Therefore, the fractal dimension is a constant value at all stages. Because this curve eventually fills the plane space, its D value is 2 as a constant number. There are many other famous examples of exact recursive process: *Koch curve, Koch Island, Snowflake and Cantor dust* (Mandelbrot 1983, 35, 41, 80). This generating method is reliable that the object is constructed in infinite stages with the replacement of the segments of itself. Moreover, there is always an equation associated with the recursive process to calculate either the length or the area of the object. The limit function in mathematics is the basis of recursive process and, for example, the length of the Koch curve is infinite because the length continues to increase with more small segments adding into the curve. On the other hand, the length of a Koch island is still an infinite value but the area is a finite value based on the equation and the limit function. The limit area depends on the side length of the Koch triangle. Detailed of the equation and theoretical framework will be discussed in Chapter Four.

The principle of the recursive subdivision is useful in the real world application. The Koch Island is a representative theoretical foundation, which can be applied to the road system. Considering the highway system and its near city, the highway is the first stage of the construction and it has several exists leading to a town or city. These exists can be treated as the next stages with a growing length. Main Street in the city is the next level and it can have some chain roads connecting to different city function areas such as shopping mall, business center and residential neighborhood. The city edge is an enclosed boundary limits the expansion of the major and minor roads. For urban sustainable development purpose, the Koch Island concept is suitable for constructing road system in a long-term development. The total length of the roads is infinite. The design of the branches makes the path shorter than the direct rectangle way. Meanwhile, the total area is limited to a constant number indicates the road system will not expand unrestrained. This recursive subdivision characteristic of fractals is the most efficient way to fill a space (Chen 2009). It has great potential in city planning and urban sustainable development application.

The above characteristics are three fundamental properties of fractals. Knowing of these characteristics is the beginning step for understanding fractal concepts, and to differentiate the fractals from other forms. Even though these three headings are reviewed separately, indeed, they are highly interrelated and complementary (Goodchild and Mark 1987). Self-similarity is the core characteristic of fractals and it bridges with scale measurement and recursive subdivision. In other perspective, characteristics of fractals can be explained in the same way and they can be treated as one characteristic. Recursive subdivision is the initial opening for constructing a fractal either based on mathematics or computer programming. As a result, the recursive subdivision generates strictly self-similar objects at all stages. At last, for a further analysis, a quantitative measurement of the size of the object is a response to the scale change. A combination of the construction and the quantitative analysis makes the fractal concept has great potential in certain spatial and geographic applications (Mandelbrot 1967, Goodchild and Mark 1987, Andrle 1996).

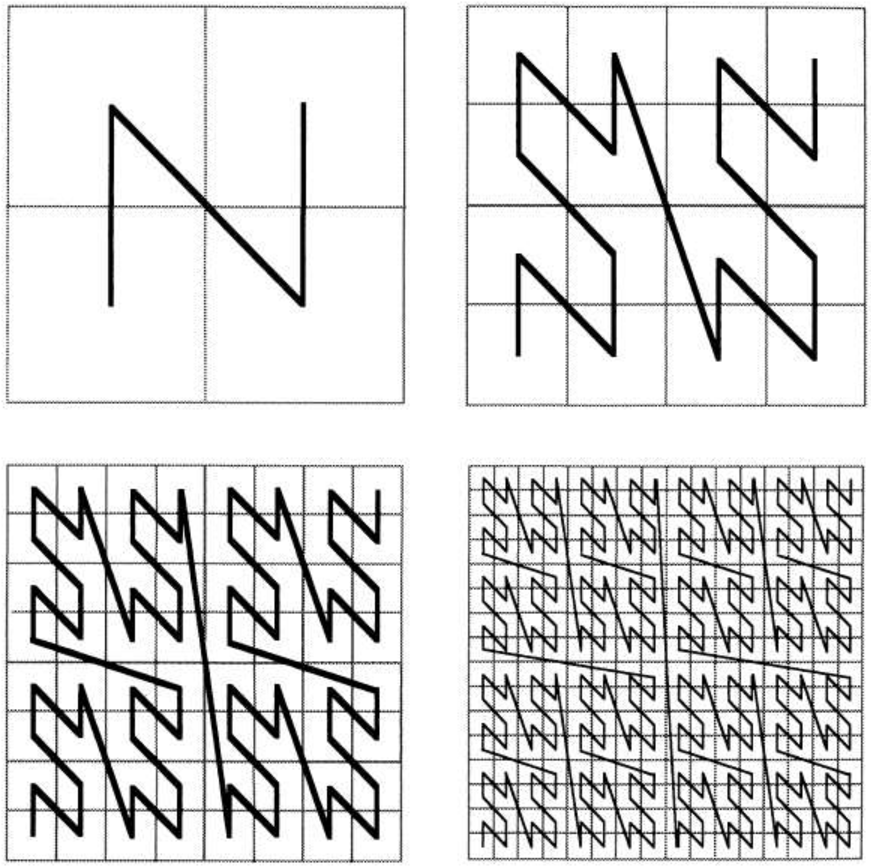

Figure 2.5 Recursive Subdivision to Fill a Space (Goodchild and Mark 1987)

2.3 Fractal Dimension

Generally, a dimension indicates how much space a geometric object can occupy near to its points (Falconer 2004, 27). The notion of dimension is essential to fractal geometry as well as other natural phenomena (Falconer 2004, 27). Traditionally, topological dimension is the standard dimension used to measure the dimension of an object. Commonly, there are four forms of topological dimension for classical Euclidian geometry: a point is 0-dimensional, a line is 1-dimensional, a surface is 2-dimensional and a volume is 3-dimensional (Figure 2.6). However, for fractals and geographic phenomena, topological dimension can hardly capture their structures and forms since fractals are too irregular, both in local and global manner (Falconer 2004). The size of fractals and natural phenomena variates in response to scale measurement, their dimensions are not integer and lie within the traditional dimension limits (i.e.

0, 1, 2 and 3) as a fractal number. The lack of the power to describe the geometry of irregular objects leads Mandelbrot (1967) to contribute the concept of fractal dimension to the public.

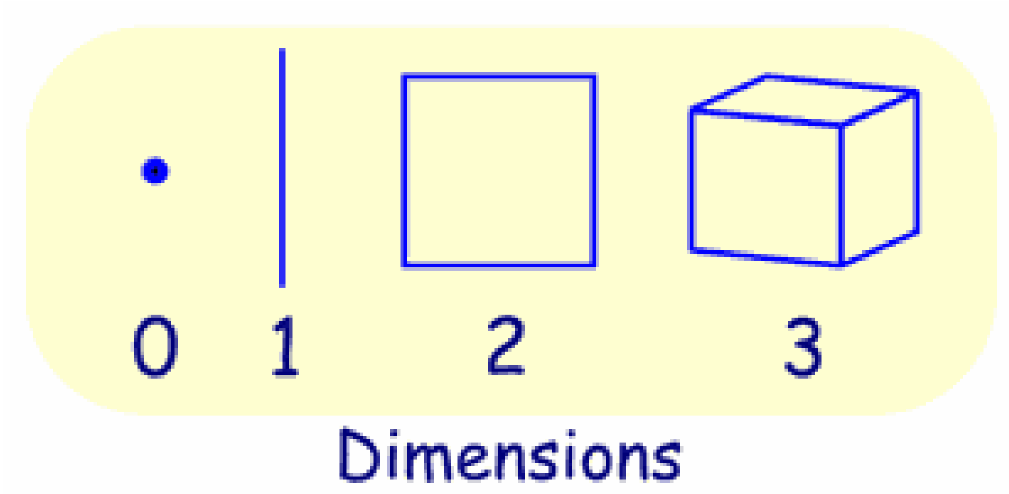

Figure 2.6 Topological Dimensions of Four Basic Classical Euclidian Geometry
Source: Google Images

A central concept and construct of fractals is termed *fractal dimension (fractal dimension)* which is a quantitative indicator of fractal geometry (Mandelbrot 1983, Sun et al. 2006). Fractal dimension extends the dimension family widely and more accurately. There are many definitions of fractal dimension have been proposed to quantitatively describe the geometric measurement of fractals. These definitions are based on different mathematical calculation and empirical estimation. The simplest fractal dimension is referred to as *similarity dimension*. Its calculation method is based on the recursive process in a repeated way. The dimension calculation of similarity dimension takes the following form:

$$S.D. = -\log m \,/\, \log r \qquad [1]$$

Where $S.D.$ is similarity dimension, m is copies of itself, r is a scale factor, and it uses logarithms which is always to be base e (Falconer 2004, 10). The calculation of similarity dimension is illustrated in

Figure 2.7. A Cantor Set starts with a line having unit of 1. As the recursive process continues, the line is replaced by two segments with 1/3 length for each. Based on the mathematical calculation, the similarity dimension of the Cantor Set is $\log 2 / \log 3$, which is a decimal number between 0 and 1. It is explainable because the Cantor Set tends to decrease its total length and arrives finally as several disconnected points. Not surprising, its total length becomes 0. The same calculation fashion can be applied to fractals with similarity dimension between 1 and 2 or 2 and 3. Similarity dimension is narrowed to be applied to the class of strictly self-similar objects and it is not applicable to the real world phenomena. Considering natural features are statistically self-similar and do not possess the exactly same value of copies and scale factor at all stages, equation (1) fails to calculate the correct dimension. As a result, similarity dimension is not widely adopted in fractal literatures regarding the physical and human geography applications.

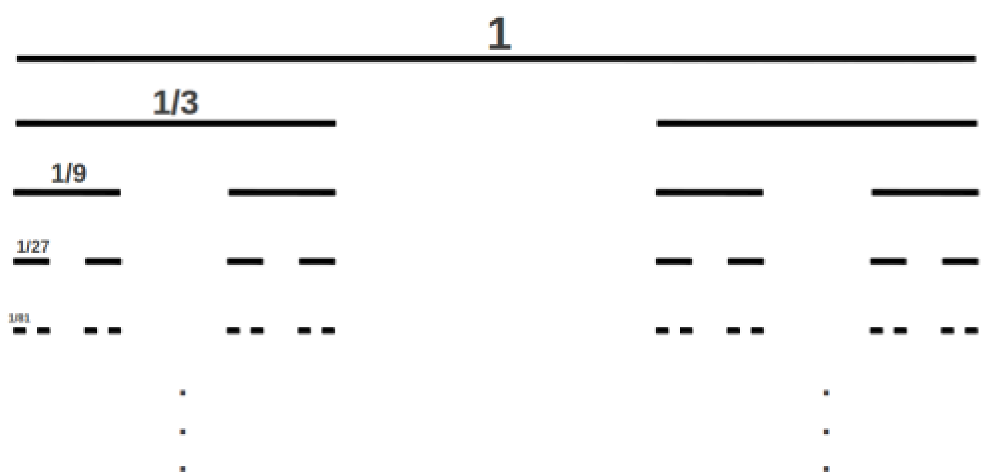

Figure 2.7 Similarity Dimension of the Cantor Middle Thirds Set
Source: Google Images

Different from similarity dimension, a more widely applied fractal dimension is termed *box-counting dimension*, which is defined not only for strictly self-similarity, but also suitable for any sets of irregular objects including the geographic features (Falconer 2004). The history of box-counting dimension can be dated back to 1930s and still is one of the most widely used fractal dimensions. Karperien (1999) stated a definition of the box-counting dimension and its method:

Box counting is a way of sampling an image to find the rate of change in complexity with scale, as well as measure of heterogeneity or lacunarity.

We recall from above that the similarity dimension can only deal with the mathematical fractals, box-counting dimension as an alternative method is more powerful and it is popular due to the simple and intuitive formulation. In addition, it can be applied to wide range of complicated fractals (e.g. trees, human lung) with an estimated dimension (Fractal Dimension 2003). For strictly self-similar objects, the box-counting dimension is equal to the similarity dimension (i.e. same dimension value for the Cantor Set). The basic procedure of estimating a box-counting dimension is to lay several boxes over an image, record the size and counts of the boxes, then change the size of the boxes for recording other pairs of size and counts. Converting both values using log transform and fit a straight line through the log transformed points. The box-counting dimension is the slope of the fitted line. This is an estimated value because the real world phenomena are not exactly recursive subdivision process and the value is an approximation. Apparently, there are two key features of box-counting dimension: 1) the count of the boxes at each sampling, and 2) the size of the square box. Box-counting dimension is important but is beyond the scope of this dissertation, interested readers are referred to Falconer (2004) for more details regarding the calculation illustration as well as the properties and problems.

Hausdorff dimension is another definition of fractal dimensions which is the oldest and the most important dimension (Falconer 2004 44, Schleicher 2007). It is also termed *Hausdorff-Besicovitch dimension* (Mandelbrot 1967, 1977, 1983). Hausdorff dimension is considered as the most precise fractal dimension when calculating dimension of geographic phenomena (Falconer 2004, University of Warwick). Moreover, it can be defined and calculated for any complex objects based on intuitive mathematical principles (Falconer 2004, 44). Not surprising, Hausdorff dimension is limited in application because it is difficult to calculate using the computational methods (McMullen 1984, Falconer 1988). The value of Hausdorff dimension is illustrated in Figure 2.8. We see that the value of the

Hausdorff dimension is acquired when the y-axis value drops to 0 as the s increases, and the Hausdorff dimension is this critical value which is the value of s. The definition and calculation of the Hausdorff dimension are complicated and difficult to understand, and the details of the Hausdorff dimension beyond the scope of this dissertation. Interested readers are referred to Falconer (2004) for better understanding.

Both of the box-counting and Hausdorff dimensions are important as a fractal dimension. According to Falconer (2004, 50), the Hausdorff dimension is equal or smaller than the box-counting dimension. Precisely, the Hausdorff dimension is equal to and smaller than lower box-counting dimension, and lower box-counting dimension is equal to or smaller than upper box-counting dimension. For most of the true fractals and the “acceptable irregular objects”, the Hausdorff dimension is no different from the box-counting dimension. However, the values of these two dimensions can be very different for some other example. There are also some other fractal dimensions (e.g. packing dimension, curves dimension) (Falconer 2004, 64) that are not discussed in this section but also have their importance and certain range of applications. In general, various definitions of fractal dimension tell different characteristics of a given set. Fractal dimension itself is not sufficient to describe the topological and geometrical property of an object, but this fractal number can convey the information of how the object formed and connected, some disconnected points or maybe an extremely rough surface.

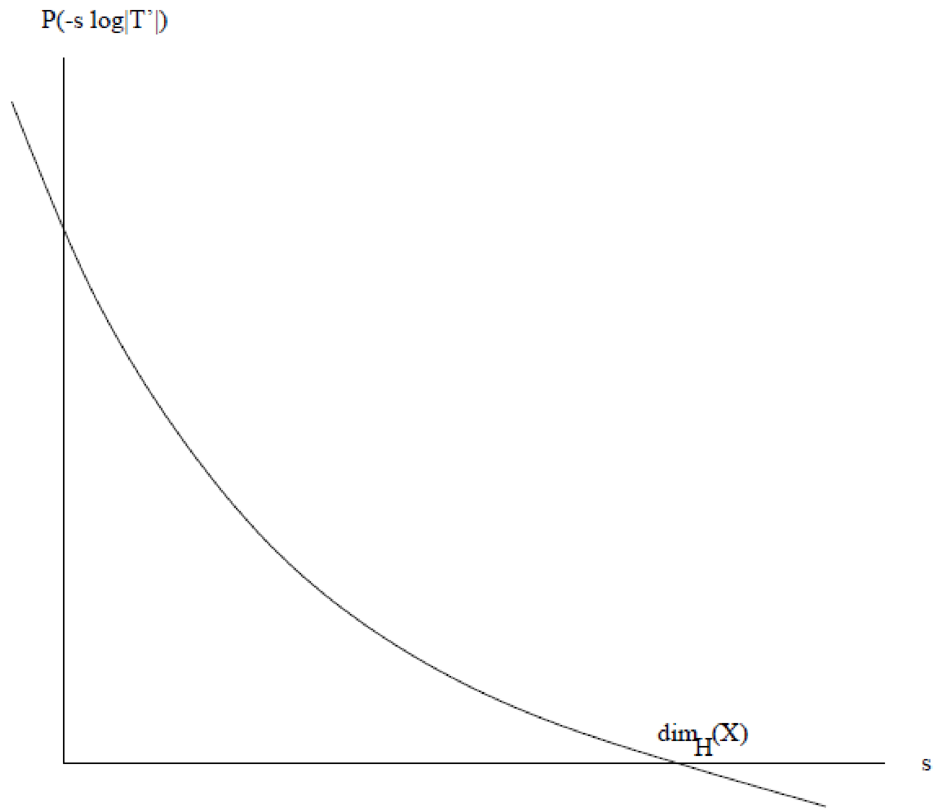

Figure 2.8 Graph of the Hausdorff Dimension
Source: University of Warwick (Website)

2.4 Fractal Geometry History of Cities

The concept of fractal geometry has been applied extensively to numerous scientific and art areas. It is proved that fractal geometry and fractal dimension can be applied appropriately to physical phenomena (e.g. coastline, air pollutant and rainfall) (Mandelbrot 1967, Mandelbrot and Wallis 1968, Burrough 1983, Lovejoy and Mandelbrot 1985, Goodchild and Mark 1987, Lee et al. 2003, Lam 2004). Recently, attention of fractal geometry has been put onto human geography and man-made world (Frankhauser 1998, Benguigui et al. 2000). Among all these many human involved phenome, city is considered as one of the best examples of random fractals (Batty and Longley 1994, Benguigui et al. 2000, Chen 2012). Batty and Longley (1994) mention that cities exhibit some fractal characteristics long time back to the ancient time, and the fractal geometry can help partially explain the development of cities, especially in a sustainable and organic way. A city originated on its own and designers are always concerned about the aesthetic aspect and ignore the functional impact on city development. One hundred years ago, we view our cities focusing on the exterior shapes to make the city "look" attractive. However, our concentration should be placed on city's social and economic efficiency in order to plan a more sustained progress (Batty and Longley 1994, 1, Chen 2010, De Keersmaecker et al. 2003).

Indeed, our city is originated from a small function area, a small group of people and limited usable land. The development then encloses more groups of people to form various function districts. An initial stage of a complete city will be settled and progresses based on the same manner of development. The physical shape of a city is an ultimate result of the combination of the economic, social and cultural development. Cities are usually classified into two development types: *natural development and planned development* (Batty and Longley 1994, 7). People also name the natural development as organic or sustainable development. This type of city evolution relies on individual decisions, which form a myriad structure, and the development is slow sometimes even draw back. This result in an irregular and chaotic internal layout of city. This type of city evolution somehow relates to the fractal geometry idea that a city starts at a small scale and expand based on the similar function needs with modest change each time. On the other hand, a planned development of a city is a result of decisions from large group of people or some agencies who dominate other people's will. In addition, this type of physical development undergoes a rapid and monumental urban growth. It is reflected by some of the decision makers and a city is highly developed in an unlimited way in order to meet their social and economic demands. As a result, the physical shape of a city is more regular and organized but not efficient and sustainable. For an illustration of these two classes, readers are referred to Figure 2.2 and 2.3.

The idea of organic development of the city has long been considered using pure geometry as a basis to guide the progress. An earliest description of city based upon geometry can be tracked back to 2000BC (Berthon and Robinson 1991, Batty and Longley 1994, 18). At that time, the concept of simple geometry has been employed to picture a town or city's settlement (Figure 2.9). This earliest city physical geometry, as well as the separate usages, was depicted in a backcloth of a military asylum. It has a circular boundary with two perpendicular straight streets in the middle that separates the city landscape into four equal sector-shaped areas. The geometry of this early city is driven by the different land usages and social purposes, and can be a general physical design for many cities at that time. That is, a central area where the main economic and social activities occur of a city is usually where a city is originated and spread out to outside edges. This pure geometry of circular shape prevails in history for European cities for forming the city boundary before middle age. Moreover, one of the advantage of pure geometry is that people can accurately measure the length and area for an area based on the known values (e.g. road length and angle). More recently, for modern cities, the geometry of a city boundary has shifted from circle to star-shape, along with incorporation of numerous grids or squares within city boundary (Batty and Longley 1994, 23). The star-shape boundary (Figure 2.10) allow the more wall spaces for stronger fortification. This design utilizes the space in an optimal way and relates to the famous fractal of Koch snowflake. The taste of aesthetic of urban form has changed but more likely since the contemporary city carries more social and economic functions and responsibilities than ancient cities. One of the biggest changes is that some transportation systems were embedded into the city layout to make city services more accessible. Subsequently, a modern city would initiate a combination of perfect circle, grids and sinuous roads, and evolve to a cluster of regular grids switched from the circle and sector. For some 20th century cities, the edges are seemingly to be not perfect circle or square but display a quite irregular and curved shape (Keeble 1969). With the development of latest city, it is desirable to exploit the third dimension to fill the volume efficiently, and free more surfaces for greenery and water body. Therefore, the focus should also be shifted from two to three dimension on future city (Le Corbusier 1987).

Figure 2.9 Pure Geometry of Circle of Early City Boundary (Batty and Longley 1994, 19)

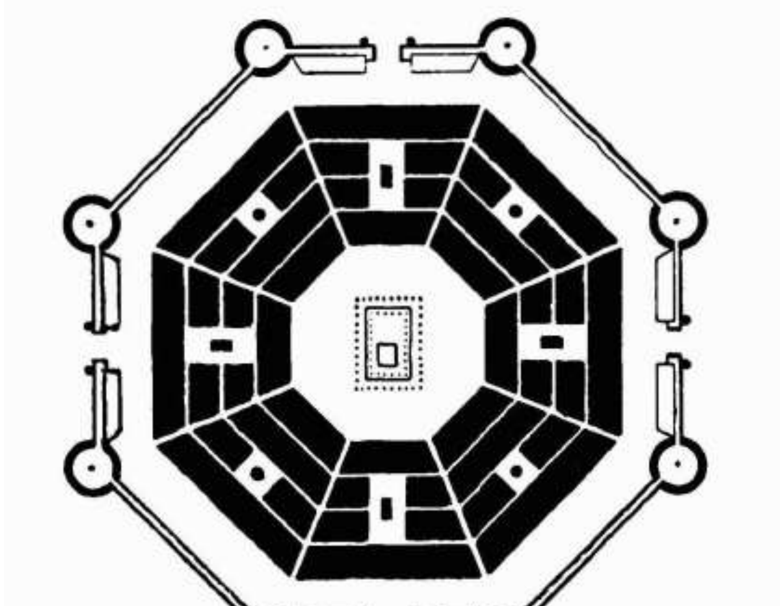

Figure 2.10 Pure Geometry of Sector Shape of Modern City Boundary (Batty and Longley 1994, 23)

North American cities in the late 18th century were completely dominated by grids rather than perfect circles (Batty and Longley 1994, 22). A new concept of company towns started to pilot the modern city plan of North American city (Reps 1965, 427). The grid design was still the dominant and popular planning type at the early years of that century for the U.S. cities, but the straight streets were replaced by the curved layout as the city expands. There were not many examples of pure geometry dominated cities in the U.S. at early ages, two examples mentioned by Batty and Longley (1994) were towns in Georgia and Ohio. They were both planned with strictly geometric structures and steadily developed to more and more regular squares. The town, with an interesting name: Circleville, in southern Ohio, was all changed to regular grids by the town company to serve its economic benefits and accessible company location. Boston as one of the major cities in the U.S. did show another type of physical structure. From 17th and until 18th century, Boston exhibited non-pure geometry type because of its advanced transportation systems and concentrated industry locations. It is noticeable to see the wall of Boston disappeared and the city reached out irregularly as star-shaped boundary (Vance 1990). Even though Boston's geometric shape is not simple, it still has its own plan of expansion to meet the specific needs of the city's social developments. This could be classified as unique urban form that originated from the pure geometry. Another important issue concerning most North American cities is that the scale has an impact on their geometric structures. Take New York City as an example, when it is considered in a smaller scale, Manhattan displayed a pure geometry development and then moved into a planned progress behavior. However, in a wider scale, from New York City to metropolitan systems of cities, an unplanned or irregular enlargement of boundaries was the dominant type but pure geometry can also been observed when the scale is zoomed into internal structures of these cities (e.g. Baltimore, Washington and Philadelphia).

The history of the development of the world and North American urban forms presents us the initial appearance of the fractal geometry. From pure geometry (perfect circle) to grids, then to the combination of circle and squares, and evolves to an irregular and messy shape, all these symbols that the idea of fractal geometry plays an essential role in urban development. Cities as one of the most complex and random systems are created by human beings based on millions of decisions and events, and closely relate to fractal geometry (Wong and Fotheringham 1990). Similar to coastlines, city boundaries show a clear self-similarity property but in a hierarchical ordering, and fractal concept can be applied to any systems analogous to cities (Batty 1991). City's complexity can be linked to chaos and fractal theory, which are non-linear tools, and to gain deeper understanding on city evolvements (Chen 2012). Therefore, at some extent, urban pattern exhibits self-similarity property, and fractal geometry as an innovative perspective has great potential in studying city structures and urban systems (Tannier and Pumain 2005, Thomas et al. 2008, Chen 2010; 2012).

2.5 Fractal Geometry Applications of Cities

The following briefly presents the applications of fractal geometry in urban structures regarding various aspects, more detail is given on the estimation of fractal dimension to examine urban forms and development. As discussed in previous section, cities have received plentiful considerations from fractal geometry and could be explained by various fractal parameters (Chen 2012). Fractal dimension of cities is a core indicator to interpret the physical structures both in global and local senses. Urban form is extremely complex in comparing to mathematical objects. The differences between these two distinctive features are listed in Table 2.1.

Table 2.1 Comparison of Urban Structure and Mathematical Object (adapted from Chen 2012)

	Mathematical Fractal	City Fractal
Fractals	Simple Structure	Complex Structure
Fractal Dimension	Constant of Time	Variable of Time
Pattern	Regular or Irregular Pattern	Irregular Pattern
Process	Certain or Random Process	Random Process

There are different issues of fractal geometry researches on urban forms. One is the focus on the optimal space filling indicating urban sustainable development, which links to the ultimate purpose of using fractal theory. This class of studies always correlates to other social and economic factors (e.g. total population, population density, proximity) for revealing more information on the relationship between fractal dimension and urban evolvement (Terzi and Kaya 2008, Feng and Chen 2010, Chen 2010; 2012). Another group of researches targeting on spatial and temporal effect of specific cities on the fractal dimension to see when and where a city shows a fractal characteristic (Benguigui et al. 2000; 2001, De Keersmaecker et al. 2003). These researches estimate fractal dimensions based on various methods for the selected cities for a period range of time. Additional, local neighborhoods are measured to see how fractal dimension varies over space. Benguigui et al (2000) concluded that the fractal dimension of Tel Aviv, Israel increased with time and only show fractal characteristic at later development stage. In addition, only central part of the city is a fractal. Other researches focus on applying fractal geometry on different urban land use to distinguish various physical structures of urban land use (Batty and Longley 1988, White et al. 2000, Herold et al. 2002, Lam 2004). Among these studies, the urban land use are divided into commercial, residential and transport. The results show that commercial land use exhibits the most complex spatial landscape. However, the results could change as the scale of the data changes (Benguigui et al. 2000).

The studies of fractal geometry in city boundary (Anas et al. 1998) is intuitive because its physical structure is similar to the shape of the coastline. As a linear feature, and with the rapid development of urban structure, nowadays boundary of modern city not only has evolved to massively large, but also to a highly irregular shape. According to Batty and Longley (1994, 202), the physical form of a city boundary is irregular and self-similar, it lies between rural and urban area that can never be clearly portrayed out. A city boundary is a place where the most interesting and dramatic changes happen. Cities can be described in many dimensions, however, the best way to analyze a city is through its 2-dimentional plane to visualize its shape (Batty and Longley 1994, 202). In this sense, the city boundary or the edge convey some useful information as it can be used to measure the city area, which is the most conceptualized quantity to describe the overall structure and form of a city. Therefore, how to define a line or curve between city and its suburban area has been studied for two centuries but it is still a problem and difficult to choose the outer boundary (Benguigui et al. 2000, Greene and Pick 2011, 42). Deciding city boundary is prerequisite and essential to the application of fractal geometry to city studies. As Peitgen and Richter (1985, 571) stated a definition of city boundary:

The fascination of boundaries lie in their ambivalent role of dividing and connecting at the same time. They mark the transition between different modes of existence. They transmit and control exchange between territories. They are the playground for discovery and conquest……They are the result of never ending competition and exhibit structure on many scales.

Another definition of city boundary focusing on the growth boundary comes from Environmental Protection Agency (EPA) (Cho et al. 2006):

A mapped line that separates land on which development will be concentrated from land on which development will be discouraged or prohibited.

Different methods have been proposed to pick up an appropriate city boundary. Batty and Longley (1994, 212) defined the boundary of Cardiff, Wales based on Ordnance Survey map, by excluding urban fringe land use, including villages connecting to the urban area as well as the man-made objects close to the coastal area. David (1998) used an automatic method based on computational experiments with the geographic data of city population distribution. Another common method for finding city boundary is to enclose the contiguity built-up area. A claim has been made that a city boundary is a fractal and Benguigui et al (2000) mentioned that it is not proved whether the fractal dimension will change for the same city by different boundary definitions. On the other hand, not surprising, some strict methods for choosing city boundary may yield more precise and reasonable fractal dimension results. Many studies have applied numerous methods and models to estimate fractal dimension of city boundaries all over the world, either for a current condition or as a function of time periods (Makse et al. 1995, Benguigui et al. 2000, Frankhauser 2004, Cho et al. 2006, Tannier et al. 2011). The city boundary encloses the city but not completely a circle or 2-dimentional object. The estimated results of fractal dimension for the selected cities lie around 1.7, which is closer to 2, indicating a relatively highly irregular boundary. A brief list of the fractal dimension of studied cities around the world is listed in Table 2.2.

Table 2.2 Fractal Dimension of Boundaries of Studied Cities (adapted from Batty and Longley 1994, 280)

City Name	Study Year	Fractal Dimension
Albany	1990	1.49
Beijing	1981	1.93
Berlin	1980	1.73
Boston	1981	1.69
Budapest	1981	1.72
Buffalo	1990	1.73
Cardiff	1981	1.59
Cleveland	1990	1.73
Columbus	1990	1.81
Essen	1981	1.81
Guatemala	1990	1.70
London	1981	1.72
Los Angeles	1981	1.93
Melbourne	1981	1.85
Mexico City	1981	1.76
Moscow	1981	1.60
New York City	1960	1.71
Paris	1981	1.66
Pittsburgh	1981	1.59
Rome	1981	1.69
Seoul	1981	1.68
Sydney	1981	1.82
Syracuse	1981	1.44
Taipei	1990	1.39
Tokyo	1960	1.31

Most of the cities were measured during year of 1981, the smallest fractal dimension is found for Tokyo in 1960, which is 1.31. This relative smooth boundary of Tokyo could be due to the early study in 1960 that the city was undergoing its early development stage. On the contrary, New York City was also studied in 1960 and has a large number of 1.71. Two kinds of irregularity of boundaries for Tokyo and New York City at the same time may result from the different economic backgrounds of development at that time. Some smaller cities in the U.S. (e.g. Albany, Syracuse) have fractal dimensions below 1.5 after 1980. The most irregular boundaries come from Beijing and Los Angeles, as well as Sydney, the fractal dimensions are 1.93, 1.93 and 1.82, respectively. All these three cities are among the largest cities in the world in terms of population and city size. Beijing and Los Angeles, not surprising, have an extremely rough city boundary that closer to 2. The fractal dimension of all the city boundaries are larger than the West Coast of Britain (D=1.25) meaning city boundary tends to fill the 2-dimentional space with diverse roughness. One conclusion can be drawn from these previous studies is that the fractal dimension of city boundary seems to have a positive relationship with the population size.

Another category concerning fractal geometry with city fractals is the measurement of surface roughness. Besides examining city boundary, the study of city landscape surface complexity could be complementary in order to understand the physical structure of a city in a whole. The fundamental model of urban landscape consisted of vegetation, impervious surface and soil (VIS) (Ridd 1995). Distribution of impervious surface is a major component of a city landscape, and can be seen mostly within urban area, especially in highly dense business district (Wu and Murray 2003). Urban surface and built-up area (urban canopy) together can generate many effects to city environment (e.g. turbulence change, storm enhancement, water storage, air pollution dispersion, etc.) (Masson 2006). Surface landscape has a tendency of filling up a volume into a 3-dimentional object. Unlike the linear fractal dimension for city boundary, city surface landscape has a fractal dimension between 2 and 3, the more rugged the surface is, the more peaks and valleys it will have, the larger the fractal dimension would be. For impervious surface, a parking lot could have a fractal dimension close to 2.0 while a building complex may generate a fractal dimension approaching to 3.0. Calculating surface roughness requires the dataset to have elevation value (e.g. Digital Elevation Model). Therefore, remotely sensed data with the digital number is the suitable data source for acquiring fractal dimension for surface landscape. Radar data is also capable of providing height value for surface landscape. As previously mentioned, one very simple and commonly used method for measuring surface landscape is the computer simulation (Fractal Brownian motion) which can generate irregular and rough surface with various levels of roughness, and the generated image can be used to test different methods in compare with the known fractal dimension. The roughness and the known fractal dimension is controlled by a parameter of H. The most successful value of H for simulating surface topology is 0.7 and it relates to a fractal dimension of 2.3 (Orey 1970). Goodchild and Mark (1987) summarized that fBm owns significant value for simulating surface topology. As for city surface topology, fBm process could be used as a reference image and help choose the most appropriate method, then apply this method to estimate city surface roughness. Lam (2004) studied Atlanta area and separated the city area into four land use: *commercial district, airport, mixed area and forested land*. These four land covers were claimed to be the most common surfaces in urban area (Lam 2004). The results of the fractal dimension of these four land covers in response to pixel size is shown in Figure 2.11.

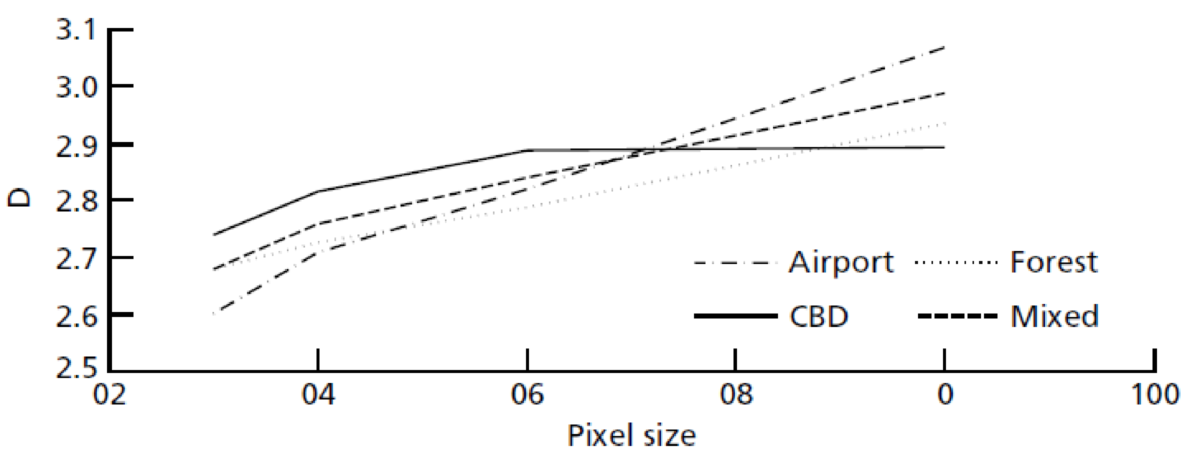

Figure 2.11 Fractal Dimension of City Surface (Lam 2004)

Commercial district exhibits the most heterogeneous characteristic with a fractal dimension of 2.7. The smoothest city landscape is airport, which is not surprising. All these four land covers show some flexibility to the pixel resolution change. Fractal dimension of commercial land increases slightly and stays close to 2.9. In contrast, the fractal dimension of all other three types of city landscape continue to increase, interestingly, airport seems to have a fractal dimension exceeds 3.0. This is unrealistic and it mainly due to either the pixel resolution effect or the fractal analysis methods (Lam 2004). In addition to the study on the present form of cities, it is also meaningful to discuss the application of fractal geometry on urban growth in a dynamic perspective.

2.6 Fractal Geometry Applications of Urban Sustainable Development

Earth's resources have been consumed to a limit and it is essential to conduct and plan a sustainable development. Cities as one of the major consumers have absorbed excessive energies and generated air pollution (Breheny 1992). It is said that 65% of the population will live in urban area by the year of 2025 (Schell and Ulijaszek 1999). Urban sustainable development is a concept in response to the growing circumstances that helps balance the social, economic and environmental systems of a city in a long-term (Campbell 1996, Diamantini and Zanon 2000, Li et al. 2009). Urban planning, especially land use planning continually changes for the cities all over the world (Li et al. 2009). Sustainable planning on urban land occupancy seems to be urgent because urban land use is remarkably heterogeneous. Complex transportation routes, green space and built-up area need enough available land and all these land use not only compete with each other, but also compete with human beings and other city systems. Finding an indicator to describe the urban sustainable development is imperative to imply urban monitoring and regulation (Repetti and Desthieux 2006, Nader et al. 2008). An effective indicator can provide a guidance for urban sustainable development, provide a quantitative measurement of how social and environment interact within city and can provide data to urban planner in the future (Nader et al. 2008).

As previously mentioned, fractal geometry provides a powerful tool in examining city physical structure. However, the previous empirical results of measuring geometric complexity of city boundary and surface only contribute a stationary investigation, it only presents to people the present physical form of the city surface with some single non-integer numbers for each city. Fractals are formed through a dynamic process from individual particle to a massive body. Therefore, studying fractals in a non-stationary way against various stages is an indispensable and necessary research concern. City fractals, as artificial complex system, can be treated as an evolved process of continually developing stages starting from central place and extending to the outer range. In other words, various developing stages are analogous to time series of urban growth. Consequently, it seems like fractal geometry of city fractals is an ideal candidate for analyzing urban sustainable development. On one hand, it has been said that land use planning is a major component of urban planning, and urban land use is closely conducted by geometric composition along with the city's density, scale and dimension (Longley and Mesev 2000). On the other hand, fractal dimension of fractal geometry is an effective and advanced indicator of urban sustainable development that it demonstrates an intrinsic property of geometric objects of urban composites.

Fractals in a whole explain the optimality of a natural system filling space from its form of origin (Rigon et al. 1998). Similarly, city structure is self-organized hierarchy and fractal structure indicates the optimal and most efficient way to fill the space in a hierarchical fashion (Wu 1996, Barredo et al. 2003, De Keersmaecker et al. 2003, Chen 2010, 2012). In this sense, this concept can be used to optimize city structure for urban planning. Moreover, as urban grow, an inevitable problem that we all face now is urban sprawl. Occupying the space in a compact way can refrain the unlimited city expansion in order to control urban sprawl issue. Analyzing city fractals is a basic and theoretically fundamental groundwork and has significant values for urban sustainable development (Frankhauser 1998, Chen 2010). Self-organized hierarchy of city may undergo several stages guided by the urban planning policy for the goal of achieving a sustainable city (Figure 2.12). Chen (2010) pointed out that sustainable development of city system is analyzed by population density models, and also stated that the inverse power law of population distribution exhibits fractal characteristic which could be used to model future regular city. Fractal geometry for space optimization plays an important role for city planning to reach the stage of real city, then a real city evolves to a future regular city.

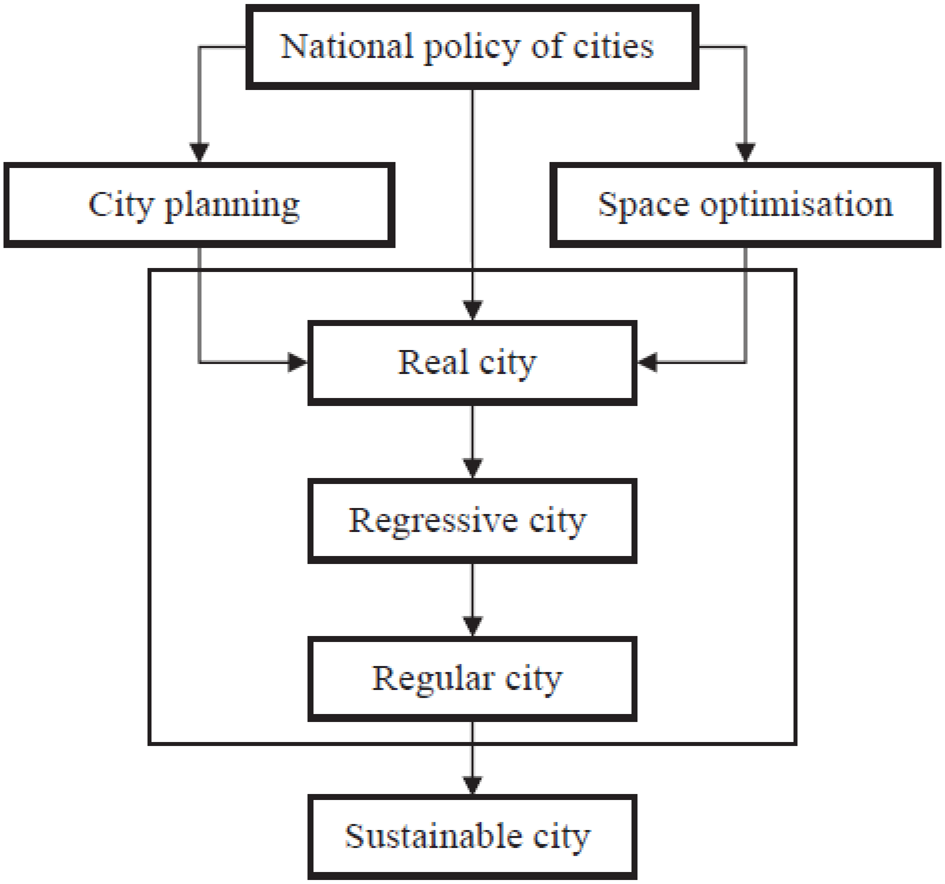

Figure 2.12 Relation between Fractal Geometry and Urban Sustainable Development (Chen 2010)

The idea of fractal geometry has great potential applications to the urban sustainable development from various aspects (Wong and Fotheringham 1990, Makse et al. 1995, Wentz 2000, Shen 2002, Huang 2007, Terzi and Kaya 2008, Chen 2010). The first collection of application is simply using scale relation ratios to calculate fractal dimension of urban boundary to quantify the urban growth throughout the city development history with the available data assistance. Batty and Longley (1994, 236) reported case study of London from 1820 to 1962, with 8 stages of growth, the fractal dimensions are 1.322, 1.585, 1.415, 1.700, 1.737, 1.765, 1.791 and 1.774, respectively. They claimed that this is a classical city growth in a fractal way and this is also confirmed by other researchers. It is noted that within the early stages of development, the fractal dimension increased from 1.3 to 1.7, which indicates a clear urban growth into a more irregular form. After that, the fractal dimension slightly increased and becomes stable within 1.7 and 1.8. It implies that London's development reached a fractal structure after year of 1880. Chen (2012) used an alternative method for calculating fractal dimension. Instead of deriving D value directly from the grid map using scale and size relationship, a self-derived equation was employed that the fractal dimension of next year can be obtained from the current and last year values. This approach is a simulation and prediction process to model fractal dimension evolution and it can be fitted into London dataset. De Keersmaecker et al (2003) measured border and surface fractal dimension of Brussel, Belgium. Several fractal dimensions were calculated and the focus is to summarize the results using descriptive statistics. The mean values are 1.822, 1.565 and 1.719 for three methods, respectively.

Fractal analysis of urban sustainable development also concerns with other geographic variables. Besides estimating fractal dimension, which is a geometric property of urban features, other intrinsic quantities are useful to be linked to the fractal dimension for revealing more insights about urban growth. Population density is an important demographic factor that conveys a homogeneous distribution over the city surface. It can be illustrated that a fractal city at the beginning contains all the population at the central place, then the population distributes to the outer edge following certain distribution laws as the city expands (Frankhauser 1998). Urban total population and population density function have been widely used to derive and relate to fractal dimension in order to understand urban growth (Wong and Fotheringham 1990, Benguigui et al. 2000, Chen 2010, Shen 2002, Thomas et al. 2008). Negative exponential model and exponential power model are usually used for the population density function and fractal dimension can be estimated from the census data. The fractal dimension ranges from1.37 to 1.86 in four time periods predicted from population density. Moreover, the information entropy increases suggesting an efficient space filling of city land carrying certain amount of people. Another way of relating population and fractal dimension is collecting population data and estimating fractal dimension separately. The fractal dimension is not positively relate to population size as D value increases while population size decrease at some points. One argument regarding the relationship between fractal dimension and population density is that fractal dimension alone is not adequate to predict city population growth. It is because some cities may experience population loss but the urban areas still expand. More caution should be carried out here for linking to population issue. One way is considering the time periods that a city population decrease. This usually happens at the later stages of urban development. Geometric shape and social factors are two types of measurements and linking them should take into account the temporal effect.

Some other geographic variables are also considered to link with fractal dimension for study urban growth. Urban sustainable development is always related to urban sprawl issue. Urban sprawl studies have been studied using fractal dimension by many scholars (Diamantini and Zanon 2000, Huang et al. 2007, Frenkel and Ashkenazi 2008). Terzi and Kaya (2008) plotted these two factors for Istanbul from 1975 to 2005. The results showed a positive relation before year of 1995 and then a negative effect. It concludes that fractal dimension is one of the methods to study urban sprawl but other methods are still needed to capture the multi-dimension characteristic of urban sprawl. Frankhauser (2004) studied European cities for different urban patterns under the context of urban sprawl. Instead of using urban sprawl index, this study measured fractal dimension and concluded a D value between 1.3 and 1.5 may indicate a limit of urban sprawl and encourage a sustainability development. A high density area of a city usually generate urban heat island effect. The temperature factor of different city areas and temporal stages can be evaluated through fractal analysis (Weng 2003). Fractal dimension was calculated for the city surface of temperature radiant. The fractal dimension has the smallest value for the spring season and largest value for the summer season. Urban development increases the spatial variation of the surface temperature as well as makes the thermal surfaces more complex and uneven. Moreover, fractal dimension has also been related to other social variables for understanding the urban morphology and evolvement (De Keersmaecker et al. 2003). Housing types, housing age, distance to CBD and household income were linked with morphology fractal dimension using correlation coefficient. The exploratory analysis suggests fractal dimension is a promising measurement for study urban planning and simulation.

Fractal geometry has a profound influence on the study of urban form and urban evolvement. Cities are complex organizations and traditional measurements fail to capture their configuration and composition. Urban form starts with a small cluster and expand to a complex system under the interaction between human being decisions and environment policies. However, the evolvement rule is quite simple, that most of the complex cities result from a simple fractal replacement at each time period. Nevertheless, the style of the spatial replacement changes at each development stage. Thus, cities are not strictly self-similar, they are not in an exact repeating structure, similar to coastlines and other natural features. Accordingly, urban form should be explained in a sense of statistical self-similarity, which the existence of city fractal attributes to chance. Fractal dimension of urban growth in real world could be assumed to be an increasing fractal number between 1 and 2 because city is not in a true fractal form, urban land use tends to fill the space in a multidimensional manner (i.e. fill more land space). It is can be said that statistical test plays an essential role for determining whether a city can be called a fractal city during its development process. Statistical distribution and hypothesis tests are in more demand to analyze fractal dimension of city morphology before carrying out systematic application of fractal geometry.

Fractal geometry applications on urban sustainable development can be divided into two dimensions (i.e. horizontal and vertical analysis). The usually horizontal analysis is the fractal dimension as a function of time periods of a city development. Previous studies have revealed some messages that city displays a fractal characteristic only through its later developing years with the indication of a relatively stable fraction dimension. The turning point (i.e. time periods of a fractal city emerges) can be located and may further studied by other social and environmental factors to examine the inner reasons of such an emergence of fractal city. The other dimension is the vertical axis that focusing on the spatial variation of fractal dimension over the internal urban area. Urban landscape is highly heterogeneous and its neighborhoods somehow would show a various characteristics of physical stricture. Therefore, measuring local fractal dimension is meaningful to pick out the hot spots (i.e. high or low fractal dimension). Also, mapping fractal dimension enhances the parameter visualization which is a central issue in geography and cartography.

As previously mentioned, the geometry of urban form has been stated to be an outcome of the fractal ideas. Urban growth can be modeled using computer simulation technique to predict the future urban model and most of the simulations result in a plane city. The fractal models, in fact, based on many aggregation or diffusion particles (e.g. diffusion-limited aggregation) which generate city simulations similar to the real city structure. One of the commonly used simulation technique is cellular automata (CA) model, which can easily yield urban dynamics analogous to fractal cities (White and Engelen 1993, Batty and Longley 1986, Wu 1996, Batty et al. 1999, White et al. 2000, Barredo et al. 2003). Using computer graphics to simulate urban growth generating urban morphology, which has comparable fractal dimension to real dataset. One finding from computer simulation is that the widely adopted CA technique embedded with fractal recursion indicates city evolves in a fractal process in a long-term period. Another contribution of urban simulation is that it can divulge risky and unrestricted development mode, which may be harmful to urban sustainable development.

Spatial complexity of city surface in a 3-dimensional form is analogous to urban morphology while can be treated as an object filling the volume space. Not similar to planar filling, volume space filling is usually interpreted as a city landscape complexity or image intensity (Sun et al. 2006). Fractal dimension of urban morphology has been related to many ancillary variables, and it would be promising to add surface fractal dimension to fully analyze urban form and urban growth. The measurement of fractal dimension of city surface commonly relies on remote sensed data, which is a large study field for fractal geometry. Chapter Three provides a general background of fractal analysis in remote sensing field, focusing on images of urban area. A brief introduction of remote sensing technique and data source is also presented. Chapter Three also covers specific issues of fractal geometry applied on remote sensing. Various fractal methods for estimating fractal dimension of city surface are reviewed, along with the applications issues proposed for fractal analysis on remotely sensed images.

Chapter Three

Fractal Geometry of Remotely Sensed Image

3.1 Introduction

Fractal geometry has been applied intensively to geographic phenomena for the studies of linear and surface physical structures. Irregular shapes such as coastlines and transit system are exhibited in a visual form to represent the real world phenomena. Therefore, the data source for fractal analysis is a crucial component for presenting physical shapes of natural features to researchers to carry out fractal dimension calculation. It is important to display the physical structure of the studying objects in a precise and digital way, and without a high quality data, fractal methods can be hardly used to fulfill the goal of measuring spatial complexity. Moreover, the heterogeneous landscape of geographic phenomena changes rapidly nowadays and both spatial and temporal analysis of fractal geometry need timely data updates. Attributes data is not appropriate for fractal analysis since it does not contain any physical characteristics. Vector data is one of the suited data source as it contains actual boundary and shape of geographic features. Point, line and polygon are the three most basic vector data type and they have geometric properties for describing their physical arrangement. Measuring fractal dimension of geographic phenomena requires additional quantity information and it based on the basic geometric measurement.

The relationship between remotely sensed images and fractal geometry could be described as a complementary communication. It is becoming more and more important and promising in geographic information sciences to study the scale effect on the geographic phenomena processes (Myint 2003). Changing scale can examine the dynamics of an indicator performance of a spatial phenomenon in order to efficiently use the data at an appropriate scale to characterize the phenomena (Emerson et al. 1999). Among all the available spatial data sources, remotely sensed images have many advantages and have attracted considerable attentions from fractal geometry studies (Sun et al. 2006). Remotely sensed image is both spatial and temporal complex and can covers large extent of geographic landscape. Remotely sensed image can be captured regularly to meet the researcher's requirement for up-to-date analysis. In addition, most importantly, it is flexible to adjust the scale of a remotely sensed image to investigate the diversity of the geographic phenomena. Nowadays, finer spatial resolution data of remotely sensed image has become available and public for easy access. This has made the remotely sensed images playing an increasingly significant role for extracting land surface properties with detailed texture information. Meanwhile, using classification technique to extract linear feature without information loss on remotely sensed images is critical for fractal analysis, and this can be done by employing various image processing methods.

On the other hand, remote sensing is an ideal community for the application of fractal geometry. Not only the estimation of fractional dimension for certain physical structure of earth landscape, but also using fractional dimension to assist related remote sensed image studies. Fractal geometry broaden the application of remote sensing area by introducing the concept for describing the irregular and complex landscape. Many applications of remotely sensed image would loss textural and geometric information without the introduction of fractal geometry. One of the most widely studied issue regarding remote sensing is the classification and it still needs to be improved at various aspects. Traditional techniques rely on the pure digital number and statistical analysis to classify heterogeneous land covers. Fractal geometry can be employed as additional information to further classify the land covers based on texture and physical structure differences, especially for the land covers with similar spectral reflectance but different physical shapes. Fractal geometry has been applied on various classification researches and proven to be a robust tool for improving classification accuracy (De Jong and Burrough 1995). However, fractal analysis alone is unable to characterize the spatial distribution of land covers in remotely sensed images, and dimension cannot even be considered as a primary tool for classifying land covers (Chica-Olmo and Abarca-Hemandez 2000, Dong 2000, Myint 2003, Sun et al. 2006). Another improvement when using fractal geometry is that multiple bands can be studied and a dimension reduction can be performed using fractal analysis other than traditional methods. Fractal methods have been studied to be a better approach than the conventional methods for dimension reduction of remotely sensed images, in a way of reducing computation complexity and yields similar classification accuracy (Mukherjee et al. 2014). Fractal geometry introduces a physical characteristic to the digital image, besides the purely digital numbers, a geometry factor replenishes to the mathematical values of the remotely sensed images and promotes the remote sensing study to a new level.

It is important to note that many fractal analysis applications on remotely sensed image rely on the overall intensity of an image surface (Myint 2003, Lam 2004). Different from coastline and urban boundary, estimating remotely sensed image complexity is more focused on 3-dimentional calculation, and this is considered as an obvious application of fractal geometry (Sun et al. 2006). A single fractal dimension is calculated for an entire remotely sensed image, a single band or different segments of an image. A higher fractional value indicates a more complex landscape surface, and this possibly happens in an urban area (Lam 2004, Liang et al. 2013). Classification of various land covers based on single fractal dimension may not always provide desirable accuracy results. Many studies have proved that similar fractal dimensions may exist for strikingly different textures (Mandelbrot 1983, Voss 1986, Roy et al. 1987, De Jong and Burrough 1995, Myint 2003). Spatial autocorrelation is a commonly used spatial statistics and has been studied to be a better approach than fractal analysis for classification purposes. In order to further distinguish land cover types, after classification techniques and fractal dimension, lacunarity has been applied to distinguish different land cover textures with similar fractal dimensions. Lacunarity is capable of dealing with spatial heterogeneity of remotely sensed images for similar fractal dimensions with different texture appearances (Dong 2000). For remote sensing application of fractal geometry, a single fractal dimension, along with lacunarity concept, could be treated as an innovative and advanced methodology for providing fundamental quantities, especially it is crucial for land cover classification purposes.

Fractal geometry application on remote sensing is necessary and powerful but is not adequate to capture spatial landscape of a remotely sensed image. It is assumed that different textures in remotely sensed images have distinguishable fractal dimensions. However, fractal dimension is not only affected by image texture, moreover, it is also influenced by other factors: (1) fractal methods, (2) parameter specification, (3) estimation procedure, and (4) image band and spatial resolution. Sun et al. (2006) summarized several research issues regarding to the fractal geometry applications on remote sensing. One promising issue is the fractal methods computation and comparison. The relationship between various fractal methods is not clear and the computed D values are not related well. Various methods often generate different fractal dimensions and it has been claimed that there could be a hidden relationship between estimated fractal dimension and fractal methods rather than theoretical inadequacy of the fractal model (Klinkenberg and Goodchild 1992). Fractal geometry application on remote sensing also concerns about the band selection. The existing fractal methods can only be applied for a single band at each time. Estimating for all the bands requires intense computation time. Developing a multivariate fractal method for remotely sensed image is desirable, and this method should be able to compute all the bands together. Such an improvement not only reduce the analysis time of an image, more importantly, fractal dimensions can be compared across all the bands and suitable band or band combination could be selected for certain social and environmental analysis.

This research dissertation focus on some of the discussed issues in the literatures. A good and thorough review of fractal analysis on remote sensing can be found at Sun et al. (2006). The study area is focused at urban landscape and multispectral remotely sensed images are collected for the analysis.

Fractal methods comparison is a focus of this dissertation. In addition, measuring spatial complexity of urban area based on fractal dimension and exploring the effect of spatial resolution are two primary goals. Fractal dimension can be treated as a summary or average statistic, similar to other statistical quantities, when applied in geographic and spatial phenomena (e.g. remote sensing), a spatial information is necessary to be considered to explore the analysis extent of fractal dimension. Sun et al. (2006) discussed that computing local fractal dimension values is a desired future research direction holds a great potential for remotely sensed images. The following part is a brief introduction to the remote sensing and remotely sensed image.

3.2 Remote Sensing and Remotely Sensed Image

In earth science field, remote sensing technique possesses unique advantages for researchers to analyze earth surface phenomena. Remotely sensed images acquired from remote sensing technique are special pictures that human do not experience often in daily life. Remote sensing has been variously defined by many scholars throughout its development history. Campbell (2002, 6) examined previous definitions and proposed his version:

> remote sensing is the practice of deriving information about the earth’s land and water surfaces using images acquired from an overhead perspective, using electromagnetic radiation in one or more regions of the electromagnetic spectrum, reflected or emitted from the earth’s surface.

A central part of the definition is the collecting distant spatial objects without toughing them. Such a broad definition omits some other geographic phenomena. Remote sensing uses overhead instrument to sense the earth’s surface and result in an image structure consists of pixels. Remotely sensed image is the ultimate form that remote sensing brings to researchers. An image consists of pixels in a row and column format. Each pixel has a digital value in an integer format, which could be the most valuable information for researchers to examine remote sensed images. Different range of digital values associate with different land covers and this could be treated as the basis and guidance for remote sensing applications, especially the classification studies.

The history of remote sensing could be traced back to early 1800s. A crucial step is the first use of photograph to record earth surface's landscape, the instrument was carried in a balloon in 1858 (Campbell 2002, 7). Following this, many more instruments carried by balloon and kites were used to capture earth surface's view in a photographic technology. The disadvantage of using low altitude platforms is that they can only cover small extent of earth surface's view, which is impossible for studying spatial heterogeneity in a national level. Not surprising, these type of remote sensing aerial image were recorded for the experiment purposes as a starting stage of remote sensing technique. The first milestone of remote sensing was the introduction of the aircraft to carry digital cameras for recording earth surface's land areas in 1909. An airplane platform dramatically increase the altitude of the instruments to acquire remote sensing images, more importantly, it can collect landscape information in a systematic way. Airplane platform is able to record a large extent of land surfaces in a state or national level. Another milestone in remote sensing would be a use of satellite carrying sensors to digitally record earth surface's land covers. Landsat-1 is the first earth-orbiting satellite launched in 1972 aims at collecting broad scale of earth's land areas (Campbell 2002, 9). It was then followed by other similar and improved earth-orbiting satellites, which formed the mainly used group of platforms for collecting remotely sensed images for remote sensing research.

There are four types of resolution associated with remotely sensed image: spectral resolution, spatial resolution, temporal resolution and radiometric resolution. Spectral resolution relates to the techniques of sensors and satellites. Multispectral remotely sensed image is the most widely analyzed image data, which usually has seven spectral bands with different bandwidths and different colors ranging from visible to infrared bands. The more bands an image has, the finer a spectral resolution is. Hyperspectral remotely sensed image has the finest spectral resolution, which contains more than 200 spectral bands. Analyzing hyperspectral image is becoming a popular research area for remote sensers, it includes dimension reduction and optimal bands selection. Temporal resolution is the frequency of the image acquired by its sensors. The more frequent the satellite is, the more images of a same area will be covered. A fine temporal resolution enables the land cover change analysis on a remotely sensed image for the covered study area, especially for a fast landscape changing area. Radiometric resolution is a color depth configuration, which means the pixel value range for an image. Spatial resolution is interpreted as at what extent the detailed information of earth surface is available to human eyes. It is reflected by pixel size of an image and it can range from more than 100m to less than 1m. A coarse spatial resolution image fails to display detailed objects but can cover large area. This is beneficial for the global level study on change analysis, environmental assessment and monitoring. A fine spatial resolution image is able to show detailed objects and can improve the classification accuracy. Spatial resolution is related to scale analysis and scale is a crucial aspect of remotely sensed image (Benz et al. 2004). Relationship between spatial resolution, scale and fractal geometry is discussed in the following section.

3.3 Fractal Geometry Characteristics of Remotely Sensed Image

Remotely sensed images can be considered as a data source, which displays the complex physical and artificial phenomena. With the improvement of precise sensors, remotely sensed images become both spatially and spectrally complex. Detailed land cover texture and narrow bandwidth both enhance the complexity of an image. In order to better understanding remotely sensed images, it is necessary to develop advanced indicators with spatial complexity information involved to measure and extract land surface properties. Various landscape indicators have been developed to quantitatively examine remotely sensed images but very few take into account the information of physical structure of land covers. In this context, fractal geometry becomes an appealing tool for characterizing complex land surface patterns of remotely sensed images (Sun et al. 2006). Moreover, fractal analysis is still unfamiliar as a spatial analytical technique to remotely sensed images, even though fractal geometry holds great potential. It has been suggested that an extended employment of fractal geometry on remotely sensed image is needed, and it is also crucial for understanding the relationship between earth surface's landscape and spatial properties of remotely sensed data (Quattrochi et al. 1997).

Even though fractal geometry has been applied on spatial phenomena extensively, its use in remotely sensed images is still limited. Moreover, fractal geometry is necessary and suitable for analyzing remotely sensed images mainly because they share self-similarity property at different scales (Lam et al. 2002, Lam 2004, Sun et al. 2006). Self-similarity is the most fundamental characteristics of fractal geometry, and it is controlled by scale change. There is a linkage between fractal geometry and remotely sensed images by connecting scale and spatial resolution. The scale definition is discussed previously in Chapter Two. Spatial resolution is one of the fundamental characteristics of remotely sensed images (Townshend 1980). A spatial resolution of a remotely sensed image can be interpreted as an average square area a pixel covers on the ground (Benz et al. 2004). In this sense, for remotely sensed images, spatial resolution can be treated as the scale of the observations (Woodcock and Strahler 1987). Scale (i.e. spatial resolution) analysis of a remotely sensed image is important for several purposes such as scale effect on dynamic process of spatial phenomena and obtaining optimal spatial resolution. However, the spatial resolution has been limited decades ago since the lack of the availability of sensors. Nowadays, scale change analysis of remotely sensed images is becoming increasingly meaningful through the change of spatial resolution from finer to coarser. Woodcock and Strahler (1987) used local models to calculate spatial statistic values for the same study area with the change of spatial resolution to obtain the appropriate resolution for certain landscape patterns.

Researches have claimed that remotely sensed image is a fractal possessing a statistical self-similarity property (Lam and De Cola 2002). This indicates scale change of remotely sensed images within certain range will not affect fractal dimensions of the overall image complexity. Scale change of remotely sensed image is analogous to resample the image for acquiring other resolution values. Changing spatial resolution of a remotely sensed image is equivalent to the dynamic processes of forming a fractal at different scales, nevertheless the remotely sensed image is not formed in an exact recursive way. Not surprising, the fractal dimension value of a remotely sensed image continues to change until it reaches to the resolution range where fractal geometry characteristic falls. Not intuitive, the fractal geometry of a remotely sensed image for image complexity is not reflected in a form of physical shape. Instead, it is exhibited through the regularly distributed digital numbers and their impacts on neighbor cells. With the spatial resolution change, the landscape of an image will most likely look different at every stage, not in a geometric shape view, but in an image detail and complexity perspective. For mathematically formed fractals and some geometric format data, one obvious way to examine whether there exists a fractal geometry is to visually look at the physical structure dynamics with the scale change. For geographic phenomena and their remotely sensed images, the fractal dimension should be a constant for a certain landscape area. Nevertheless, resolution change changes the image structure and therefore affects the estimated fractal dimension values. Finding an acceptable resolution range of an image with no fractal dimension change (i.e. statistically significant) benefits the scale analysis for the image and it is becoming a favored research area for fractal geometry on remote sensing.

Besides the spatial resolution, spectral information is another research focus of a remotely sensed image. A spectral information is reflected by multiple bands, each band is a single image and they have the same spatial extent but different digital numbers. Characterizing spatial complexity based on estimating fractal dimension across spectral bands of remotely sensed images is a primary research of fractal geometry application on remote sensing (Lam 1990, Qiu et al. 1999, Chica-Olmo and Abarca-Hernandez 2000, Emerson et al. 2005, Liang et al. 2013, Mukherjee et al. 2014). These studies have transformed the original remotely sensed images to a newly derived image. NDVI image is one of the most studied derived images, which is a single grey scale image indicating a broad land cover spatial distribution and served as an important environmental indicator in general (Lam 2004). It is calculated by using the ratio between red and infrared bands and several land covers including urban landscape can be examined using fractal dimension. Besides NDVI bands combination, another widely used technique for spectral bands aggregation is principal component analysis (PCA). PCA is developed to transform redundant band information into three principal components, which are PC1, PC2 and PC3. The spectral information contained in all the multiple bands are treated as variance, and the goal of PCA is to transfer all the information into the three PC bands without any information loss. As a result, the first PC band contains almost 99% variance of the entire image. Instead of applying fractal geometry on all the spectral bands, only use the PC bands not only keep the important spectral information, but also make the fractal analysis more efficient. Chica-Olmo and Abarca-Hernandez (2000) calculated fractal dimensions for each of the PC bands, the fractal method is adapted from "structured walk" method. Hyperspectral remotely sensed image have attracted much attentions recently from fractal geometry since hyperspectral sensor is a group of sensors different than traditional multispectral sensors. AVIRIS sensor is the main source of collecting hyperspectral imagery and it is promising to examine the spectral variation of fractal dimensions. Results have shown that there is a clear fluctuation and several peaks of fractal dimension values across the entire 224 spectral bands for both the urban and rural areas (Figure 3.1).

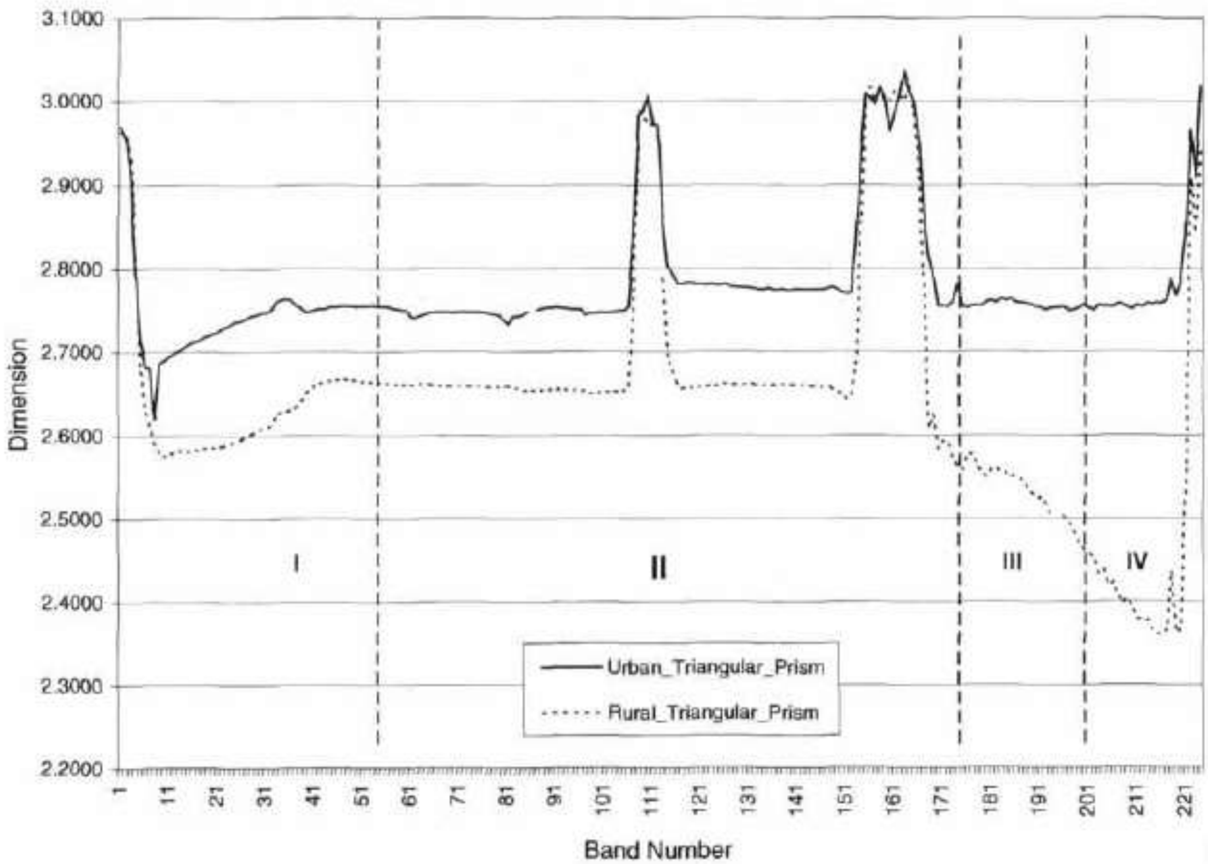

Figure 3.1 Variation of Fractal Dimension Values across 224 Spectral Bands (Qiu et al. 1999)

Remotely sensed image is highly related to fractal geometry characteristics. Previous studies have proved that the self-similarity property exists for the entire image within certain spatial resolution range. In addition, calculating fractal dimension values for the entire spectral bands also reveal a fractal geometry characteristic (e.g. Figure 3.1). Fractal dimension values stay the same in a statistical way for most of the bands, moreover, the variations across the spectral bands can help identify noisy spectral bands and select the appropriate bands for image classification, segmentation and other related image analysis (Sun et al. 2006). Fractal geometry application on both the scale and spectral analysis introduces a valuable spatial complexity information to the remotely sensed image, calculating a single fractal dimension value does not convey much information about the image, on the other hand, a dynamic analysis of the fractal dimension is desirable for researchers to truly understand fractal characteristics. Specifically, the analysis of fractal dimension should include a comparison between various spatial resolutions, a comparison between interested land cover types, a comparison between the available fractal methods and a comparison between the multiple spectral bands. Additionally, not limited to these, a relation can also be made through examining fractal dimension and temporal change on a remotely sensed image for the same study area for a temporal resolution study. It would be promising and encouraging to investigate the time series analysis of scale effect of fractal dimension on remotely sensed images and store the results in a matrix format. This process is particularly useful for urban sustainable development based on remotely sensed images where a fractal may exist for both urban form and an image structure.

3.4 Fractal Geometry and Spatial Statistics

The key ideas of fractal concepts are developed from a map data source, and continue to draw applications on spatial phenomena (Goodchild and Mark 1987). Map data is presented in a spatial way that position information is associated with each location. This is a crucial difference than the ordinary statistical data where the statistical data does not possess coordinates information. GIS data is a digital type of traditional map and it conveys wide variety of spatial characteristics. Fractal geometry analysis using GIS data in either a vector format or a raster format highly relates to spatial analysis. Goodchild and Mark (1987) claims that fractal ideas have some direct relevance to spatial analysis and it is necessary to undertake some reviews of the fractals to the spatial analysis in geography. They also state that fractals are themselves with the consideration of spatial data handling. Many early researches have attempted to use different types of fractal methods and applied to wide range of spatial and atmospheric phenomena.

Burrough (1983) estimated fractal dimension for soil data and compared with other environmental data as well as the Brownian fractals reference data. He concluded that soil data are fractals, not a strict fractal, and also implied that some bulking and block kriging method should be used to interpolate soil property values. Lovejoy and Mandelbrot (1985), Lovejoy and Schertzer (1986) used a fractal model to study rain and cloud, they concluded that the boundaries of rain and cloud on the earth ground possess a fractal property and this research settled the application of fractal geometry in meteorology. Lovejoy et al. (1986) took a network of worldwide meteorological stations as an example of highly spatially heterogeneous distributed phenomena and estimated an empirical fractal dimension of 1.75. They implied that meteorological stations network is a fractal set and the dimensional resolution is associated with geophysical statistics. Most of these early studies of fractal geometry mentioned remote sensing as an advanced measurement technique and implied some related issues such as problems in calibrating remotely sensed information and the importance of the mesoscale processes (Lovejoy and Schertzer 1986, Lovejoy et al. 1986). Similar contributions to the early studies of fractal geometry and geospatial analysis include Hubert et al. (1993), Olsson et al. (1993), and Anagnostakis et al. (1996), which provide a basic description of rainfall events and surface soils as spatial distributed natural phenomena using fractal and multifractal analysis. These studies reveal the fractal characteristics and suggest new spatial analysis ways on these physical events.

The early studies of the fractal geometry have mainly focused on various physical phenomena, which spatially distributed in a highly heterogeneous manner, especially the rainfall events have inspired many studies linking fractal geometry with spatial phenomena. The following briefly discusses the concepts of spatial analysis and spatial statistics which are widely used to quantitatively analyze various geographic phenomena, and the linkage between fractal analysis and spatial analysis is also reviewed. For traditional or aspatial statistics, the assumption behind this is that there is no variation across the study area. In other words, there is no spatial information attached to the dataset and the calculated statistic is the same everywhere. This is also interpreted as spatial stationarity and a static model is used to analyze these spatial relationships (Fotheringham and Brunsdon 1999). Stationarity is an essential concept not only in spatial analysis, but also to temporal analysis, where a stationarity model has the same parameters and result in similar statistical properties (e.g. mean and variance) across the entire study area (Lloyd 2010, 9). However, this assumption does not always hold true for spatial data and other geographic phenomena. The important distinction here is that spatial data contain both attribute and locational information while aspatial data only possess attribute information (Fotheringham et al. 2003, 3). The locational information is additional information and somehow the most valued property of spatial data. Space (i.e. places) is a key element in geography and often times treated to be of fundamental importance for the concern that people is interested to see what factors influence certain social phenomena (e.g. unemployment or soil erosion) (Lloyd 2010, 1). Different from stationarity, a process for analyzing spatial data over space can be called spatial nonstationarity, that is, a statistic result varies from place to place within certain scale range. In reality, it is impossible to observe any stationary processes across geographical spaces, which are controlled by intrinsic variations, and there is a crucial change in geography that focus has been switched from similarities to differences across space (Unwin and Unwin 1998, Fotheringham and Brunsdon 1999). Classical statistical methods in this case are favored to be replaced by spatial analysis methods and a new perspective of observing geographical data is therefore emerged and expanded.

In a spatial statistic, the locational arrangement of data values have an impact on the value of the statistic (Unwin 1998), and if the various data arrangements always generate the same statistical results then it is aspatial statistic. As previously mentioned, global statistics are a group of spatial statistical methods which use all the available data to calculate a single statistic to characterize the general trend of the variable itself. Representative examples include global mean, global variance, global autocorrelation and global regressions. A global statistic intends to characterize the entire region with the mutual locational relationship of the data values. A major category of the measurement of global statistic is spatial autocorrelation which is a general statistical property, and can be briefly defined as values of random variables taking pairs of locations, that departs from or similar to the complete spatial randomness (CSR) pattern (Legendre 1993, Lloyd 2010, 80). There are several commonly used global statistics for demonstrating the spatial autocorrelation. A global K function can be used to study the departure from a CSR point pattern and has been applied on Mediterranean subshrub of plant study (Ripley 1979, Haase 1995). A global nearest neighbor statistic is a simple and intuitive statistic to measure the spatial pattern of an event, it is based on contiguity relationship and can be applicable to wide range of geographic data (e.g. cancer mortality) with easy implementation (Hudson 2000, Rogerson and Yamada 2008, 43). Two of the most frequently encountered global statistics in GISystems literatures are Moran's I and Geary's C methods, which are formulated in a similar manner in a contiguity ratio way (Lloyd 2010, 81, 82). Both of C and I have been applied to various social and environmental phenomena including population distribution, epidemiology rates and species distributional data (Oden 1995, Waldhör 1996, F Dormann et al. 2007, O'Sullivan and Unwin 2014). Some other theoretical researches focusing on identifying extreme values, adjusting current methods and improving the test methods of these two statistics, as well as combining with other statistical methods (Jong 1984, Assuncao and Reis 1999, Li et al. 2007). An appropriate term for this process could be called global spatial statistical analysis.

Global spatial statistics have several drawbacks in spatial data analysis. Some of the properties and foundations were reviewed previously for global analysis but they are doubtful under geographic data analysis domain. Unwin (1996) pointed out three limitations of global statistics in spatial analysis. The main limitation is that a single global statistic fails to explain the real process and pattern of a spatial phenomenon, especially GIS and remote sensing techniques have the ability to store and display large extent and fine resolution spatial dataset, it is even more heterogeneous of the large area landscape and more likely that earth's surface exhibits diverse characteristics. A secondary limitation of spatial global statistic is that the calculation is subject to edge effect and a so-called modifiable area unit problem (MAUP), which is a fundamental problem of geographic analysis and exhibited for spatially aggregated data (Openshaw and Taylor 1979). Another important issue with global spatial statistic is the cartographic visualization purpose. A single global statistic value cannot be displayed in a map format, which does not take the advantage of the capability of cartography and geographic illustration. Exploratory spatial data analysis tends to use visualization as a direct approach to display the pattern of spatial phenomena and choropleth mapping has become a useful tool for displaying various parameters estimation results based on different color scheme, which can be synthesized by human eyes and brain (Unwin 1996, Fotheringham 1999, Goodchild and Haining 2004, Cromley and Hanink 2014).

The other group of spatial statistic is *local* statistics. Lloyd (2010, 4) reviewed that the term local can have multiple definitions in many disciplines. In physical geography, a local analysis could be some focal areas within a study are and this particular process has a noticeable effect. A landscape in geomorphology discipline may be considered as different land uses and spatial analysis could be carried out in each these land use areas. For socioeconomic study, a local analysis could happen in the neighborhood or particular districts with which individual or a group interact on a regular basis. In the field of spatial analysis, a local space could be treated as a distance from a focal point to its neighborhood points or areas. In use of local statistics, we focus on learning more for each individual location including point, line or area and comparing with neighbor values (Unwin 1996). The foundation and core principle of local methods is spatial dependence (Lloyd 2010, 5). Spatial dependence is also termed the "First Law of Geography", that is, objects are located closer tend to be more similar than objects located further apart (Tobler 1970). Spatial dependence indicates that spatial data is not independent and, the nearer the objects are located, the more similar the values they share. Objects with similar values located closer is termed positive spatial autocorrelation or strong spatial dependence, objects with dissimilar values located closer is termed negative spatial autocorrelation or weak spatial dependence. Fotheringham et al. (2003, 6) mentioned that local statistics are a set of statistical techniques which are spatial disaggregation of global statistics. There are some differences and relations between global and local spatial statistics (Table 3.1).

Table 3.1 Differences between Global and Local Spatial Statistics (adapted from Fotheringham et al. 2003, 6)

Global Statistics	Local Statistics
Summarize data for a whole area	Local disaggregation of global statistics
Single valued statistic	Multi valued statistic
Non mappable (GIS unfriendly)	Friendly (GIS friendly)
Aspatial or spatially limited	spatial
Emphasize similarities across space	Emphasize differences across space
Search for regularities or “laws”	Search for exceptions or “hot-spots”

Global and local spatial statistics vary in many ways. One of the main difference is the mapping purpose. The results of global spatial statistics cannot be analyzed within GIS environment. Global statistics generate one single value, which cannot be mapped using cartographic technique. As a result, the results of global statistics may only be presented in a table format and lack of a spatial display capability. On the other hand, local statistics are able to generate mappable statistical results, parameter values and can be further studied in a GIS environment. Indeed, spatial phenomena possess large amount of variation and it is essential to map the results for better understanding of the spatial pattern (Fotheringham et al. 2003, 7). Another difference is that global statistics try to capture a general trend or a universal rule for the spatial phenomenon. It is important, for certain applications, find a general rule or law is a first goal for other analysis to follow. In contrast, local spatial statistics tend to search for extreme areas or exceptions, which present some highest or lowest values of the spatial property, this process helps, identify particular local regions and relate to other factors to study the causes of this consequence.

Anselin (1995) proposed a new concept of local statistics, which is a general class of local indicators of spatial association (LISA). Spatial dataset becomes increasingly heterogeneous and largely available with the needs of using GIS to visualize the spatial characteristics. Moreover, it is claimed that a new group of techniques should be developed for exploratory and confirmatory nature (Anselin and Getis

2010). There are two definitions for a statistic to be considered as a LISA. One is that a LISA for each individual observation provides an indication of the clustering extent of similar values around that observation; the second requirement is that the sum of the LISA for all observations is proportional to the corresponding global indicator of spatial association. The concept of LISA is a fundamental idea for analyzing local spatial statistics and models for studying spatial autocorrelation and spatial association, and has been widely discussed in the literature (Unwin 1996, Fotheringham and Brunsdon 1999, Boots and Okabe 2007, Fotheringham 2009, Cromley and Hanink 2012). However, these literature focus on various aspects of LISA and relate to other concepts and methods, LISA has been related to GIS that incorporating LISA into GISystems may improve the functionality of local spatial statistics of GIS software, indicating the local spatial statistics can turn into GISable (Unwin 1996). Other studies mentioned LISA style to imply that some statistical methods and significant tests possess LISA characteristics, examples of this including a spatial version of the chi-square test developed by Rogerson (1999) and a spatial alternative of location quotients. The results of using LISA as an alternative method to examine spatial clusters can be evaluated by visual inspection, but can also be examined by inferential norms (Jacquez 2008). Another recent and similar concept was proposed by Boots and Okabe (2007), which is termed local spatial statistical analysis (LoSSA), a concept based on integrative structure of the existing methods. LoSSA is a framework for facilitating the development of both global and local spatial statistics. When developing a particular local spatial statistics, LoSSA can reveal some features and limitations including the nature of the datasets surrounding an observation, spatial relationship between a subset and the whole dataset, as well as the relationship between global statistics and the corresponding local one.

At this point, after review the concept and foundation of both global and local spatial statistics, the focus is switched to more details of local spatial statistics, which is a main part of this dissertation research. This section further review the principle for creating a local statistic and model. The construction of a local statistic and a local model depend on spatial dependence, and spatial dependence reflect on spatial nonstationarity, it is also claimed that creating a local analysis in this manner follows a logical way (Fotheringham 2009). Distance plays a crucial role for constructing local methods or adapting from global alternative. Calculating distance matrix between a focal point and neighbor observations is usually a first step for deciding the influence of each attribute. A widely used and a key approach to localization method based on distance is geographical weighting scheme (Brunsdon et al. 2002, Lloyd 2010, 24). This scheme is informed by spatial dependence that observations locating closer to focal point have higher weights than the further observations. Euclidean distance is the most intuitive and common notion for calculating distances between pairs of observations or focal points (Pinkse and Slade 1998, Dray et al. 2006). Besides Euclidean distance, other parameters would also be used based on empirical results to formulate local statistics in various manners. There are some other options of geographical weighting scheme based on distances but in a different weighting assignment. The existing geographical weighting schemes are listed in Table 3.2.

Table 3.2 Common Geographical Weighting Schemes (adapted from Getis and Aldstadt, 2010)

	Geographical weighting scheme
Contiguity-based weighting scheme	Spatially contiguous neighbors
	Lengths of shared borders divided by the perimeter
	n nearest neighbors
Distance-based weighting scheme	Inverse distances raised to some power
	Bandwidth as the n^{th} nearest neighbor distance
	Ranked distances
	All centroids within distance d
	Constrained weights for an observation equal to some constant

A local statistic consists of distances calculation and various geographical weighting scheme. With the attribute values distributed at the whole study are, many local statistics and models can be developed to perform local spatial analysis for diverse geographical applications. Global statistics and models are discussed previously. Similarly, widely used local methods are reviewed as well as the corresponding applications of spatial data. One of the most important outputs of local statistics is the mapping of spatial distribution and they are presented here for some examples to distinguish from global statistics results. Geographically weighted summary local statistics are a group of local statistics derived from mean, variance, standard deviation and skewness. Calculating of local summary statistics is intuitive and can be applied to almost every spatial phenomena for descriptive purposes. The most widely used geographically weighted variants of standard local statistics include geographically weighted mean and geographically weighted standard deviation. These local statistics have been applied to various situations include racial population distribution (Lloyd 2010, 76), housing price spatial pattern (Brunsdon et al 2002, Cromley and Hanink 2014), hydrology and surface waters (Harris and Brunsdon 2010) and atmospheric data of wind direction (Brunsdon and Charlton 2006). The results can be used for measuring spatial variation of the general values and in assist of calibrating spatial regression models.

Commonly used local statistics for measuring spatial autocorrelation are local G and G^* (Getis and Ord 1992), local Moran's I and Geary's C (Anselin 1995), together these popular local statistics focus on revealing various local clusters of spatial phenomena. Wulder and Boots (1998) employed local Getis statistic to measure the spatial autocorrelation of digital numbers of remotely sensed image. Goovaerts and Jacquez (2005) used local Moran's I to detect the clusters of high cancer mortality rate across space and time. Zhang et al. (2008) adopted the index of local Moran's I to identify pollution hotspots in urban soils. Some other applications of exploring spatial dependence using local statistics have also been widely discussed in the literature (Fortin et al. 1989, Ping et al. 2004, Tsai et al. 2009). Another important and broadly studied local statistic is geographically weighted regression (GWR) which is developed to measure spatial association between multiple variables in contrast to spatial autocorrelation (Brunsdon et al. 1998). GWR assumes the regression model parameters vary locally and multiple regression models can be generated over space for the spatial relationship. Different from global regression, the concept of local regression allows the exploration of spatial variation on each calibration location. Consequently, using subsets of the entire spatial dataset would be a simple solution for achieving the various spatial parameters combination (Lloyd 2010, 109). GWR have been extensively applied on broad fields to understand the spatial relationships between independent variables and dependent variable. One of the applications is to study the causing of limiting long-term illness within UK (Brunsdon et al. 1998). Another application includes the relationship between average rainfall altitude and gauge elevation over Great Britain (Brunsdon et al. 2001). Some other applications are the study of the relationship between level of China regional industrialization and various factors (Huang and Leung 2002), linkage between housing attribute price and some key variables in the housing market (Bitter et al. 2007, Cromley and Hanink 2014), and the connection of gross state output with capital and labour (Cromley et al. 2013).

Besides the reviewed local statistics and regression models, there are also some other local statistics and methods which have been developed specifically for some local measures. One of the examples is the development of geographically weighted colocation quotient, which is developed for measuring spatial interaction between categorical data such as housing types (Cromley et al. 2014). Another example is the local version of the Index of Dissimilarity, which can be used to measure spatial pattern of disparity such as spatial segregation and regional income inequality (Lloyd et al. 2004, Reardon and O'Sullivan 2004, Feitosa et al. 2007, Berentsen and Cromley 2013). In addition, a local variant of the K function (Getis 1984, Getis and Franklin 1987) have been applied to analyze spatial clusters of white-tailed deer habitats and clusters constrained to roads (Potvin et al. 2003, Yamada and Thill 2007). The selection of local statistics and models subject to spatial applications as well as scale consideration. It is encouraged to maximize the power of existing local methods and spatial data, and meanwhile generate innovative outputs (Lloyd 2010, 274). Two examples of local statistical results are provided below for the purpose of visual interpretation.

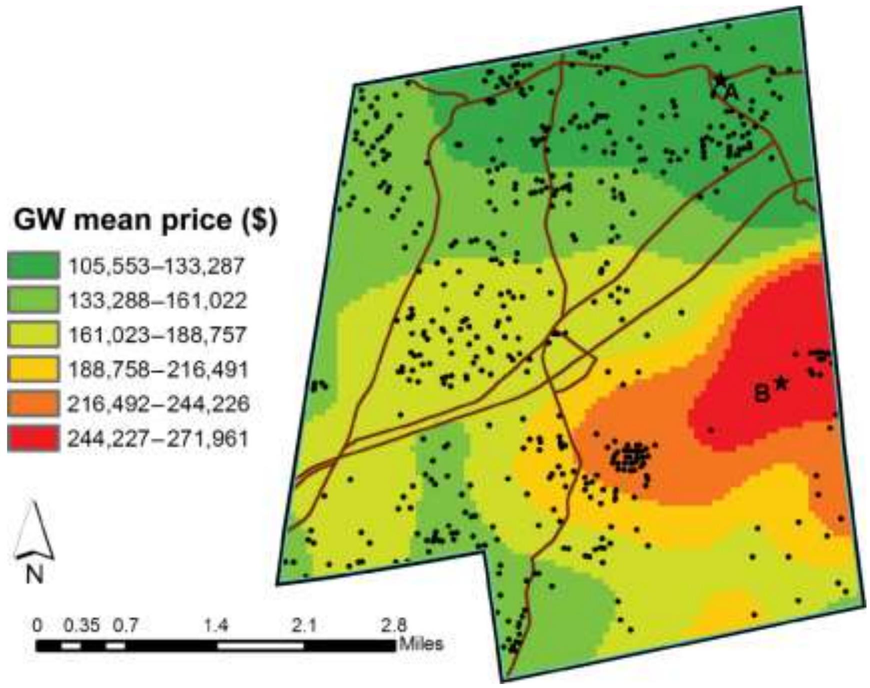

Figure 3.2 Geographically Weighted Mean of Housing Price (Cromley and Hanink, 2014)

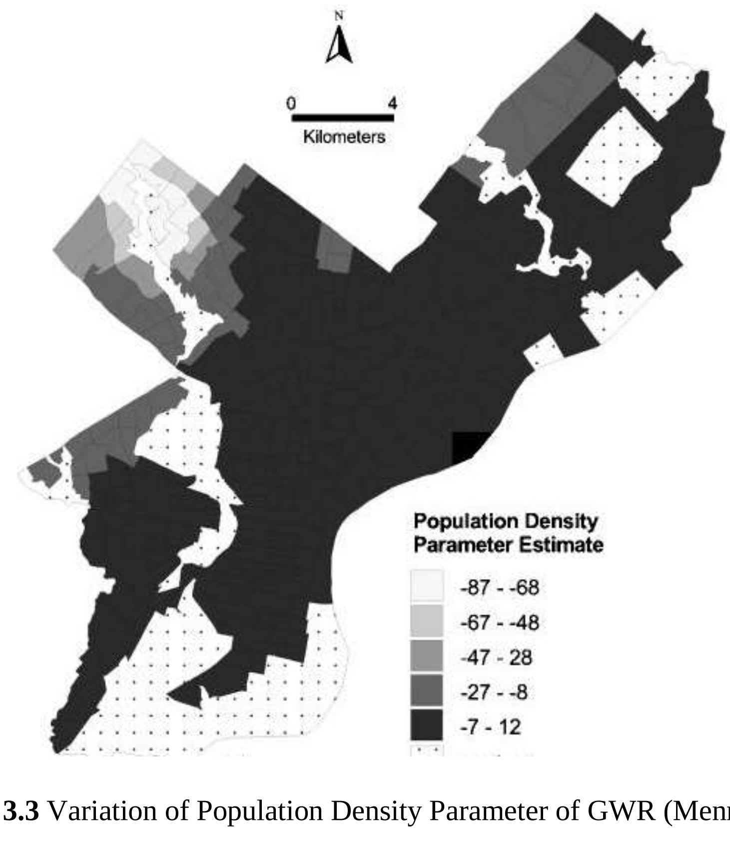

Figure 3.3 Variation of Population Density Parameter of GWR (Mennis 2006)

Many previous analysis of fractal methods focus on estimating one single fractal dimension values for the entire study landscape. Fractal analysis falls into the category of spatial global statistical analysis since the arrangement of data values affect the fractal analysis results and they use the entire dataset to measure the spatial complexity of a linear or surface landscape on earth. Sun et al. (2006) mentioned that estimating local fractal dimension values should be a next step research direction, which holds great potential for fractal analysis in remote sensing community. Local measurement of remotely sensed imagery mainly relies on moving windows technique. Queen's case and Rook's case contiguity are the basic three-by-three pixel moving windows for grid analysis (Cliff and Ord 1970). However, many different fixed sizes of moving window have been widely applied for neighborhood analysis to achieve local level results (Haralick et al. 1973, Thomas et al. 1981, Lee 1983). In addition, approaches with pixel weights and adaptive window sizes are studied as well (Chang et al. 2000, Sun et al. 2004, Harris et al. 2010). De Jong and Burrough (1995) employed a local fixed moving window technique to compute local fractal dimension values. In their study, they claim that local fractal analysis may inform us some valuable information of spatial pattern of the land covers in addition to global fractal dimension values. They modified the Triangular Prism Surface Area method to a local version by using 9 by 9 kernel moving window in consideration of computation time and number of points for fitting the regression line. The local fractal dimension method was applied to a TM image and the local fractal dimension ranges from 2.00 to 2.55 where rangelands have the lowest fractal dimension and agricultural areas have the highest fractal dimension values. The results prove that fractal dimension values vary locally for different landscapes as well as or different fractal methods.

There are few studies focused on developing local fractal methods to generate local fractal dimension for measuring landscape complexity. One issue associated with computing local fractal dimension based on remotely sensed imagery is that the size of the moving window affects the local fractal dimension values. Sun et al. (2006) claims that choosing an appropriate window size depends on two conditions. The first condition is large window size, which allows more regression points, but may cause many heterogeneous land cover types. The other one is a small window size covers homogeneous landscape with realistic local fractal dimension while it contains fewer pixels, which may be insufficient for regression technique. Using moving window technique of local spatial analysis to compute local fractal dimension is intuitive and straightforward and this needs great potential researches to develop approaches to couple local moving window with appropriate regression techniques to estimate local fractal dimension. However, only considering a moving window may cause some issues (e.g. blurring and boundary effect) which result in a map of spatial distribution of local fractal dimension values with loss of several edge pixels. An alternative method to compute local fractal dimension values is to employ geographically weighting scheme on remotely sensed imagery, which has not been tested. Geographically weighted scheme ensures that every chosen focal location can be visited without pixel loss, also all the pixel values can be assigned a weight to decide the local fractal dimension value. In addition, various bandwidths also play an important role for generating a comparison of the spatial pattern of local variations (Bucci and Franceschetti 1987, Gatrell et al. 1996, Fotheringham et al. 1998).

There are some previous researches relating fractal analysis to spatial statistics. Chica-Olmo and Abarca-Hernandez (2000) computed several image texture measurements including fractal dimension based on spatial autocorrelation concept using moving window technique to quantify the image data at a local level. Myint (2003) employed spatial autocorrelation statistics using Moran’s I and Geary’s C to analyze the image texture of urban landscape. Based on a discriminant analysis, the spatial autocorrelation technique is more favored than fractal analysis methods for urban land cover classification. Luan (2012) compared three fractal methods based on simple mean and variance to analyze the computed fractal dimension values. Liang et al. (2013) adopted coefficient of variation to measure the strength of the raw pixel relationship of five Landsat data and then perform fractal analysis. Some other similar literatures analyzed fractal dimension results using simple descriptive statistics and some measurements of spatial relationships (Palmer 1988, Lam 1990, Cheng 1999, Emerson et al. 1999, Lam et al. 2002, Sun 2006).

3.5 Results Visualization of Local Spatial Analysis

In geography and geographic information system environment, maps could be the most important interface to convey information to the public and an effective visual tool in communicating geospatial data (Chang 2015, 170). Maps are a necessary display method for transforming numerical results into a plane format with both a static and dynamic representation. A well-designed map is rich in data and can effectively transmit the information to map reader (Tufte and Graves-Morris 1983). One advantage of computing local statistics results is that researchers can map the computed statistical results or model parameters over the study area and use GIS cartography technique to present a spatial pattern. As the spatial statistical methods and models become popular, the numerical result itself becomes an intermediate step. How to effectively visualize the results according to their associated focal points remains a next level issue for spatial local analysis research. Furthermore, researchers are not only interested in plotting the numerical results over the extent of the study are, but also they are concerned with the cartographic techniques to improve the appearance of the spatial pattern of the local variations. Local spatial statistical analysis has been claimed to be a visual exploratory analysis and an effective mapping approach needs to be developed in order to allow people to explore the spatial non-stationarity property of the spatial data (Mennis 2006).

Cartography is defined as the making and study of maps for all their aspects (Robinson 1958). Cartographers have been using various formats of maps to visualize many kinds of spatial phenomena. No matter what type of map it is, cartographers always present a map by using symbols, colors, data classification and generalization (Chang 2015, 172). Among these map elements, researches mainly focused on two components for an informative map. One is the classification method for the local spatial analysis results, different classification method may yield different number of classes and range values. The other one is the color scheme associated with each class. There are some challenges relating mapping techniques, which needed to be resolved for better visualization. The main goal of mapping is to classify the numerical results into several groups to display a spatial variation of the results. The principle of classifying the numerical results is to minimize the difference within each category and maximize the difference between classes. In other words, the goal is to minimize variance within category and maximize variance between categories. ArcGIS packages offer several classification methods to users, which includes equal interval, mean & standard deviation and natural breaks, et al. Another challenge is the choice of color scheme for each category. There are various color schemes available over the years and a key rule among these color schemes is that map-readers can easily recognize the progress from low to high values (Antes and Chang 1990). Some of the color schemes are single hue scheme, the hue and value scheme, the diverging or double-ended scheme, the part spectral scheme and the full spectral scheme. The conventional cartographic technique mainly uses an equal step classification and a no-hue color scheme for mapping statistical and model parameter results (Mennis 2006). The equal step classification method, which classifies data into equal range, appears to be the most common data classification method (Dent 1999), especially the most appropriate method for uniformly distributed data (Mennis 2006). However, this may not be an appropriate approach for some non-uniformly distributed spatial data, and other classification method should be considered or developed as alternatives for normal data distribution or other data distribution. For the choice of color scheme, a no-hue color scheme assigns classes of intervals an increase of grey shade (Brewer 1994). Map-readers can perceive the gradual increase of the importance of the values based on the sequential colors. However, for some statistical results and statistical tests, the sign plays an important role as both the positive and negative values indicate the same importance (Huang and Leung 2002, Mennis and Jordan 2005), and a no-hue color scheme fails to convey the information of the significant statistical results.

Maps are classified into several types with different concentrations. One of the cartographic style is quantitative map, which communicates quantitative results such as city population, ratio between ethnic groups or salary ranking (Chang 2015, 172). The choropleth map is one type of quantitative map plots derived data onto administrative units using graduate colors. The calculated data are classified before mapping and a graduate color scheme is used to present the spatial variation. Therefore, the appearance of a choropleth map is affected by the classification strategy. Indeed, one main question regarding choropleth mapping is that the classed versus unclassed maps or it can be rephrased as how many classes are necessary to demonstrate the spatial data distribution (Cromley 1995). The ultimate goal of choropleth mapping is to class or unclass the unique parameter results for a better discrimination for map-readers. Cartographers often make several choropleth maps with different classification schemes and choose the best final map product. The simplest approach for data classification is an unclassed choropleth map on which each unique data with its color scheme is mapped. However, this process will result in many colors and symbols that makes it difficult to capture the spatial organization. Cartographers and geographers seek to develop several classification methods for applying to generate improved choropleth maps.

Choropleth mapping has been widely applied on local regression parameter estimations. Geographically weighted regression can generate multiple parameter results for each local area and choropleth mapping of the derive data is an important part for data exploration. Many researches have used choropleth maps to visualize spatial pattern of parameters results of both geographically weighted regression and quantile regression (Mennis 2006, Matthews and Yang 2012, Cromley and Hanink 2013, Cromley et al. 2013). Among all the classification methods, a natural breaks classification scheme is employed. Besides, researchers have also used simple mapping technique to combine parameters estimations with t-value in a single map for further exploration of spatial nonstationarity. On one hand, regression technique generates spatial data for choropleth mapping. One the other hand, choropleth mapping has also been applied to demonstrate spatial variation for direct social and economic data (Dixon 1972, Cromley and Cromley 1996, Berke 2001, Brewer and Pickle 2002, Poulsen and Kennedy 2004, Cromley et al. 2015). These spatial data includes crime data, population density, regional count data of red foxes, epidemiological and disease data, and birth rate data. All these data were mapped across spatial units using various data classification methods for a better understanding for map-readers. Table 3.3 shows a summary of commonly and newly used data classification methods for choropleth mapping.

Table 3.3 Data Classification Methods for Choropleth Mapping (adapted from Brewer and Pickle 2002)

Data Classification Method	Summary
Natural Breaks (Jenks)	Jenks optimization procedure, minimize within class variance and maximize between class variance
Quantile Method	Place equal numbers of enumeration units into each class
Standard Deviation Method	Middle class centered on the mean, classes above and below are 0.5 standard deviation (+-1 each time)
Minimum Boundary Error Method	Iterative optimization method, the only method considering data spatial distribution
Shared Area Method	Used ordered list of polygons ranked by data value to accumulate land areas in each class
Box-Plot Based Method	Middle Class centered on interquartile range
Hybrid Equal Interval Classification	An Improvement of Standard Equal-Interval Method
Concentration-based Lorenz Curve Method	A Concentration-based Approach using Lorenz Curve

Local fractal dimensions are derived across the study area, which is in a great need of choropleth mapping technique for visualizing the spatial pattern of how urban surface complexity varies over heterogeneous landscapes. Most of the current data classification methods can be applied to explore local fractal dimensions for map-readers, especially for city planners for a better perception of how neighborhoods of a city differ in terms of the fractal dimension numbers. A comparison of selected methods for visualizing local fractal dimensions could be carried out in this dissertation for generating several maps with different classes and map appearances. Scale effect is the main characteristic for fractals and it could be taken into account for relating with local fractal dimension values in one map to show a multi-level spatial organization of how scale affects fractal dimension. It is essential to explore choropleth map techniques for mapping local fractal dimension to better visually interpret the results. Moreover, mapping of spatially derived data can add additional insights into the spatial nonstationary process (Cromley and Hanink 2014).

Chapter Three can be separated into two parts, which is consistent to Chapter Two. The focus of this chapter is it covers the primary data source for fractal geometry application. Remotely sensed images nowadays as a public and easy access data source has many advantages for carrying out fractal geometry analysis. First, remotely sensed images possess spatial resolution characteristic, which is in consistency with self-similarity property in response to scale change for fractals. Changing resolution of remotely sensed images can generate a series of digital data where fractal analysis can be directly applied to test how the fractal dimension values change. Further, many remotely sensed images now available for urban area across the U.S, which makes it possible to compare the cities located in different areas using the fractal analysis. In addition, the availability of remotely sensed images ensures multi-time digital data can be accessed and tested for time series analysis. However, some other unique characteristics of remotely sensed images may affect the results of fractal dimension and are needed to be analyzed in addition to the standard analysis. One of the analysis is the information extraction from all the multiple spectral bands and then apply fractal geometry on the main band, which is called PCA. Overall, remotely sensed images provide a rich resource for fractal analysis on various aspects, and also fractal analysis can assist to identify more characteristics and issues for image analysis.

Applying fractal concept and estimating fractal dimension are connected with geographical and spatial data analysis. Another reviewed section of Chapter Three is the relationship between fractal analysis and spatial statistics analysis especially the local spatial statistics. Fractal analysis falls directly in spatial analysis category. The main property of the fractal analysis for geographical phenomena is statistical self-similarity that the fractal dimension will vary, but if they are within the acceptable range then the geographical phenomena can be treated as a fractal. There are very few researches address the fractal dimension results using hypothesis test methods and there is not a statistical distribution has been proposed for fractal dimension distribution. Some commonly used spatial statistical methods have been applied to compare with fractal methods for remotely sensed images analysis including classification analysis. The results show that the spatial statistical methods outperformed the fractal analysis methods when carrying out classification accuracy assessment. The previous studies have demonstrated that there is a great potential for relating spatial statistical methods and models to fractal analysis on analyzing remotely sensed images. Moreover, local spatial statistical scheme has not been widely studied for fractal analysis and it has been mentioned that there is a great need for developing new local methods for calculating local fractal dimension because earth surface exhibits heterogeneous landscape and local spatial analysis scheme can help reveal local variations of spatial nonstationarity. Many schemes have been developed for calculating local spatial statistics and the principle is to convert global statistics to its local version by using decomposition rule. De Jong and Burrough (1995) attempted to use moving window technique to calculate local fractal dimensions. However, some of the issues may be released using moving window including burring and boundary effect. Alternatives could be considered for using geographically weighted scheme to avoid missing pixels calculation. In general, there are much spaces for exploring local fractal dimension to add to the fractal analysis field, and furthermore, seeking local fractal dimension values could be treated as additional variable which can be used in regression analysis as an information about landscape complexity.

Chapter Four reviews existing fractal analysis methods for estimating surface geometric complexity. The theoretical background and estimation procedure are demonstrated and illustrated. Similarities and differences are discussed and compared. Some of the fractal models are reviewed through graphs. Moreover, geographically weighted scheme is reviewed and related to fractal models for local analysis. Some of the spatial analysis methods are also discussed for analyzing fractal dimension results. Chapter Four focuses on the major methods of this dissertation. All the mathematical models and formulas are discussed in the following chapter.

Chapter Four

Data and Methodology

4.1 Introduction

Mathematically constructed fractal objects possess strict self-similarity characteristics. People can easily compute the true fractal dimension for the mathematical objects by using the ratio function between length, area or volume and scale factor. The computation principle of strictly self-similar objects can be extended to estimate the fractal dimension for non-mathematical objects, or natural phenomena. Because of the roughness of the natural objects, estimation of fractal dimension can only be performed through an empirical analysis.

There is a large number of methods for computing fractal dimension for remotely sensed image for the image surface intensity. Sun (2007) collected six common methods for computing 3D fractal dimension based on satellite image. Every method has its own calculation process but they all share the same statistical relation between the measured quantities and the step sizes to derive fractal dimension. There are many researches dealing with applying these fractal methods and comparing between two or three methods results. It is important to systematically compare the computation results between the methods and also relate to a real fractal dimension value. There is a lack of research that brings together the methods for an exploration purpose, and also some of the methods have not been tested previously.

Chapter Four focuses on introducing the algorithm of the common methods for the estimating 3D fractal dimension for remotely sensed images. The methods are illustrated for the subsequent analysis using the remotely sensed images of city surface. First, the general process of acquiring fractal dimension for non-mathematical objects is outlined, followed by a demonstration of how to apply on remotely sensed image. Then it focuses on describing and illustrating the theoretical background of the chosen fractal methods. This dissertation research focus on three fractal methods for measuring the image surface intensity: Triangular Prism, Differential Box Counting and Fourier Power Spectrum methods. With the availability of the remotely sensed image, these fractal methods can be applied directly to calculate the image surface intensity using digital number value.

The fractal methods are followed by an introduction of the methods for developing local statistics. Several local schemes have been proposed for incorporating local information into the global statistics. This dissertation is mainly focused on employing the geographically weighted scheme, which is used to combine with the original fractal methods for the calculation of local fractal dimensions. The last part of Chapter Four presents the new developed local version of the fractal methods. Each fractal method is incorporated with the geographically weighted scheme in different manners.

4.2 Data

The focus of this dissertation is the comparison of fractal methods and exploration of calculating local fractal dimension. Therefore, the datasets in this dissertation serves as implementation purpose. The study areas of the datasets are not limited to specific area. Instead, several sample subsets of the original datasets are extracted to be used for the fractal analysis. To implement the comparison between these three chosen fractal methods as well as the idea of calculating local fractal dimension, this dissertation research consists of two different types of images: aerial photograph and Landsat remote sensing images.

Both of these two datasets are in raster format, which are appropriate for calculating fractal dimension. These two kinds of datasets have different ways of acquisition and therefore, they have distinct characteristics so that the results can be compared not only across methods but also between datasets.

An original aerial imagery is downloaded from the Center for Land Use Education and Research (CLEAR) which is a GIS data center at University of Connecticut (http://www.clear.uconn.edu/data/index.htm). The aerial imagery was captured in March of 2012 and it covers the entire State of Connecticut. The data used in this dissertation is an aerial photograph of New Haven area. This area is chosen because it is a large city located near Storrs, Connecticut. This 2012 Ortho Imagery of New Haven are composed of 4 bands, and representing colors of red, green, blue and near infrared. This original imagery covers an area of about 176.9 km^2 including Connecticut River and Yale University. Each band comprises a series of pixels containing digital number ranging from 0 to 255, with a spatial resolution of 1 foot. For simplicity, only the red band is used in the dissertation analysis, and several samples with various image sizes are extracted from the original image for the further fractal analysis in this dissertation.

Another dataset is remotely sensed imagery compiled from Global Land Surveys (GLS) which were created by NASA and U.S. Geological Survey. The datasets are terrain and geometrically corrected, with a consistent a period of time series of the same area across the globe. The Landsat data has a spatial resolution of 30 meters, with a Universal Transverse Mercator (UTM) coordinate system. The data used in this dissertation research are the GLS images of New York City, New York and Houston, Texas. Selected years are used for computing the fractal dimensions to see whether these two cities have undergone landscape changes as well as making comparison with aerial photograph in terms of global and local fractal dimension. For the GLS imagery, it is composed of several spectral bands and only the red band is used in the fractal analysis.

.

4.3 Mathematical Foundation of Fractal Geometry

The theoretical foundation of fractal geometry originates from mathematics and calculus. The mathematics of non-smooth objects worth a great deal of study because irregular objects provide a better representation of the geographical phenomena than the classical geometry. However, there are two sets of objects that can be described as non-smooth geometric shape. A mathematical object discussed in previous chapters of this dissertation represents a regular and strict fractal, which has a constant value of fractal dimension. The following part illustrates the theoretical background of how to acquire the fractal dimension for mathematical objects, and this can be treated as a basis for estimating the fractal dimension for non-mathematical objects.

Chapter Two outlined some of the common characteristics of the fractal geometry in general. Chapter Four continues to summarize some attributes, which serves the purpose of the explanation of the mathematical calculation for the true fractals, not limited, this mathematical background can also be extended to study natural phenomena. For mathematical fractals, besides the common features, we can also ascribe the following characteristics, in a more specific way (Falconer 2004):

- Object has a fine structure containing details at small scales. Visually the more we enlarge the picture of the object, the more texture and information we will see (either more gaps or more lines)
- Object is too irregular to be described using classical geometry terms, not only globally, but also locally.
- Although the mathematical object has an intricately detailed structure, its definition and measurement of fractal dimension are straightforward
- It is difficult to describe the local geometry of a fractal since every local part of a whole is connected with other large number of local parts, which makes the local measurement nearly close to a global one.

A basic representation of mathematically constructed fractal is shown in Figure 4.1. Different than the Cantor Middle Third Sets in Chapter Two, Figure 4.1 displays another common used true fractal object which is called the *Koch Curve*. The Koch Curve is constructed based on a strict recursive procedure. It is similar to the Cantor Middle Thirds Set that they starts with a straight line. The Cantor Set removes certain length of itself and continues to an infinite stage with a length close to zero and fractal dimension is between 0 and 1. In Figure 4.1, Let S_0 be a line segment of unit length, then the second stage S_1 consists of the four segments obtained by removing the middle one third from the whole first and replacing it at the removed segment by an equilateral triangle with two sides with a length of each side of one third of unit. S_2 is the third stage, and it is shaped by applying the same procedure to each of the segment of S_1 and this process continues to infinite stages. Each recursive stage is formed based on the last stage using the same construction procedure and when the stage N continues to a large number, the two sets S_{N-1} and S_N are closely similar and only differs in fine details.

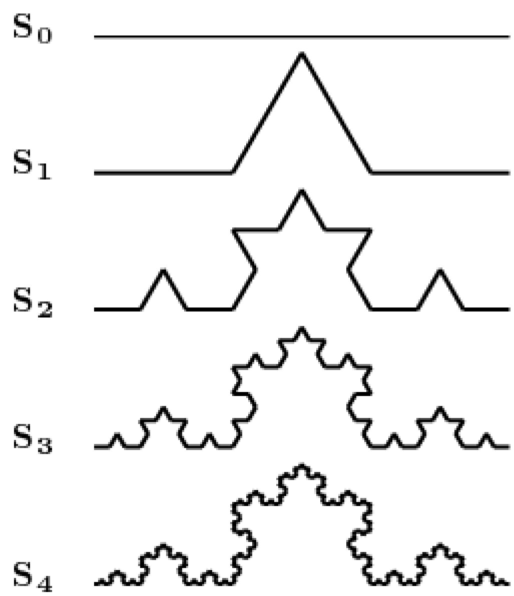

Figure 4.1 Construction of the Koch Curve
Source: Adopted from inspirehet.net

The Koch Curve approaches to a detailed and limiting curve, which is similar to the Cantor set and many other mathematical fractals. The construction of Koch Curve is simple and forms an intricate structure. Each quarter of the Koch Curve is similar to the whole but scaled by a factor 1/3. The length calculation of the Koch curve is straightforward and S_N is of length $(4/3)^N$ where N starts from 0 to infinity. However, the length of Koch Curve is not useful for describing the geometrical characteristic, neither the area because there is no meaning of area for Koch Curve as a 1-dimensional geometry. Based on the formula in Chapter Two, and convert it to remove the negative sign, we can have a more meaningful way of calculating the fractal dimension for mathematically constructed objects:

$$D = \frac{\log N}{\log 1/r} \qquad [2]$$

Where N is the number of copies by itself and r is the scale factor. For the Koch Curve, its fractal dimension can be obtained by using the above the equation that N is equal to 4 and r is equal to 1/3. The fractal dimension of Koch Curve is 1.2618, which is between 1 and 2 because it is a curve shape and occupies zero area in the plane. It is encouraging to compare the Koch curve with the Cantor Set since a Koch Curve represents a geometric shape of line approaching to fill the plane while a Cantor Set proceeds to unconnected dots with fractal dimension between 0 and 1. Another mathematical fractal based on the Koch Curve is called snowflake curve, which is formed by putting three Koch Curve together to make a symmetrically enclosed shape. It is clearly not adequate to describe a mathematical fractal using only one traditional geometric parameter, incorporating of fractal dimension, it is anticipated to use a set of parameters including traditional geometric descriptors and the fractal dimension to better interpret a true fractal.

Some of the fractals are not strictly constructed and may be randomly formed. It is not an equal chance to replace each side of the line segment. Figure 4.2 shows a random Koch Curve, that a coin is tossed at each step to determine either the above or below side of the line segment is to be replaced by the equilateral triangle. The random Koch Curve is not symmetrical and looks more intricate than the regular Koch Curve. The measurement of its geometric property is difficult that fractal dimension cannot be calculated using the empirical equation (2). This random Koch Curve is a fractal but possess statistical self-similarity property. In other words, the resemblance may seem weaker than the strict self-similarity, this could also be interpreted as approximate and statistical (Falconer 2004). The family of statistical self-similarity fractals can be seen more easily in the geographical environment and this dissertation research focused on studying them.

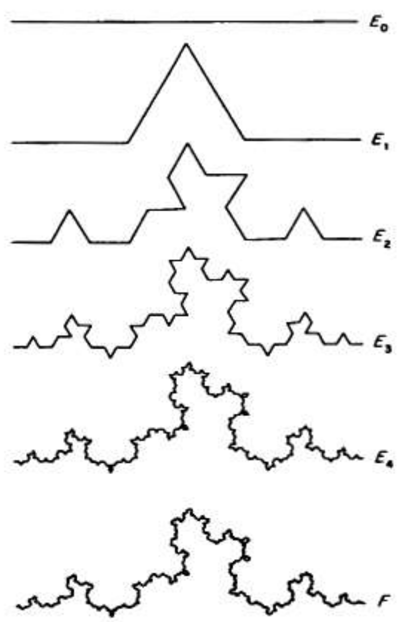

Figure 4.2 Construction of the Random Koch Curve
Source: Isaravia.github.io

The random Koch Curve represents one of the statistical self-similarity fractals which show some of the patterns that slightly deviate from the true fractals, and which share similar characteristics with the natural phenomena. The study of geographic features directly relies on fractal dimension and the calculation is based on equation (2) but needs more process since the natural phenomena does not possess the strict self-similarity and it does not have the same number of copies and scale factor at each step. Therefore, the fractal dimension of non-mathematical objects needs to be estimated empirically not analytically (Sun et al. 2006). A large number of methods have been developed to estimate the fractal dimension for natural objects based on the empirical equation. The fractal dimension calculation of geographic features consist of two measurements which are quantity and step size, the quantity is the length, area or number of cells and the step size is the scale or resolution change. In general, all the fractal methods used in this dissertation research have different quantity measurements but requires the same statistical relationship between the two quantitative results. The methods are also directly suited in applying on remotely sensed images. A common procedure for applying these methods for estimating fractal dimension for natural objects (e.g. remotely sensed image) consists of three steps (Sun et al. 2006):

- Compute the quantities of the object based on various step sizes
- Plot the log version of quantities against the log version of various step sizes and fit it through a straight line using univariate least-square regression technique
- Based on the slope of the regression line to derive the fractal dimension of the studied object

This procedure of estimating fractal dimension for natural objects is based on regression technique, which is an approximate method to obtain the desired result values. The reason for using regression technique is that the natural features are not constructed based on the same recursive procedure and the simple ratio equation is no longer applicable. The methods applied in this dissertation research are 3-dimensional methods for calculating surface features including the remotely sensed images. Sun et al. (2006) mentioned that a remotely sensed image can be viewed as a hilly terrain surface whose elevation value is proportional to the digital number value. Therefore, the digital number can be treated as a value that fills up in the volume above surface and can be used to extract 3-dimenstional fractal dimension for the earth surface feature. There is a number of methods for computing the fractal dimension for remotely sensed images, three methods have been selected because their wide application in remote sensing and low intensity of computation complexity. Moreover, these three methods have the similar calculation process of not using contour line or profile measurement. The methods reviewed in next section will be applied to several remotely sensed images of test images and city surfaces in the following chapters. Moreover, a new developed set of local fractal methods are tested.

4.4 Estimation Methods of Fractal Dimension for Surface Features

The Triangular Prism Method

The triangular prism method was developed by Clarke (1986), this is also known as triangular prism surface area method, and it is initially developed for calculating the fractal dimension of topographical surface. This method has been widely adopted to analyze the surface landscape complexity of remotely sensed images. Taking elevation or digital number of the image as input, Figure 4.3 illustrates the process of the calculation. This method decides an analysis window as a square box first, and then uses a, b, c, d as four corner digital number values to interpolate a central value e. This value is usually the mean of the four pixel values. The middle point divides the square into four triangles: abe, bce, cde and dae. In Figure 4.4, the 3D version of the triangular prism method, the top surface area is calculated by adding four triangles A, B, C and D. Geographically increase the step size δ, a relationship can be established between the total top surface areas and step size. Using univariate regression, a slope is obtained and the fractal dimension of the surface area can be derived from the slope. The relationship can be described as follows:

$$S(\delta) \propto \delta^{2-D} \qquad [3]$$

Where δ represents the step size and S is the total top surface area for the corresponding step size. The slope of the regression line is 2-D, then the fractal dimension is 2-slope. Triangular Prism method is not computationally intensive compared to other methods, and has been broadly applied to calculate surface complexity (Emerson et al. 1999, Qiu et al. 1999, Myint 2003, Luan et al. 2012, Liang et al. 2013).

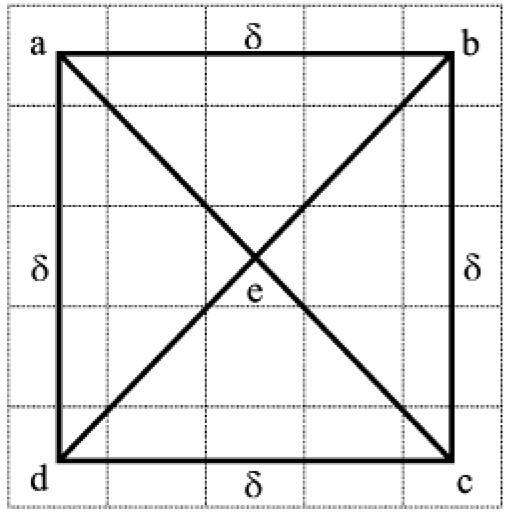

Figure 4.3 Plane View of Triangular Prism Method (Sun et al. 2006)

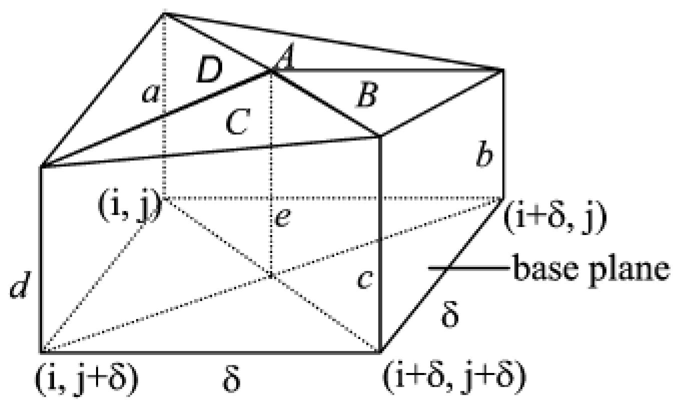

Figure 4.4 3D View of Triangular Prism Method (Sun et al. 2006)

Another three variations of the triangular prism methods are also included in this dissertation for a comparison with other fractal techniques. These three versions: the Max-Difference method, the Mean-Difference Method and the Eight-Pixel method are based on the original triangular prism method (Sun 2006). These three proposed new versions are inspired by the structure of the triangular prisms but focus on adopting more rigorous ways for constructing the triangular prisms. In general, this modification causes two changes to the original method. The first is that all these three variations use the actual digital number of the center instead using the mean DN values. The second modification is, instead of using the

DN of the four corners, they use different positions of the "corner pixels" to form the triangular prims, and this is the main improvement for these three methods.

The Max-Difference method takes all the edge pixels and calculate the difference with the actual DN of the center, and then select the edge pixels with the largest deviations for each edge. In this way, it captures more details of the difference between the edge and central pixels, in other words, this selection procedure captures the largest DN differences, which can be interpreted as covering the actual surface elevation. The Mean-Difference method performs similarly with the Max-Difference method, instead of using the four edge pixels with the maximum differences to the central pixel, it considers the edge pixels whose DN values differences with the central pixel are the closest to the mean differences of all the edge pixels. The Mean-Difference method, however, does not consider the highest elevation contrast, but utilize the average elevation difference to represent the triangular prisms. The third method, other than using four edge pixel for a square, similar to the original method, it uses the four corner pixels and four middle pixels together to construct triangular prisms. In this way, it could be better to approximate the image surface because eight pixels are taken into account with more details. The first two methods rely on searching the specific edge pixels following predefined rules while the third method is based on the number and the position of the edge pixels. These three modified versions along with the original triangular prism method are applied to the dataset in this research especially to examine the local version of each.

<u>Differential Box-Counting (DBC) Method and its improved version</u>

The improved differential box counting method is used in this dissertation. However, it is important to include the original box counting method first. The Differential Box-Counting (DBC) method was proposed by Sarkar and Chaudhuri (1994) for estimating the fractal dimension of image (Figure 4.5). In the case of a remotely sensed imagery with $M \times M$ pixel size, each original pixel will be divided by s where $M/2 \geq s > 1$ and s is an integer. The original image will be seen as scaled down image with new number of grids. A ratio of $r=s/M$ will be acquired. Then using the grey level range of the image which is denoted as G, s' is calculated by using G/s'=M/s. Now, a vertical set of boxes with size s×s×s' can be acquired for each grid and the number for the boxes is counted starting from 1. For the (I, j) th grid, the grey level of the pixels will be displayed as intensity surface and intersect with the set of boxes. The minimum and maximum grey level will intersect with two different counted boxes noted as k and l, respectively. Then we have the following equation:

$$n_r(i,j) = l - k + 1 \qquad [4]$$

For all the grids:

$$N_r = \sum_{i,j} n_r(i,j) \qquad [5]$$

Different r will generate different quantity of N_r, the log form of $N_r$and 1/r will be fitted a linear line using univariate regression technique and the fractal dimension is equal to negative of slope. The regression relationship is as follows:

$$N_r \propto (\frac{1}{r})^{-D} \qquad [6]$$

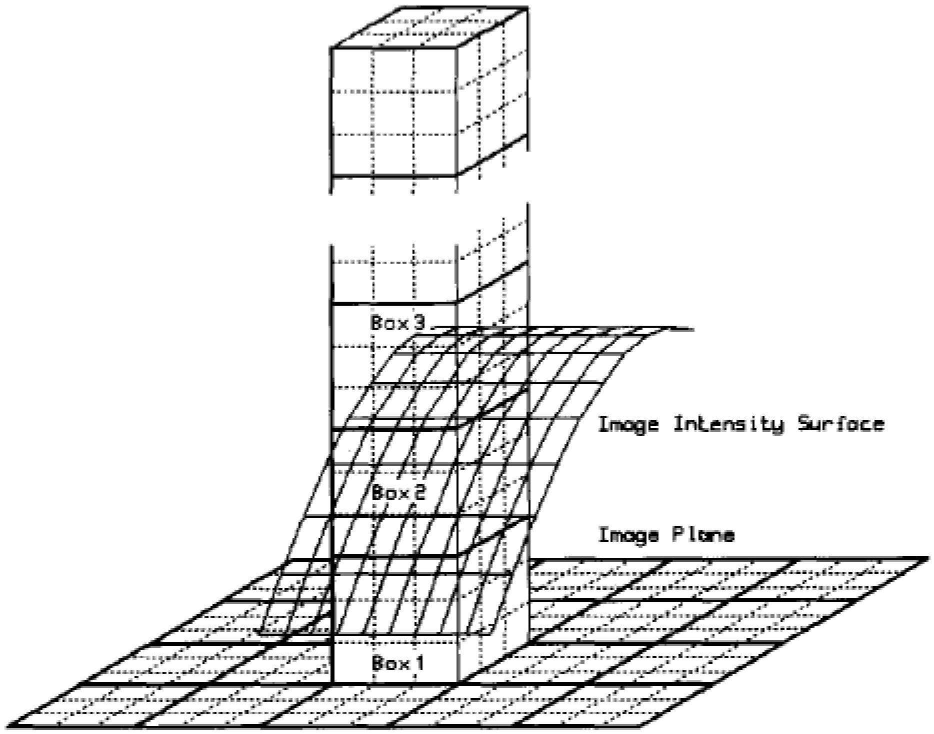

Figure 4.5 Calculation Illustration of Differential Box-Counting Method (Sarkar and Chaudhuri 1994)

One improved version of differential box counting method is adopted in this research. Three major problems were identified from the original method and the modified version tends to improve the estimation accuracy of fractal dimension. The improved differential box counting method is similar to triangular prism method as they both measure the quantity directly from the image data and constructs the quantity in a 3D manner. The improved differential box counting method can be implemented in the following steps. First considering an M by M image and partition the image into blocks with s by s size. In the improved version, we consider the blocks to be overlapped with each other by one row or one column. We will have a scale parameter r equals to s -1. Then the box height for each block is selected as:

$$r' = \frac{r}{1 + 2a\sigma} \quad [7]$$

where $r' =$ the box height for each block;

$a =$ a positive integer number;

$\sigma =$ the standard deviation of the digital number of the image;

$r =$ the scale parameter of each block.

A column of boxes with scale $r \times r \times r'$ are acquired and used to cover each block. The quantity of box counting is decided as follows:

$$n_r(i,j) = \begin{cases} ceil\left(\frac{l-k}{r'}\right), & l \neq k \\ 1, & l = k \end{cases} \quad [8]$$

where $n_r(i,j) =$ the number of boxes needed to cover the (I, j)th block with scale r;

$l =$ the maximum digital number in (I, j)th block;

$k =$ the minimum digital number in (I, j)th block.

The function ceil (.) indicates that the division result round to a nearest and greater integer. Considering contributions from all blocks for scale r, the total box counting number is:

$$N_r = \sum_{i,j} n_r(i,j) \quad [9]$$

Plot the log of N_r and r with least squares regression and the fractal dimension is equal to the negative slope of the fitted straight line.

Previous researches have been mainly focusing on comparing the following three methods: triangular prism, variogram and isarithm method, since only these three methods have been incorporated into an analysis software package known as the Image Characterization and Modeling System (ICAMS), which is a GIS software module, used for measuring the fractal dimension for remotely sensed images (Quattrochi et al. 1997). Most studies have tended to compare fractal dimension results between these three methods based on remotely sensed images with various spatial resolution (Qiu et al. 1999, Emerson et al. 1999, Lam et al. 2002, Myint 2003, Liang et al. 2013). ICAMS provides researchers these fractal methods to be conveniently implemented to study the raster format data. Among the studies, the triangular prism method is the most widely adopted fractal method since almost every literature mentioned using it with one or two other methods. This research dissertation also decides to use the triangular prism method for its easy computation complexity. Lam et al. (2002)'s studies have shown that triangular prism method can produce accurate fractal dimension results for highly complex surfaces, and meanwhile, the variogram method performed poorly for all the tested surfaces. Liang et al. (2013) concluded that the triangular prism method holds the greatest potential for future research on urban change detection based on the experiments that this method yielded the lowest fractal dimension values. Their studies found that the variogram method produced some unrealistic values as the fractal dimensions exceed the upper limit of 3.0. Fractal algorithms have also been applied to hyperspectral remotely sensed images for method comparison purpose. The advantage of using hyperspectral data is that there are numerous spectral bands can be tested and it is more likely to reveal extra information of suitability of the applied methods. Qiu et al. (1999) applied both triangular and isarithm methods to examine the entire 224 bands of hyperspectral image and disclosure that triangular prism method is more sensitive to image noises than isarithm method, on the other hand, isarithm method is robust to image contrasting for generating high fractal dimensions.

This dissertation does not employ isarithm method since its principle relies on that the contour lines can be used to approximate the complexity of a surface. The methods selected in this research dissertation share the similar characteristics of calculation procedure using the direct DN values to extract fractal dimensions from a remotely sensed image. However, the isarithm method constructs isarithm lines (i.e. contour lines) on the image surface and a length is calculated for each of the contour line based on the neighborhood number of cells. This method computes a length quantity using the number of cells instead of directly computing the DN values. Furthermore, as described above, many researches have studied isarithm method and have included it in the method comparison.

Given the focus of this dissertation on the exploration of fractal methods, it is central to switch attentions to other methods and compare the fractal dimension results for a broad understanding. This research dissertation employs the differential-box counting method for the comparison purpose to add some new information to the fractal methods comparison studies. Sarkar and Chaudhuri (1994) proposed the differential-box counting method and compared it with other three methods. The findings of the comparison showed that the differential-box counting method is an efficient method and can produce accurate results. Furthermore, some modifications have been applied to the original method for an accurate estimation (Buczkowski et al. 1998, Theera-Umpon 2002, Liu 2008, Li et al. 2009). All these modified version of differential-boxing counting method based on the principle of using the smallest number of boxes to cover the image surface at each scale for estimating precise fractal dimensions. The experiments tested the modified methods on various images including the synthesized fractional Brownian motion images, texture images and remotely sensed images, the results proved that the improved methods outperformed the original methods of differential-box counting. Many disciplines have received attentions from this method including the applications on remotely sensed images (Myint et al. 2006, Marghany 2009, Tzeng 2012). Its broad data sources containing high resolution image, hyperspectral imagery as well as radar dataset. The focus still remains on the development of novel differential-box counting method serving the general purpose of improving the classification accuracy as well as for detecting specific land cover types and natural phenomena.

The Fourier Power Spectrum Method

Fourier analysis is another technique, which can be used for computing the fractal dimension of surface. This method is selected in this dissertation is because the Fourier analysis technique represents another category of the fractal methods for computing fractal dimension for surface feature (Sun et al. 2006). The first category for fractal methods is the methods, which directly use the derived information from the image and perform the log-log regression to obtain the fractal dimension. On the other hand, the second category methods require a more sophisticated data preprocessing step than the first category and the fractal dimension is acquired based on secondary derived information from the original image. In this dissertation, the triangular prism and differential box counting methods belong to the first category and the Fourier power spectral density approach fits into the second category.

The Fourier power spectral density approach consists of several steps to derive a fractal dimension. The first step is to perform a two-dimensional discrete Fourier transform on an N by N image in order to extract an array of complex coefficients which are obtained by the following equation:

$$H_{st} = (\frac{L}{N})^2 \sum_{n=0}^{N-1} \sum_{m=0}^{N-1} h_{nm}\, e^{[-\frac{2\pi i}{N}(sn+tm)]} \quad [10]$$

where H_{st} = the complex coefficient array corresponding to each original digital number value;

L = the linear size of an equally spaced grid;

N = the size of the grid image;

n, m = the index of each pixel in the original image;

h_{nm} = the digital number values of row n and column m;

N = the length or size of the image;

s, t = the transformed index of the complex coefficients.

Then each transformed complex coefficient is assigned an equivalent radial number using the following relation:

$$r = (s^2 + t^2)^{1/2} \quad [11]$$

For two dimensional cases for Fourier transform, the mean power spectral density is derived based on the following equation:

$$S_{2j} = \frac{1}{L^2 N_j} \sum_{1}^{N_j} |H_{st}|^2 \quad [12]$$

where S_{2j} = the mean power spectral density for each radial wave number;

N_j = the number of the complex coefficients

satisfies the condition that r is greater than j and smaller than $j + 1$.

Notice that the summation is performed over all the complex coefficients in the condition. For a fractal distribution, the relationship between mean power spectral density and the radial wave number is as follows:

$$S_{2j} \sim K_j^{-\beta-1} \qquad [13]$$

Given the log-log relationship, acquiring the slope value of the regression, the fractal dimension of surface features can be calculated using the following equation:

$$D_2 = \frac{7-\beta}{2} \qquad [14]$$

4.5 Geographically Weighted Scheme

The main contribution of this research dissertation is to adapt the global fractal methods to corresponding local version, as it is essential to explore the local variations for earth surface landscape. Therefore, local adaptation approaches are needed to transform stationary method to its local form. There are many approaches have been proposed for local methods development. As discussed above, the moving window technique is one of the popular approaches often used on grid data. For remotely sensed image, it is intuitive and convenient to apply moving window approach for calculating local results. The window size determines the analysis boundary for the local analysis and the commonly used window sizes are 3 by 3, 5 by 5 and 7 by 7. The global method is repeatedly calculated at each studied window area. As a result, many global statistical results are computed for the entire grid image and each global value is treated as a local value compared to the rest of the global results. This dissertation is aimed at adopting an alternative approach for developing local statistical results for gird data, geographically weighted scheme, to address the issue of local variations of fractal dimension.

A geographically weighted scheme is a widely used approach for introducing local variations to the global methods (Lloyd 2010, 24). The core principle of geographically weighted methods is that it incorporates spatial information and it adjusts the traditional weight of one to a nonstationary value for different locations. Prior to the adoption of the geographically weighted scheme, a focal location is selected and it is the location of each point or the centroids of the polygons. Then a geographically weighted statistic will be calculated for each focal location. This method treats distances as the main factor and calculates spatial weights based on various schemes. Besides the distance factor, a bandwidth is also crucial which has direct influence to the calculated results. A bandwidth can be treated as an operational scale or scale of action, which indicates the spatial extent that certain processes operate in the studied area (Lam 2004). Changing the bandwidth results in different distance decay profiles, which will affect the local estimates varying over space (LeSage 2004). For remotely sensed image, a bandwidth can take from several to hundreds of pixels. Based on various weighted scheme, along with the distance and bandwidth, the calculated geographical weight is between 0 and 1, where 1 indicates a strong impact and 0 means weak impact to the focal location, respectively. However, for certain applications, instead of using distance representation, a spatially contiguous neighbor scheme may be adopted for simple calculation of weights (Getis and Aldstadt 2010). This typically well-known scheme is based on topological relations between two observations and simply assign weight of 1 to the nearest n^{th} observation and 0 to the other observations.

This dissertation focus on using distance-based weight scheme, and using a Gaussian kernel scheme to attempt to calculate local fractal dimension. A Gaussian distance weighting scheme is based on a Gaussian kernel function which is constructed by using distance and bandwidth parameters (LeSage 2004). The Gaussian kernel scheme used in this research can be formulated as follows:

$$W_{ij} = \exp[-0.5(d/b)^2] \qquad [15]$$

where W_{ij} is the weight between focal location I and observation j. d is the Euclidean distance between focal location I and observation j, b is the bandwidth of the kernel. The Gaussian function illustrates an exponential decay relation with the distance increases. When the distance is zero, the weight will be one indicating a full weight because the observation overlaps with the focal location; when distance increases to a very large value, the weight approaches to zero indicating the observation has no impact on the focal location. Another situation is that the weight equals to 0.61 when the distance has as the same value as the bandwidth. The spatial weights dramatically decrease when the distance becomes larger than the bandwidth. Empirical experiences decide the negative constant parameter and the default value is -0.5. Another factor of Gaussian kernel function is the selection of kernel types. The most commonly used kernel types are fixed kernel and adaptive kernel functions. The fixed kernel function used a constant value of bandwidth and a changing number of observations for each focal location. On the other hand, the bandwidth varies in order to fix the total number of observation count for each focal location. Comparison between fixed and adaptive kernels has been examined in various geographical data applications (Guo et al. 2008, Cromley et al. 2013). This dissertation focuses on applying fixed kernel function and comparing local fractal dimension by using selected bandwidths. An example of Gaussian function using fixed kernel for calculating spatial weights is illustrated in Figure 4.6. Three bandwidths are selected for comparison: 5m, 10m and 15m.

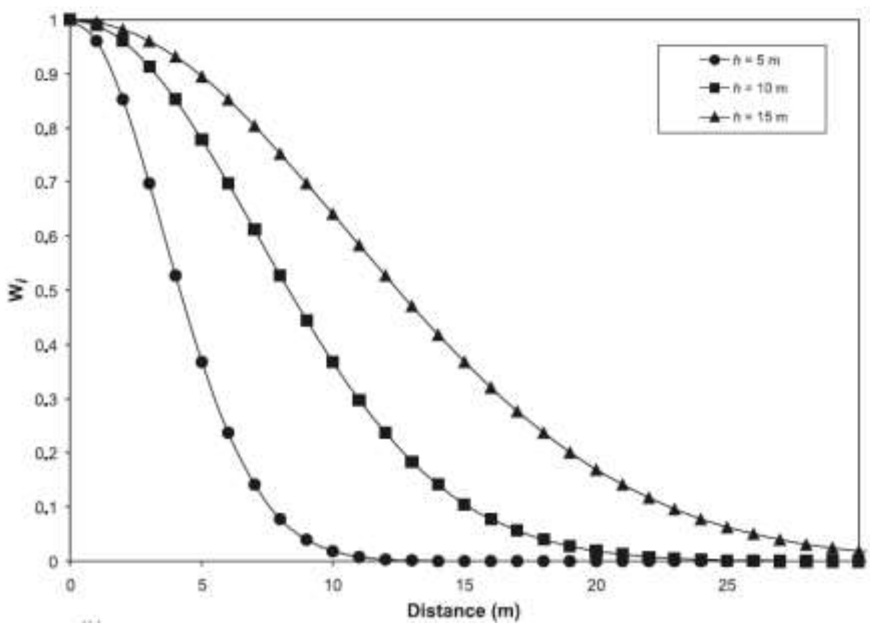

Figure 4.6 Comparison between Various Bandwidths of Gaussian Weighting Scheme (Guo et al. 2008)

For remotely sensed data with regular lattice pattern, a suitable method for applying local models is to use a moving window, which is defined by various window sizes. Taking 7 by 7 window as an example, despite the function we use, for a specific focal location, only the observations in the 7 by 7 window are taken into consideration for calculating a local value. This local method does not provide sufficient information for a focal location because not all the pixels are used. A Gaussian kernel function calculates distances between all the observations and focal location, and generates a full set of weights. In this case, the local adaption based on Gaussian function uses all the observations, which provide more observation information than moving window technique. The advantage of the Gaussian function is that it not only considers the neighbor observations, but it also considers the rest observations as a decisive part. Gaussian function has not been widely applied on remotely sensed data, and it is intuitive to apply it since each pixel can be treated as a point data. Focal location can be selected as pixel location and the distance calculation is more convenient because of the regularity of the arrangement of the pixels. Given the focus of this dissertation on estimating local fractal dimension, not on applications of fractal analysis, the exploration of the effect of various fractal analysis methods becomes important, and the estimation of local fractal dimension is the core concentration of this research. In order to achieve the research goals, the Gaussian weighting scheme is combined with the three local analysis methods mentioned previously, in this way, this dissertation proposes three new methods for estimating local fractal dimension on remotely sensed images.

4.6 Estimation Methods of Local Fractal Dimension

In order to extend the basic global methods for computing local fractal dimension, the three global methods presented above are the basis here and the Gaussian weighting scheme is used here for achieving the goal of the extension. This extended approach is aimed at assessing the nonstationarity of landscape complexity through the study area and the functionality of using the geographically weighted scheme which is widely used in many global methods but have not been tested for the methods of fractal analysis. The computation of local fractal dimension can be quite complex due to the lack of previous attempts and consideration of the computation scale for the local analysis. This becomes increasingly true when applying on remotely sensed images because there are various types of spatial resolutions. The most intuitive way for obtaining local value of fractal dimension is to partition the entire image into several subparts and apply the global methods to calculate the value separately. However, for a coarse resolution image, the small parts could still covers a very large land space and the landscape could still be complex that a single local fractal dimension value may still fail to explain the phenomenon.

Recalling the moving window technique presented above in this dissertation, it is similar to the image partition approach that the only factor considered here is the window size. The computation scale is restricted by the window size that the local value of fractal dimension may lack of significance due to the possibility of having a large window size with a coarse spatial resolution. Even more, in order to acquire sufficient training data for regression in the estimation methods for fractal dimension, a large window is usually considered to make sure the method can at least compute results for specific partitioned area. In order to satisfy the computation procedure, it has to compromise to cover ample pixels which means a large and heterogeneous land covers. In a Gaussian function based methods, the computation scale can be targeted on a single pixel which is the finest operating scale for a raster data format. With either high or low spatial resolution, Gaussian function can perform the same procedure on a single pixel for acquiring a fractal dimension value. A coarse spatial resolution image may still result in a complex land cover for a single pixel but this is the ultimate scale for a local fractal dimension. Although this single local value may not be representative for this specific land cover, it has been improved from the traditional moving window technique in terms of the computation scale for local fractal dimension. For a very fine spatial resolution image, neighbor pixels may exhibit similar landscape complexity (e.g. region of lake), so the local value of fractal dimension will be statistically the same for this specific area. It does not seem worthy for presenting the local value in such detail but it is valuable for assessing the land cover types by recognizing a gathering of similar fractal dimension values. The geographically weighted scheme (Gaussian function) has the advantage of aiming at the smallest distinguishable parts (i.e. the measurement scale) of an object and using all the observations for contributing to the estimation of a local fractal dimension (Tobler 1988, Lam 2004). In this dissertation research, the measurement scale refers to pixels in a remotely sensed image which is the main dataset used here.

The proposed methods for the dissertation research are three adjusted approaches for computing local value of fractal dimension. Each of the three methods discussed above is adjusted to a local version of itself, by using Gaussian function, respectively. The selected three estimation methods are all suited for modifying to a new version and forms three new estimation methods which has not been developed previously. The general formula of a Gaussian-based methods for estimating local fractal dimension is as follows:

$$\ln[Q(x,y)] = a(x,y) + b(x,y)\ln SS \qquad [16]$$

where ln is natural log transform, Q is the quantity of the object under consideration, (x, y) is the coordinate of the focal location for local fractal dimension, a and b are the intercept and slope of the regression line, respectively, SS is the various step sizes. As discussed above in the global version, the local version based on the same formation of the global methods, incorporating a coordinate of a focal location and a weighting function. The general regression rule has not changed, the dependent and independent variables are various quantities and step sizes, respectively. The differences occur within the three methods in terms of the quantity measurement and relation between slope and fractal dimension. In fact, the fractal dimension mentioned here is recognized as a local value.

<u>Local Triangular Prism Method</u>

This section introduces the local version of the three selected estimation methods for computing fractal dimension. The first method is the Triangular Prism method which we name it the local Triangular Prism method here. Previous section presents this method focusing on the measurement quantity and the global estimation procedure. The measured quantities of this method are the total top surface areas and they plot against the step sizes to form a least-squares regression line. In the corresponding local form, based on the Gaussian function, the spatial weights are constructed on the surface areas. For a remotely sensed image, the original input are the digital numbers of the pixels and these values stay unchanged because these are not observations for the estimation method. The top surface areas are the observations since they are used directly in the regression. Therefore, the spatial weights are placed on the surface areas for specific focal location. First the Euclidian distances are calculated between a focal location and each of the center pixels. The center pixels are the central locations for the triangular prism. In other words, the central pixels are the actual locations for the observation (e.g. top surface area). The calculated distances can be used in the Gaussian function to compute spatial weights for each observation. Then the summed top surface areas multiply their corresponding spatial weights to result in a series of weighted areas. On the other hand, the step sizes stay the same and not weighted. At last, this procedure is repeated for other step sizes in order to construct a series of weighted summed areas (i.e. dependent variable) and step sizes (i.e. independent variable) for establishing the linear regression. Once the least-squares regression is performed with the weighted area, the fractal dimension equals to 2 minus the slope. This fractal dimension explains the land surface complexity for the focal location (i.e. local area) only. The only difference of the local estimation from the global method is the merging of the Gaussian function with the top surface areas. The geographically closer triangular prisms have higher spatial weights and the geographically further ones have lower spatial weights. In other words, the spatially further triangular prisms are not influential for the resultant fractal dimension. For geographic phenomenon, within a predefined bandwidth, we may not be able to see the land surfaces which are far away from the focal location, accordingly, the surface complexity does not remarkably affect land surface we observe surrounding the focal location area. Therefore, for triangular prism method, the land surface complexity is reflected on the top surface area of triangular prisms and the spatial weights are small or even zero in order to remove their influences.

The integration of the Gaussian function discussed for triangular prism method is an example of how local estimation of fractal dimension can be achieved based on the geographically weighted perspective. We assume that the local fractal dimension changes over space, and the Gaussian function modifies the top surface areas that result in variations of the parameters of the least-squares regression from space to space. Although the Gaussian function makes use of all available data, it places spatial weights on each of the observation and some of the further observations may be assigned a zero weight. Different from geographic mean, for triangular prism method, the spatial weights are not standardized because there is no ratio form in the estimation process. The triangular prism local method displays a basic rule for incorporating Gaussian function to a global estimation method and following two methods presented next also based on the same procedure here.

Local Differential Box Counting Method

The second estimation method for local fractal dimension is based on the improved differential box counting method. Follow the triangular prism method, it is not difficult to modify the differential box counting method to a local form. The quantity here is the number of the box counting, or the difference between the box numbers associated with the largest and smallest digital numbers. Recall from previous discussion of the global differential box counting method, each grid contributes a box number which is the total value for covering that grid. In this case, applying the local perspective, the grid is considered to be an observation location and the difference between box numbers is treated as an observation. The Euclidean distance is calculated between a focal location and the grid center, then a spatial weight can be acquired for this observation. A weighted differential box counting number is acquired by multiplying the spatial weight and the original box number. Repeating this process for all grids, the total weighted box numbers are counted by summing all the weighted box numbers from each grid. For different values of step sizes, the quantities (i.e. weighted box numbers) are counted and a fractal dimension for a specific focal location is derived from a least-squares linear fit.

This simple adaption is similar to triangular prism method in a way of placing spatial weights on the corresponding quantity and the step size stays the same, also the fractal dimension is obtained by using the least-squares regression technique. Another change is that the original box counting number is an integer, and after the weighting process, the resultant box numbers become a fractional value because the spatial weights are fractional values. The differential box number becomes a weighted value under a different understanding and this does not affect the fractal dimension estimation because it uses the linear regression to estimate the parameters. The original differential box counting method has not been widely applied to remotely sensed images, therefore, the local form of this method seems to be more desirable to be explored with remote sensing images for a better understanding (Tso and Mather 2001).

This chapter first presents three widely used estimation methods for computing fractal dimension. These methods focused on computing global fractal dimension on remotely sensed images and can be applied on various land covers. In Chapter Four, a discussion is presented for the three methods focusing on theoretical foundation and the mathematical formulation. For remotely sensed images, different from the regular objects, the strict calculation method is no longer suitable for measuring the geometric complexity of these complex and irregular land surface features in remotely sensed images. Therefore, the regression technique is favored as a basis because this technique aims at searching for an optimal solution based on a trend line for different types of observations in a dataset. Various methods have been developed using least-squares regression technique as the core principle and try to capture the geometric details of real phenomenon. Among these methods, some can be applied to land surface features in remotely sensed images directly. One of the most critical issues in fractal domain is that there are many fractal techniques and each one has its own unique characteristics. Since the complexity of fractal objects, it is understandable that one method is not sufficient and these numerous methods attempt to fully study the nature of fractals. In this dissertation, three commonly used estimation methods are chosen for a comparison purpose. It is interesting to correlate the results of the computed D values to find out the performances of each method in the following chapter.

The fractal dimension of land surface features which measures the geometric complexity of image texture can be recognized as a summary or global statistic (Sun et al. 2007). This summary statistic appears to have many similar aspects to other popular summary statistics that a fractal dimension represents an overall measurement by averaging each fractal dimensions from local neighbors. For a homogeneous land covers, a single fractal dimension can be appropriate quantify the geometric complexity of an image. However, such homogenous land covers are extremely difficult to be seen in real world especially when dealing with remotely sensed images covering large scale. For remotely sensed image acquiring the real world land covers, the focus should shift from a summary statistic (i.e. global fractal dimension) to several local statistics (i.e. local fractal dimensions) in order to measure the detailed geometric complexity more accurately. In this case, this dissertation research tends to explore the possibility of calculating local fractal dimensions to explain the variations of landscape complexity. It is important to note that there is an R package developed for computing geographically weighted local fractal dimension. This package uses set of point data to estimate the multiscale behavior.

A Gaussian function is integrated with the original methods to achieve the goal of obtaining the local values. In the previous sections of Chapter Four, the Gaussian function is introduced and discussed in detail. The conjunction between a Gaussian function and the original methods is needed to formulate equations for obtaining fractal dimensions for local areas. It is important to inspect where to place the spatial weights on the original estimation methods. Unlike other summary statistics, fractal techniques contain a regression step and the spatial weights are needed to be blended in before the step of least-squares regression. For all these three methods, the Gaussian function needs to be added to the quantities which are constructed from different aspects of counting the digital number. Such construction aims at strengthening the spatially closer land surfaces and weakening the spatially further ones. One of the focus of this dissertation is the bandwidth selection, the Gaussian function only uses a fixed filter for the bandwidth to compute Euclidean distances so the effect of the bandwidth can be examined. Overall, Chapter Four introduces methods for computing summary statistic or fractal dimensions and the Gaussian function separately. Then a combination between these two parts is proposed to explore the possibility of decomposing a summary fractal dimension value to local values.

Chapter Five focuses on the application of both global and local methods for calculating fractal dimension for test data using the triangular prism and differential box counting methods. The purpose of using test data is to give a general impression of how the estimation methods work especially the local ones. A comparison between these two methods is performed in Chapter Five. The central part of Chapter Five is to compute the local values of fractal dimension and compare them with the global value in order to assess the effectiveness of geographically weighted fractal estimation.

Chapter Five

Results of Triangular Prism and Differential Box Counting Methods

5.1 Introduction

This chapter mainly evaluates the performances of the first category method, the triangular prism and differential box counting methods. Five methods in total are evaluated and compared using the aerial photograph for computing the two dimensional fractal dimension. Several sample images extracted from aerial photography are examined for each of the method. For aerial photograph, some global fractal dimensions are calculated for large areas of various landscape features. Each of the methods are applied and the results are compared.

For local analysis, this dissertation only uses small samples with certain sizes because of the computation complexity. The local fractal dimension is calculated for every pixel and the results are visualized and compared with the corresponding global fractal dimension. The algorithms of triangular prism and differential box counting methods are not computationally complex and, however, when carrying out the local analysis for each pixel, the computation complexity is dramatically increased.

Therefore, the sample images used in this dissertation for local analysis are limited to several small sizes. For each of the local methods of triangular prism and differential box counting, the Gaussian function is used for the local adaption for computing the local fractal dimension values. Moreover, the effect of bandwidth on the range of local fractal dimension is examined for exploring the behavior of the local models on fractal approaches.

In this Chapter, the triangular prism and differential box counting methods are first studied, both global and local, for the first category methods. The algorithms are comparable and they can be directly modified to local forms. The global and local results complied from this Chapter are expected to compare with the Fourier power spectral density method which is discussed in next Chapter.

5.2 Evaluation of Triangular Prism Method Results

The triangular prism method is the first fractal approach examined for the global fractal dimension results. The focus for this section is to implement the four types of triangular prism methods on the aerial photographs to study the land cover complexity. Because of the high spatial resolution of the aerial photograph, various land-cover types can be visually selected for the analysis. Two different land-cover types are selected representing two complexity levels of the image surface. Figure 5.1 shows the two sample images extracted from the original aerial photograph for global fractal dimension computation.

Figure 5.1 Sample Images of Aerial Photograph for Global Fractal Dimension Analysis

As we can see from Figure 5.1, two sample images demonstrate two completely contrasting landscapes from the red band of aerial photograph. The location of the sampled images are not the focus in this dissertation, however, the land covers of the sample images play a key role here. With the high spatial resolution, it can be seen that the first sample image covers a large body of water area with a few waves captured at the right side. The rest of the land cover is filled with highways, several parking lots, etc. All the impervious surface areas are found at the left hand corner of the image. On the other hand, the second sample image, is an example of a more developed landscape than the first image. A visual inspection of the second image tells us the main land covers of this area are residential, also high buildings can be seen in the business district area. Moreover, a small portion of highway is visualized at the lower right hand corner. Both of the sample images are defined by 4097×4097 pixels with a pixel size of 1 foot. This length of the image is equal to $2^{12} + 1$ which is the predefined rule ($2^{n} + 1$) of the image size for triangular prism methods. The raw digital number values are used in the analysis with a pixel depth ranging from 0 to 255.

Each of the four versions of the triangular prism methods is used to compute the fractal dimensions of the two images. The results are shown in Table 5.1 for a comparison between the four methods and also between the two distinct landscapes. We can see from the results that the fractal dimension in summary for the first image ranges from 2.20 to 2.32 indicating a relatively low geometric complexity and, on the other hand, the fractal dimension for the second image ranges from 2.40 to 2.48 which are larger values than the first case. Given the differences of fractal dimensions between these two landscapes, it is encouraging that based on fractal dimension, people can somehow distinguish the dominating land cover types of given images. Here, a water dominated area would generate small fractal dimension because of the nature of low geometric complexity of the water body itself. The residential dominated area, with high contrasting elevation because of the buildings, exhibits high geometric complexity and result in large values of fractal dimensions. The descriptive statistics of these computed results are shown in Table 5.2. Among these four methods, the original triangular prism method consistently generate the smallest fractal dimension values for both of the two sample images. The largest

D value for water area is given by the Max-difference method and, for the residential area, the Mean-difference method produces the largest D value. The mean fractal dimensions for the two images are 2.45 and 2.26, which shows a good distinction for these two land covers. Another interesting finding is that all the three modified versions give larger D values than the original method for both the water and residential areas.

Table 5.1 Global Fractal Dimensions of Four Triangular Prism Methods

Sample Images	The Original	Max-Difference	Mean-Difference	Eight-Pixel
Water Area	2.2038	2.3168	2.2622	2.2465
Residential Area	2.3976	2.4679	2.4811	2.4538

Table 5.2 Descriptive Statistics for Computed Results of Triangular Prism Methods

Sample Images	Mean	Standard Deviation	Min	Max
Water Area	2.2573	0.0404	2.2038	2.3168
Residential Area	2.4501	0.0318	2.3976	2.4811

Figure 5.2 and 5.3 present the results of the regression used for deriving the fractal dimension values for water and residential areas, respectively. Starting from upper left and clockwise are the original triangular prism, Max-difference, Mean-difference and the eight-pixel method. All the three modified versions use 11 regression points for carrying out the univariate linear regression analysis while the original one uses 12 data points for the regression analysis. The R square value of the original triangular prism method for the water area image is 0.7656 corresponding to a slightly curved regression line. All the three new versions yield higher R square values than the original method, especially the Max-difference method, the R square values are 0.9651 and 0.9806. By looking at the regression results of the Max-difference method, it displays a relatively straight line compared to other regression results. The R square values of the original triangular prism method increase from 0.7656 to 0.9031, which may suggest

that the original triangular prism method is more suitable for fractal analysis of high geometric complexity image. The four R squared values for the residential areas are all greater than 0.90 and, all the R squared values of the residential image are greater than the water area image. This finding may imply that the triangular prism method, in general, is appropriate for analyzing the earth surface with middle or high geometric complexity.

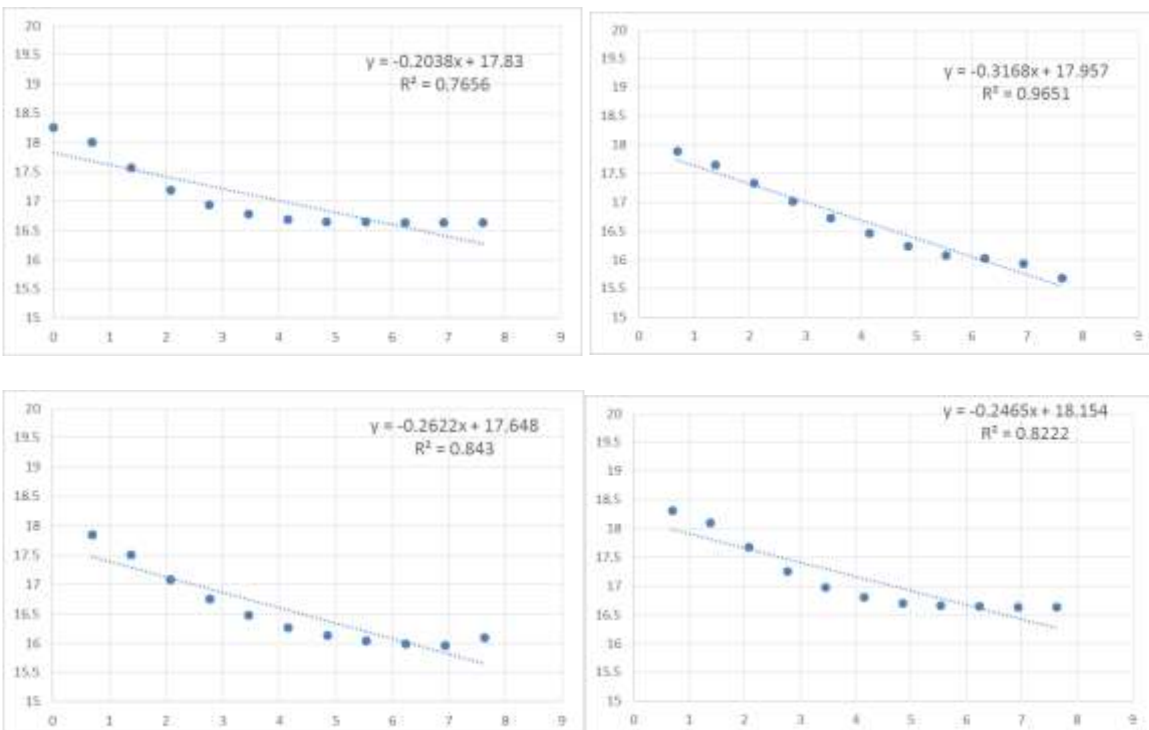

Figure 5.2 Regression Results of Triangular Prism Methods for Water Area (horizontal axis: log form of step sizes; Vertical axis: log form of total triangular areas)

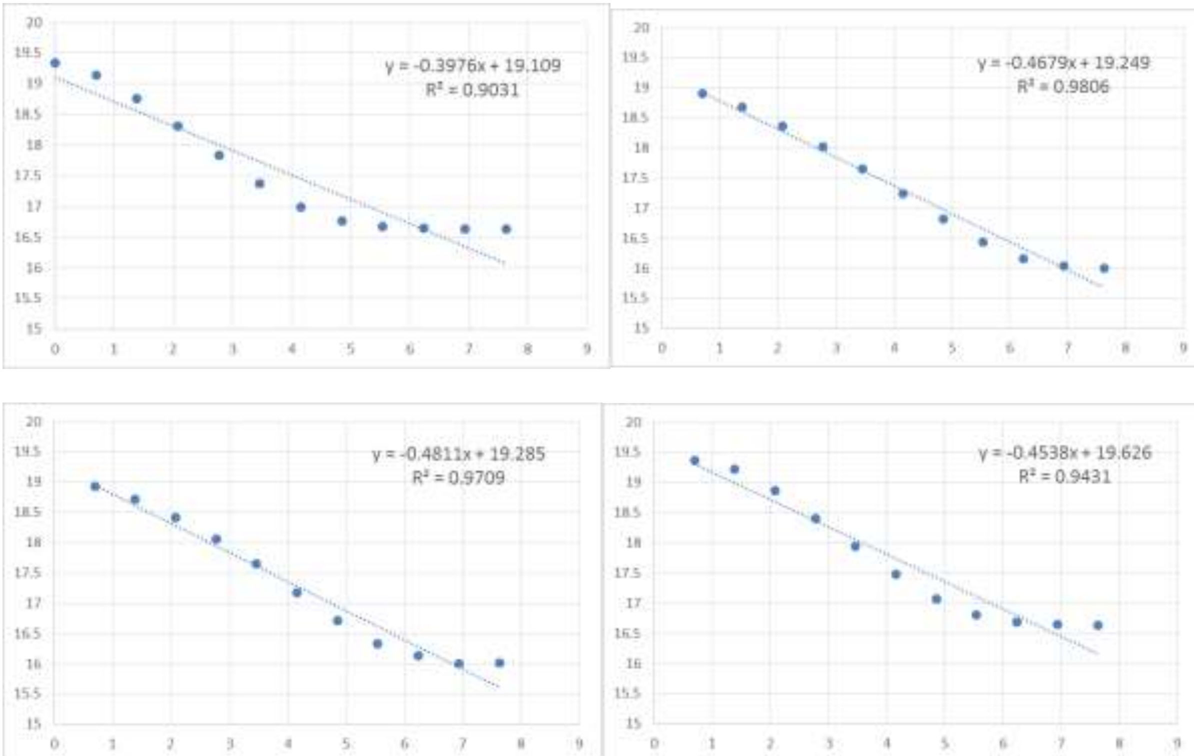

Figure 5.3 Regression Results of Triangular Prism Methods for Residential Area (horizontal axis: log form of step sizes; Vertical axis: log form of total triangular areas)

5.3 Evaluation of Differential Box Counting Method Results

Another selected method which belongs to the first category method is the differential box counting method and is analyzed as well as compared with the triangular prism methods. Based on the results of the triangular prism methods, the original triangular and the max-difference methods are analyzed in this section and together with the improved version of differential box counting method. The Max-difference method is chosen because of the best performances in the last section. This section is a mixture of analyzing one kind method and comparing it with another type of methods. The sample images used in this section are shown in Figure 5.4. These two images are different from the images used for the triangular prism methods but the structures are similar. These two images consist of a water area which has a large patch of water in the middle and harbor constructions on both sides of the image, for the second image, it is also a residential area but the distribution of high buildings is denser than the first case based on the visual comparison. These 4097×4097 pixel images are analyzed following the same procedure as the last analysis.

Figure 5.4 Sample Images of Aerial Photograph for Differential Box Counting Method

Table 5.3 presents the analysis results of the global fractal dimension for the chosen three methods. The original triangular prism method still generates the lowest D values among these three approaches. The results of the two triangular prism methods (original and the max-difference) for the two image sets are the same, 2.2038 and 2.2074 or 2.4679 and 2.4908, which are slightly different but can be considered as the same values because the nature of the fractal dimension itself. As mentioned before, these two sets images have similar landscapes and it is no surprising that the triangular prism methods produce the similar results. The improved differential box counting method, on the other hand, computes very large D values for both of the sample images. A fractal dimension value of 2.5518 of a water area seems larger than the normal value that, usually, the D value for low geometric complexity landscape is slightly exceeds 2.0. The first sample image in Figure 5.4, however, is greatly dominated by water with a few built-up land covers, which is a low complexity landscape and is expected to have a small D value. Another explanation could be that the built-up land covers, even though only occupy a limited space of the whole image, may still display a significant contrast to the water body and cause a high D value. The other case, the residential-city area, results in a D value of 2.7058 which is dramatically increased from the triangular prism method results. A comparable analysis of the improved DBC method of the first set images results in fractal dimension values of 2.5441 and 2.6863, and this is consistent with the results acquired from the second set images.

Table 5.3 Global Fractal Dimensions of Triangular Prism and DBC Methods

Sample Images	Original Triangular	Max-Difference	Improved DBC
Water Area	2.2074	2.3051	2.5518
Residential Area	2.4150	2.4908	2.7058

Figure 5.5 shows the regression results for the improved DBC methods, left is the water area and right is the residential area. The R square values are extremely high and close to 1.0 indicating a good fit for both two analyzed landscapes, for Max-difference method, the R square values are 0.9239 and 0.9836,

which are similar to improved DBC method but generate much lower fractal dimension values. The quantity used for improved differential box counting method is integer values of pure box counting, different from the fractional quantities used for triangular prism method. Moreover, the range of the dependent variable for DBC method is wider than the triangular approach. In general, although both belong to the method of the first category, the results of improved differential box counting method show a quite different outcomes, however, the distribution of high and low geometric complexity based on the sample images is the same for these two methods.

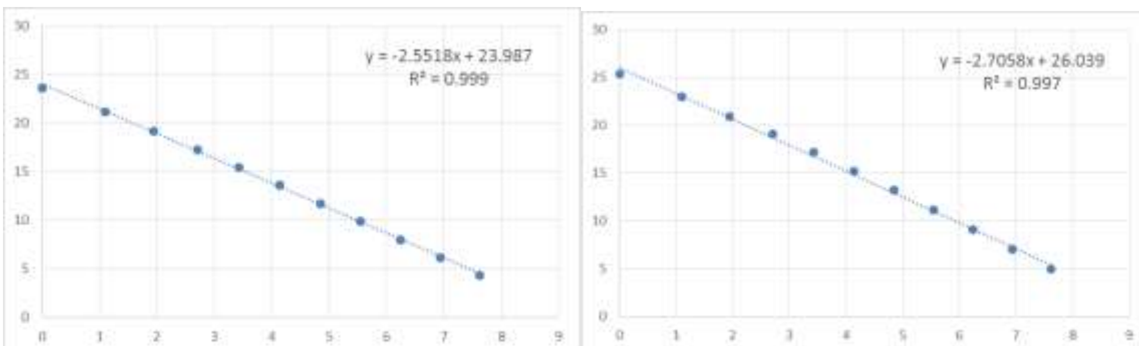

Figure 5.5 Regression Results of Improved Differential Box Counting Method (horizontal axis: log form of step sizes; Vertical axis: log form of total box counts)

5.4 Evaluation and Comparison of Local Fractal Dimension Results

The focus of this section is to explore the results of local fractal dimension, a core idea developed in this dissertation research. Three methods are selected here which are the Max-difference, Mean-difference, eight-pixel. The reasons for choosing these three methods are that they are all modified from their originals. In addition, all these three methods use the same number of regression data for deriving the slope and fractal dimension, the original triangular prism method uses one more regression data, thus it is omitted from the local analysis in this part. Sample images are also extracted from the original aerial photographs but, as indicated before, the computation complexity is an essential factor considered for analyzing local fractal dimensions, which are computed for each single pixel. Therefore, the sample images used for calculating the local fractal dimensions for entire images are much smaller than the images used for the global analysis. However, the same sample images are used again for computing the local fractal dimension values for several separate locations (i.e. pixels) to first test the idea of acquiring the local D values using kernel density functions.

The image of the water area for the improved differential box counting method is used for analyzing the fractal dimensions for single pixels, with the involvement of Gaussian kernel density function to the global approaches. Figure 5.6 shows the sample image and the regions of interested areas. Three regions are selected and compared in terms of the fractal dimensions. It is observed from the image that these three locations display various textures, with different landscapes complexity shown in the image, which contains water and road land covers. It is expected that the surface complexity of these three landscapes are not as the same as the global fractal dimension value and, because of heterogeneity, the D values should be varying based on the global value.

Figure 5.6 Sample Images and Locations for Local Fractal Analysis

Because of the image length is 4097, the bandwidths used for local analysis are 2000 feet for this part test. The results of the local analysis are shown in Table 5.4. Again, the global values are listed in the table, which are generally below 2.3. It is important to examine the separate local D values for these methods. The bandwidth does play a role for changing the D values based on the landscape textures. The smallest D values are all acquired at the lower left corner which is reasonable because that area is pure water and the geometric complexity is very low. The smallest fractal dimension is 2.1955 acquired by the Eight-pixel method. The largest D value is obtained at the middle right location, which is a more complex surface than the water area and, it is as expected to have a high fractal dimension.

Notice that the global fractal dimension values are all within their corresponding local D results which is the rule for the local adaption. The local analysis results are promising because they provide us with the desired outcomes. First, the local results reflect the corresponding surface textures, for example, pure water generates the smallest D values. Second, the local results are in the range (i.e. between 2 to 3), with the incorporation of Gaussian kernel, the results are within the theoretical boundary. The results of the three locations are similar and consistent among these three methods. Max-difference method has the largest D value and also has the largest D values for each of the three locations than the other two methods. It is encouraging that a kernel density function is compatible with fractal approaches, for calculating D values for single pixel, instead of large patch of pixels.

Table 5.4 Local Fractal Dimension for Individual Locations

	Upper left	Lower left	Middle right	Global
Max-difference	2.2702	2.2576	2.3346	2.3051
Mean-difference	2.2406	2.2202	2.2996	2.2710
Eight-pixel	2.2187	2.1955	2.2796	2.2492

To further evaluate the effectiveness of the local adaption of fractal approaches, the regression results of the local fractal methods are included for illustration (Figure 5.7). Only the results of the Max-difference method are shown here, from top to bottom are upper left, lower left and middle right locations. It is clearly demonstrated in the figure that the R square values are equal and greater than 0.9, which means a great fit of the data points. However, it is obvious that, with the Gaussian Kernel function and the bandwidth value, the quantities (i.e. total areas) are decreased for each step size. Furthermore, it is found that the last point is an outlier for all these three methods, the log transformed values of the dependent variable of these three points are larger than a few of their previous data points. For example, the upper left, the value of the last point is 15.06, while the values of its previous three step sizes are 14.82, 14.90 and 15.01, which is not as expected as for the regression technique used for fractal analysis, because the regression data points resulted from triangular prism method are distributed in a descending order based on the step sizes and the regression line is expected to display a straight trend. This could be a potential problem found in the local triangular prism methods which may lead to a poor estimation of fractal dimension. Another consideration of this problem is that using the full step sizes may be another reason for causing the outliers, the last step size could be a potential source of generating this nonlinear tendency of the derived data points.

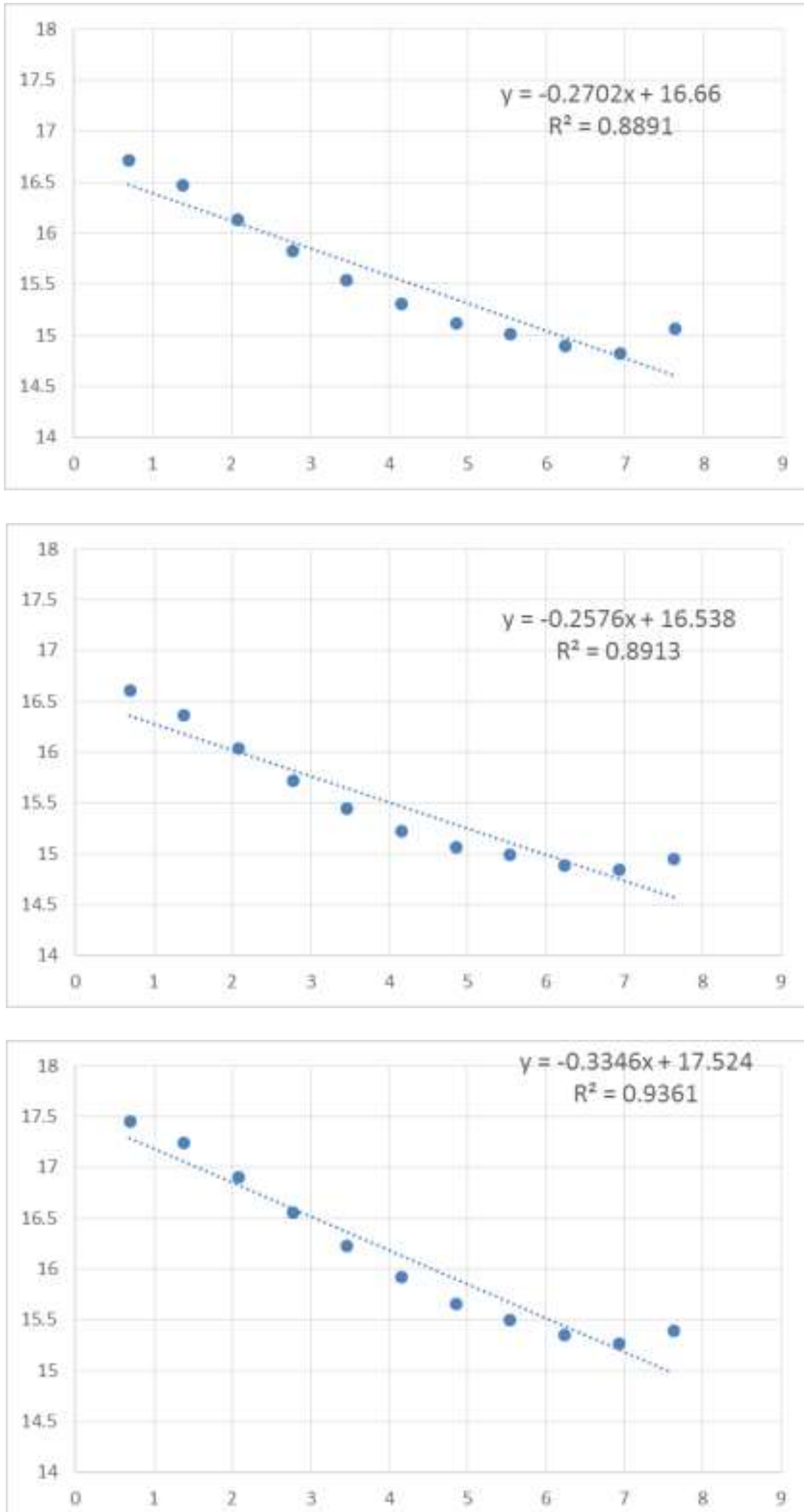

Figure 5.7 Regression Results of Local Fractal Analysis (horizontal axis: log form of step sizes; Vertical axis: log form of total triangular areas)

A general discussion of the findings of the local analysis is that the Gaussian kernel density can be applied to fractal approaches. Although only the triangular prism method is tested, the procedure is similar for other methods. On the other hand, the results from this local analysis suggest that the number of step sizes is essential and much more attention should be put on the last step size. Also, a single bandwidth cannot fully reflect the effectiveness of the kernel density function, therefore, more bandwidths should be added to examine the relationship with the fractal dimension values.

In order to evaluate the relationship between fractal dimension and bandwidth, as well as the number of step size used, various bandwidth values are tested. Figure 5.8 shows the test image for the analysis in this part. This image consists of 1025×1025 pixels. For simplicity, only the original triangular prism method is used for the analysis. The geometric complexity of the entire image based on the visual inspection is low and the summary D value is 2.3340. The left corner of the image is selected and the bandwidth used are 800, 700, 600, 500, 400, 300, 200, 100, 80, 60, 40 and 20 feet. From bandwidth 800 to 200 feet, the fractal dimension values ranges from 2.3192 to 2.2384, which are smaller than the global D value. With the decrease of the bandwidth, the value of the fractal dimension becomes smaller which is as expected, because narrow the bandwidth to a limited space will restrict the local analysis focus on a small area, in this case, water area, and this may lead to lower roughness of the surface. However, when it comes to the bandwidth of 100, 80, 60, 40 and 20 feet. The problem emerges that the values of fractal dimension increase to 2.4917 and then dramatically to 2.766, 3.418, 5.455 and 17.151 (Figure 5.9). It is clear to argue that these small bandwidths (i.e. bandwidth smaller than 1/10 of the original image size in this case) marked by red dots in Figure 5.9 cause an unacceptable result of the large D value, which exceed the upper theoretical boundary of 3, and for bandwidth of 20 feet, the values is 17.151 which is a disappointing finding because it is an extremely large value.

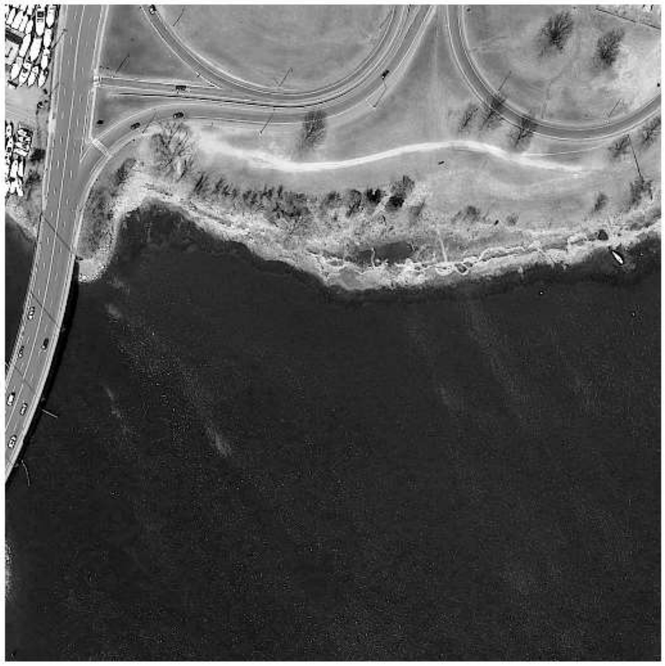

Figure 5.8 Test Image for Examine Effect of Bandwidth

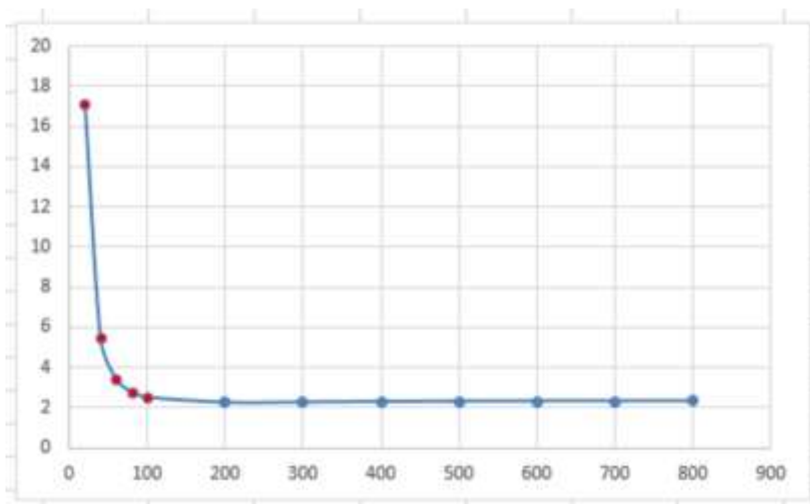

Figure 5.9 Trend of Local Fractal Dimension of Different Bandwidths
(Horizontal axis: bandwidth; Vertical axis: local D values)

By looking at the regression results of the goodness of fit of these small bandwidths, the R square values reflect the poor estimate. The R square values are 0.5681, 0.4679, 0.4106, 0.3953 and 0.4074. All these R square values are very low and decrease gradually with the bandwidth becomes smaller. Take an example of the result of bandwidth of 20 feet, which is the last bandwidth, used in this analysis, and this is shown in Figure 5.10. It is clearly observed from this regression result that the slope is quite a small negative value result in a very large fractal dimension. An outlier is clearly identified from the last step size that the log transformed value is much smaller than its previous regression data points. In addition, not only for this last step size, but also for the 8th and 9th step sizes, the log transformed value of the dependent variable are both smaller than zero, which is hard to interpret since the dependent variable of triangular prism method is total areas of prisms and the values should not be negative.

This analysis results have shown that the small bandwidth may cause an issue for calculating the fractal dimension at a local scale using Gaussian kernel density function. A number of problems have been identified to improve the local analysis procedure. It is still unproved that whether use the full step sizes is the major issue as the bandwidth becomes smaller. The desired result of the local analysis should be, at least, that the regression data points are in a linear trend and the log transformed dependent variable is positive for all step sizes. These conditions may ensure a fractal dimension within the theoretical limit.

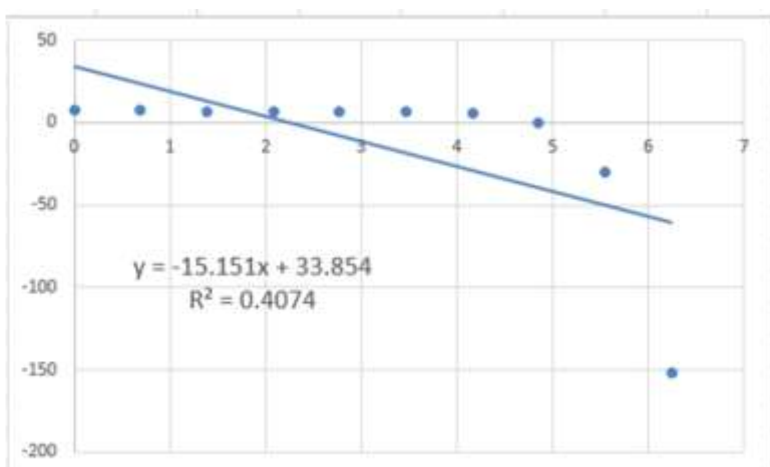

Figure 5.10 Regression Result of Bandwidth 20 Feet (horizontal axis: log form of step sizes; Vertical axis: log form of total triangular areas)

It is important to note that the fractal analysis technique does not have to use the full step sizes, in other words, it is flexible to use different number of step sizes and this is an important adjustment for small bandwidth local analysis. To examine if the small bandwidth is an issue for the other locations of the image, two other locations are selected and together with the current one, three different location: lower left, upper center and image center are analyzed for small bandwidth effect. Table 5.5 shows the selected bandwidths and the number of removed step sizes for each of the location. Notice the 10 feet is a very small bandwidth and for these three locations, the last four step sizes need to be removed from the regression analysis. For a 1025 × 1025 image, the left number of regression data points are 6. The table also demonstrates that as the bandwidth becomes smaller, the number of removed step sizes increases and the removed number are the same for all these three individual locations. It may be inappropriate or impossible to remove many step sizes since a regression analysis technique needs to be performed based on not very few data points. However, for the local analysis with small bandwidth, this strategy may seem the most straightforward way to acquire a normal fractal dimension value. It is also observed from the table that the removed number of step sizes are identical for each bandwidth for all these three locations. It is still not safe to conclude that a rule (relationship between removed number of step sizes and value of bandwidth) has been made here because only three locations cannot represent the general situation. The number of step sizes used for other individual locations for local analysis may vary slightly.

Table 5.5 Number of Removed Step Sizes for Various Bandwidths

	Lower Left	Upper Center	Image Center
10 feet	4	4	4
20 feet	3	3	3
40 feet	2	2	2
60 feet	2	2	2
80 feet	1	1	1
100 feet	1	1	1

After remove the certain number of step sizes for the small bandwidths, the R squares of the regression plot for 10 feet to 100 feet are 0.9353, 0.9524, 0.8949, 0.8236, 0.8624 and 0.8405, respectively. There has been significant increase of the R square values and the corresponding fractal dimension values are 2.5719, 2.4143, 2.2740, 2.2177, 2.2689 and 2.2346. Figure 5.11 shows the trend of the fractal dimension values of the whole range of the bandwidths including the corrected D values for bandwidths 10 to 100 feet. It is noticeable that for bandwidth 10 and 20 feet, the fractal dimension values are slightly smaller than the rest of the values, which is not consistent with the selected surface landscape. The reason is that the bandwidth gets smaller, the locally analyzed area of the lower left corner becomes narrower with only water and the surface roughness should be low compared to the wider bandwidths areas. However, it would be inappropriate to argue at this stage that the fractal dimension values of the small bandwidth of the water area are necessarily smaller than the values of the large bandwidth. For the rest values of the fractal dimension, they are distributed between 2.22 to 2.27 and fluctuate within this range. Starting from bandwidth 100 feet, the fractal dimension values increase gradually until the bandwidth of 800 feet.

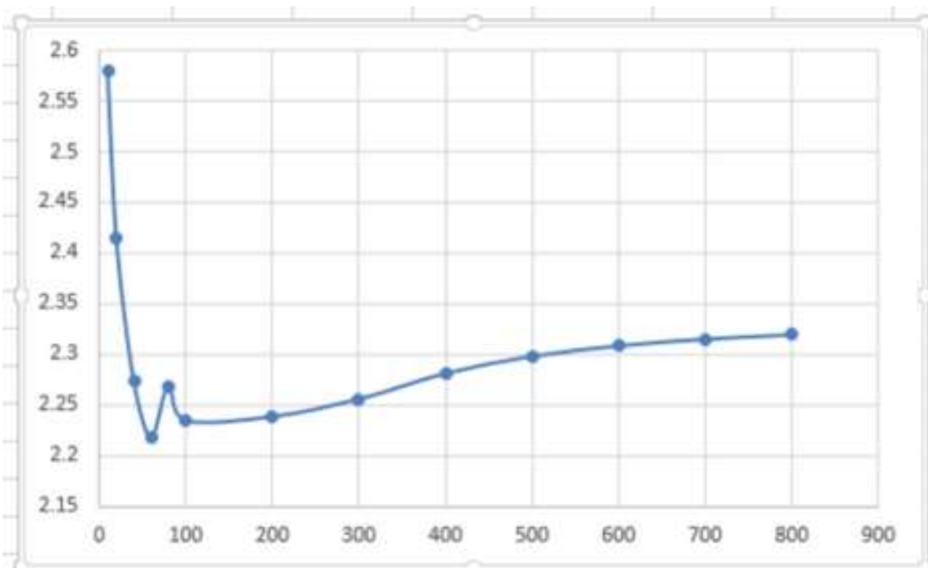

Figure 5.11 Corrected Fractal Dimension Values for Various Bandwidths (horizontal axis: bandwidths; Vertical axis: local D values)

To test the performances of the modified regression analysis for acquiring new fractal dimension values further, the other two selected locations are also examined using the same procedure in the last part for the bottom left location. Figure 5.12 shows the trend of the corrected fractal dimension values for these three different locations. The red, green and blue lines represent upper center, image center and bottom left locations, respectively. It can be observed from the following chart that, for both of the bandwidths of 10 and 20 feet, all these three locations possess higher D values than the rest of the bandwidths. From bandwidth 20 feet and forward, it can be seen that these three locations display a similar trend of the estimated D values. Compare the image textures of these three locations, the upper center location shows the highest fractal dimension and the bottom left displays the lowest D values. Among these three locations, the D values can be easily distinguished at the bandwidth of 100 feet, then as the bandwidth becomes larger, the D values gradually converge to a similar value. This finding is consistent with the rule of the local adaption that as the bandwidth becomes large enough, all local values become the same value and equal to the global one. It is encouraging and recommended that, with the correction of the number of the step sizes used in the regression analysis, this local concept for calculating local fractal dimension for single pixel could be extended to the entire image.

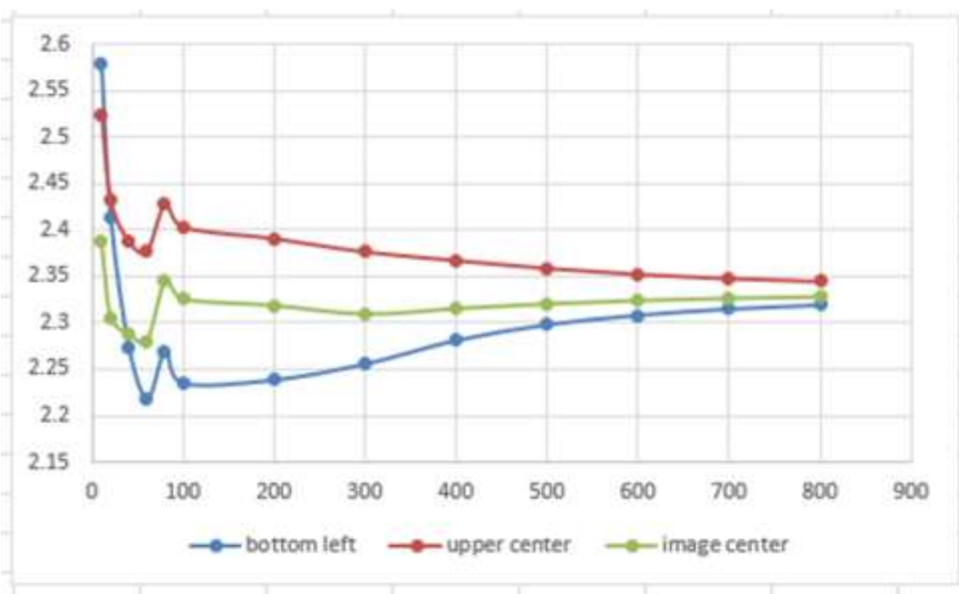

Figure 5.12 Trend of Corrected Fractal Dimension Values for Three Locations (horizontal axis: bandwidths; Vertical axis: local D values)

In addition to the local analysis for the different image textures, it is necessary to carry out another similar test for a few locations with the similar surface textures. In order to examine the same textures, two locations are selected which are located at the bottom left and bottom right. The calculated fractal dimension values for these two locations are shown in Table 5.6. Again, for bandwidths of 10 and 20 feet, the D values are high and not recommended for use for real world applications. As the bandwidth becomes 200 feet, the D values for both of the locations approximate to same D value. The mean fractal dimension values for both locations in the bandwidth range of 200 to 800 feet are 2.2879 and 2.2739 which can be considered as identical value. This result follows the rules of incorporating local and spatial information to the analysis, and is also consistent with their highly similar image textures.

Figure 5.13 presents the general trend of the fractal dimension values for these two locations. The chart presents the results of the D values in a different way than the table form and, as discussed earlier, the geometric complexity of these two locations are highly analogous and this is reflected in the chart that the two curves of the trend of the estimated fractal dimension values eventually converge to a same value. As noted earlier, when the bandwidth becomes larger than 100 feet, these two values differ somewhat but steadily approach to the same D value. Now the main issue of the local analysis for calculating fractal dimension is clear that the small bandwidth does have a huge impact on the fractal dimension values. The previous analysis all focus on exploring single locations (i.e. pixels) of the same or different image textures using a wide range of bandwidths, the results of this kind of analysis are limited and can only present a part result of the local analysis. Rather than using the single location, it is also recommended to explore the local fractal dimension values for the entire image, by doing so, the results can be displayed in map format and a lot more details and comparisons can be made through visual exploration.

Table 5.6 Local Fractal Dimension for Bottom Left and Bottom Right of Image

	Bottom Left	Bottom Right
10 feet	2.5791	2.6731
20 feet	2.4143	2.5403
40 feet	2.2740	2.4308
60 feet	2.2177	2.3507
80 feet	2.2689	2.3584
100 feet	2.2346	2.3131
200 feet	2.2384	2.2545
300 feet	2.2556	2.2418
400 feet	2.2812	2.2580
500 feet	2.2980	2.2744
600 feet	2.3083	2.2874
700 feet	2.3149	2.2972
800 feet	2.3192	2.3044

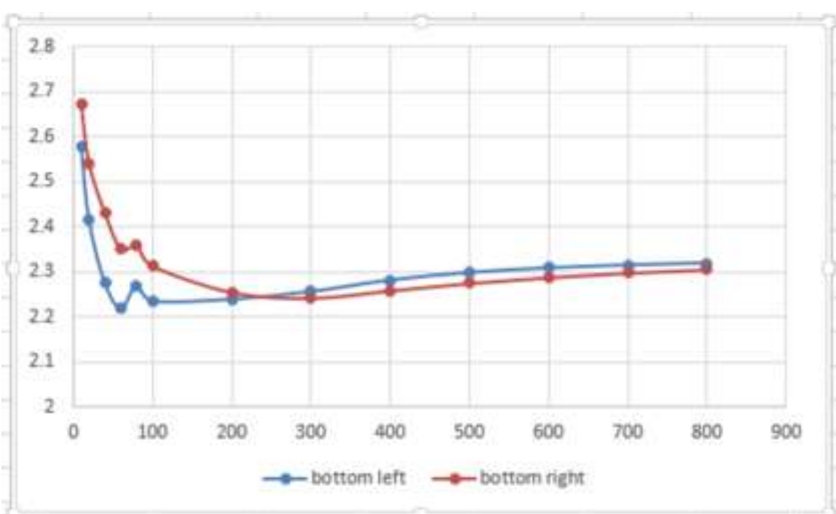

Figure 5.13 Trend of Corrected Fractal Dimension Values for Two Similar Locations (horizontal axis: bandwidths; Vertical axis: local D values)

The last test of the local fractal analysis section in this dissertation is computing local fractal dimension values for the entire image for every single pixel. This is the full range of the number of pixels for an image and each pixel will have its D value to form a range of the fractal dimension result. Because each pixel is used for calculating a D value, for ease of computation, a much smaller test image is used to demonstrate how the ranges of the fractal dimension values look like and vary by applying selected bandwidths and fractal approaches.

Figure 5.14 shows the test image, a 257×257 image with some water body, sand and building land covers. It can be seen from the image that there is a clear contrast between the land covers and their surface complexity would be different. The full number of the pixels in this case are 66049. Firstly, the four triangular prism methods are applied on the this test image for calculating the fractal dimensions for all the pixels using Gaussian Kernel, the bandwidth used for this image is 70 feet which is approximately 1/3 of the image size. Figure 5.15 presents the spatial pattern of the geographically weighted fractal dimension values for each pixel based on a Gaussian function for the four triangular prism methods. The original triangular prism method uses the full step sizes and the computation time for a 66049 pixel size is about 1 hour and 40 minutes, while for the other methods, they skip the first step size and the computation time is about 25 minutes which is a lot fewer than the original method because the first step size result in the largest number of triangular prims for summing the total areas.

Figure 5.14 Test Image for Local Fractal Analysis for Entire Pixels

The spatial distribution of the local fractal dimensions in Figure 5.15 is presented using 5 classes for all the four methods, also range and color for each class is identical for each method so the results can be fully compared across these four method. The global fractal dimension for original triangular prism, Max-difference, Mean-difference and eight-pixel methods are 2.4976, 2.4691, 2.4943 and 2.5360, respectively. The corresponding R square values are 0.9857, 0.9960, 0.9931 and 0.9945. The R square value of the original triangular prism method is improved from the test image used in the previous analysis. The original range of the local fractal dimension values for the original, Max-difference, Mean-difference and the Eight-pixel methods are 2.3414 - 2.6062 (global: 2.4976), 2.3280 - 2.5642 (global: 2.4691), 2.4200 - 2.5350 (global: 2.4943) and 2.3820 - 2.6562 (global: 2.5360), respectively. It can be seen from the result that the global values are all within the range of their corresponding local value range, which are as expected. Among the results, the mean-difference method yields a different result that its values fall into the medium range of roughly 2.40 - 2.60. The other three results display a similar spatial pattern that the max-difference method yields the most pixels in the smallest range, which are 2.33

- 2.40, on the other hand, it does not have the values in the largest range. The eight-pixel method yields the most pixels in the largest range which is 2.59 - 2.66. The original method, Max-difference and the eight-pixel method exhibit very comparable spatial distribution of the fractal dimension values that, the lowest geometric complexity exist at the bottom part of the image and the highest geometric complexity is observed at the top right region of the image. This is somehow consistent with the test image landscape that the water area is at the bottom area of the image with low complexity and the top right corner is identified to be a built-up and shadow area, which is considered to be a high complexity area.

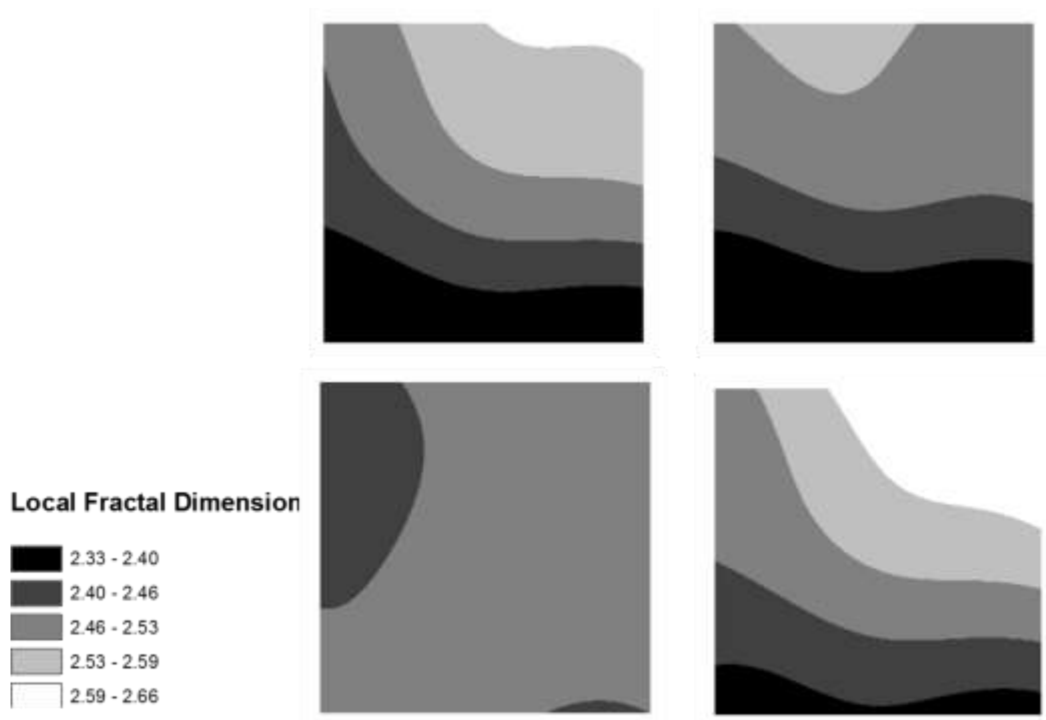

Figure 5.15 Spatial Pattern of Local Fractal Dimension for Four Triangular Prism Methods. Upper Left: Original Triangular; Upper Right: Max-difference; Lower Left: Mean-difference; Lower Right: Eight-pixel.

In addition to the within method comparison, another analysis on the comparison between methods is also carried out for the local fractal analysis. For simplicity, the Max-difference method is chosen to compare with the improved differential box counting method. The same test image is used for this part analysis. Figure 5.16 presents the spatial distribution of the local fractal dimension results for these two methods. The global fractal dimension value using the improved differential box counting method is 2.4643, compared to the value of the Max-difference method which is 2.4691. These two values can be considered as the same value. Recall from the previous analysis for a large image, the global fractal dimension values for the improved differential box counting method is much larger than the Max-difference, however, for a smaller image, the global values are quite the same. The local fractal dimension of the improved DBC method ranges from 2.39 to 2.51. It is narrower than the range of the Max-difference method. Also compared with other triangular prism methods, the result of the improved differential box counting method is somehow within the range of all the triangular prism methods. From Figure 5.16, it can be seen that the improved differential box counting method does not yield any fractal dimension values within 2.33 to 2.38 and 2.51 to 2.56. Most of its results are within 2.40 to 2.50. The general distribution of the local fractal dimension of improved DBC is comparable to the Max-difference method, also to the other triangular prism methods based on the results from previous part. Both of the methods yield the same values fall in the value range of 2.47 to 2.51 at the top right area. The Max-Difference method yields the largest D values (2.51 - 2.56) at the top left region of the image while the improved DBC method has lower values for that area.

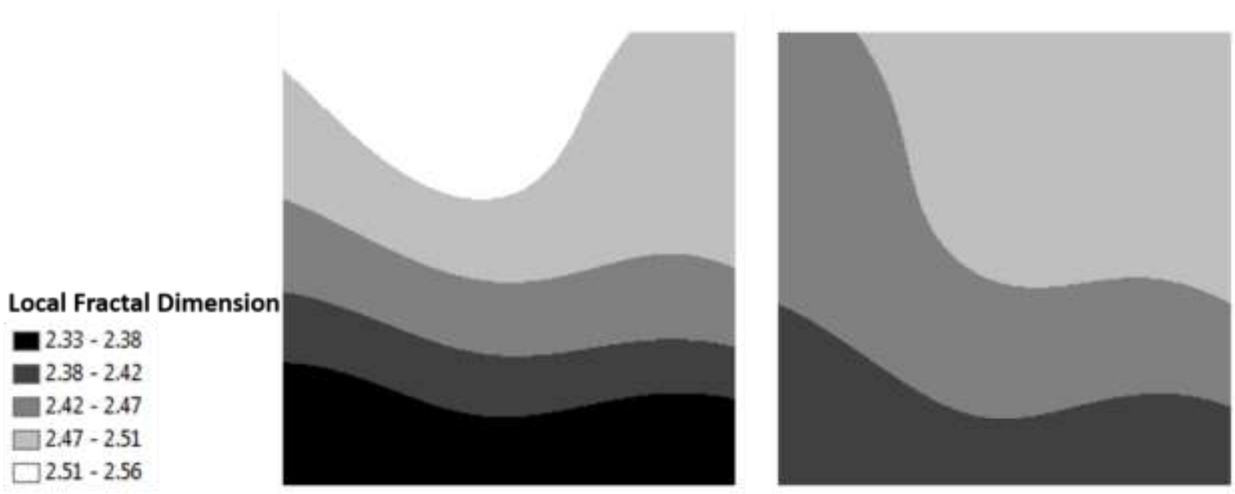

Figure 5.16 Spatial pattern of Local Fractal Dimension for Max-Difference and Improved DBC

It is also important to explore the effect of bandwidth of Gaussian function for computing local fractal dimension for the entire image. As mentioned before, two rules of local adaption are targeted for the analysis. The first one is the global result needs to be within the range of each local results for each bandwidth. Secondly, the range of the local fractal dimension values should vary according to the value of bandwidth, that is, specifically, as the bandwidth becomes larger, the maximum value decreases and the minimum value increases for the entire image. On the other hand, as the bandwidth becomes smaller, the maximum value increases and the minimum value decreases. As a special case, when the bandwidth is becoming large enough, usually from the image size to infinity, the results become narrower and eventually all the values become the same value which is the global value. In this dissertation research, the fractal dimension value is very different from the other spatial statistics because the fractal dimension value, for surface feature, has two theoretical boundaries that the result is expected to be within 2 and 3. Unlike geographically weighted mean, such spatial statistic does not have any boundaries for the results, therefore, the fractal analysis requires much more care for the local fractal dimension analysis.

In order to examine the bandwidth effect, the Max-difference method is used for testing various bandwidths. The same test image from last part is used for the bandwidth effect analysis. From last part analysis, the spatial distribution of D values can be observed and the general trend of the pattern is shown for bandwidth of 70 feet. Based on the same test image, the numerical results of local D values for various bandwidths are presented in Table 5.7. The bandwidths used in this analysis roughly cover the whole range from 5 feet to 200 feet. From bandwidth 200 feet to 60 feet, the interval is 20 feet. The results of bandwidth 200 feet is 2.45 - 2.49, with the global D value of about 2.47. The bandwidth of 200 feet is approximately the image size and yields the narrowest width of result compared to the smaller bandwidths. With the bandwidth becomes smaller, the maximum values become larger and the minimum values become smaller, the range of the results become wider. Recall from previous statement, the behavior of this results is consistent with the rules of the geographical weighted scheme.

It is noticeable from Table 5.7 that from bandwidth 200 to 100 feet, the change of the ranges of the local D values are small, for minimum and maximum values, the average change for both boundaries is 0.01. However, when the bandwidth becomes smaller than 100 feet, the extreme values (maximum and minimum values) change more dramatically than large bandwidths. For example, from bandwidth 50 feet to 40 feet, the minimum value decreases from about 2.25 to 2.19, and for maximum value, it increases from roughly 2.63 to 2.73. The change interval is 0.06 and 0.1 for minimum value and maximum value, respectively. The change interval can increase to as large as 10 times (0.1 / 0.01). In addition, from bandwidth 200 to 30 feet, the behavior of the bandwidth effect is correct. When it comes to bandwidths 25 to 5 feet, there are many unexpected values that caused by the small bandwidths. The minimum values for bandwidths 20, 15 and 10 feet are 1.99, 1.96 and 2.07. Although the values of 1.99 and 1.96 are below 2.0, they are extremely close to 2 and still be considered as a value of 2 which may seem correct since a very small bandwidth covers a highly homogeneous surface and can yield a fractal dimension of 2. The maximum values of bandwidths 25 to 5 feet are strange which are 3.28, 3.87, 5.20, 9.17 and 31.29. It is interesting to find out that the maximum values exceed 3.0 and continue increase dramatically.

Table 5.7 Local Fractal Dimension Values of Entire Image for Various Bandwidths

Bandwidth	Local Fractal Dimension Values
200 feet	2.4469 - 2.4876
180 feet	2.4420 - 2.4913
160 feet	2.4352 - 2.4959
140 feet	2.4258 - 2.5026
120 feet	2.4121 - 2.5129
100 feet	2.3922 - 2.5279
80 feet	2.3590 - 2.5493
60 feet	2.2892 - 2.5869
50 feet	2.2474 - 2.6311
40 feet	2.1882 - 2.7320

35 feet	2.1472 - 2.8293
30 feet	2.0976 - 2.9919
25 feet	2.0416 - 3.2846
20 feet	1.9878 - 3.8662
15 feet	1.9624 - 5.2000
10 feet	2.0697 - 9.1661
5 feet	3.4645 - 31.2917

In order to further examine the small bandwidth effect, similar to the previous analysis, but instead of analyzing for single pixels, the entire test image is used and three bandwidths are selected for comparing the result of removing certain number of step sizes with the original result. Dark color indicates small values and bright color means large values. The left image is the original result and the right image is the corrected image. Figure 5.17 shows the original and corrected spatial distribution of fractal dimension values for bandwidth 5. The last three step sizes are removed for correction. The original image looks interesting that it has four circles with small D values distributed at four corners of the image. The large values are found at the middle and four edges of the image. The spatial distribution of the D values seem very regular but not as expected. After removing the last three step sizes, the local D values become smaller but still not within the range of 2 and 3. The spatial distribution changes to a completely different form. There are many small circles distributed across the image and some small values are found at the top right edge of the image.

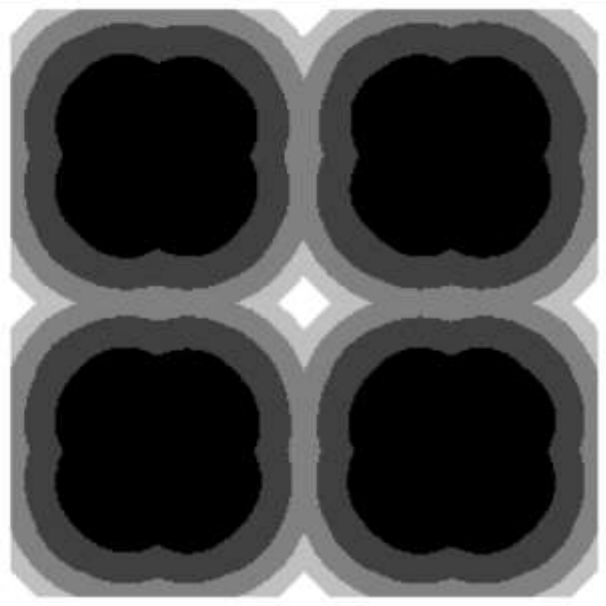

3.4645 – 31.2917

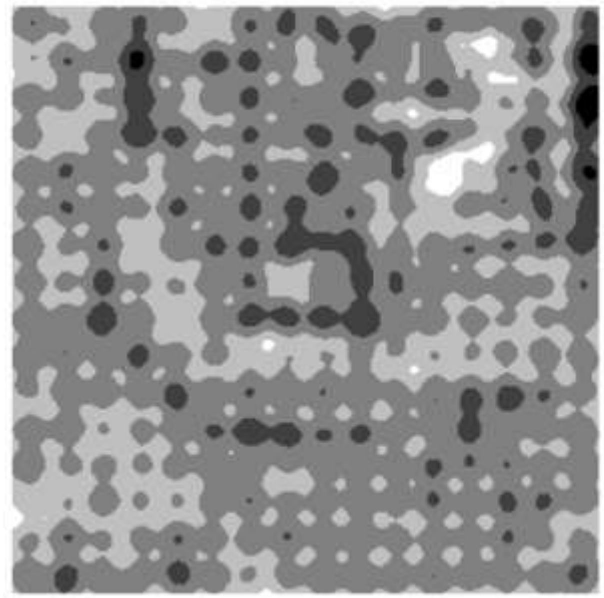

1.3011 – 3.5853

Figure 5.17 Comparison of Spatial Distribution of D Values between Original and Corrected for 5 Feet

Figure 5.18 shows the comparison of bandwidth of 10 feet. Increasing of 5 feet bandwidth, the original image shows the same pattern with the bandwidth of 5 feet. The corrected image displays a similar spatial pattern to bandwidth of 5 feet, but the small circles become larger. The possible explanation is that the bandwidth plays a role for changing the local analysis area wider. Figure 5.19 shows another comparison for bandwidth of 30 feet. Different from the bandwidths of 5 and 10, the original image has four circles that are not regularly distributed in the image. Also, the values of the bottom two circles are smaller than the top two circles. The corrected image shows different pattern from bandwidths of 5 and 10 too. The spatial distribution of 30 feet looks smoother than bandwidths 5 or 10. The small values are found at the top left and bottom right corners. The middle of the image shows a small area of large fractal dimension values.

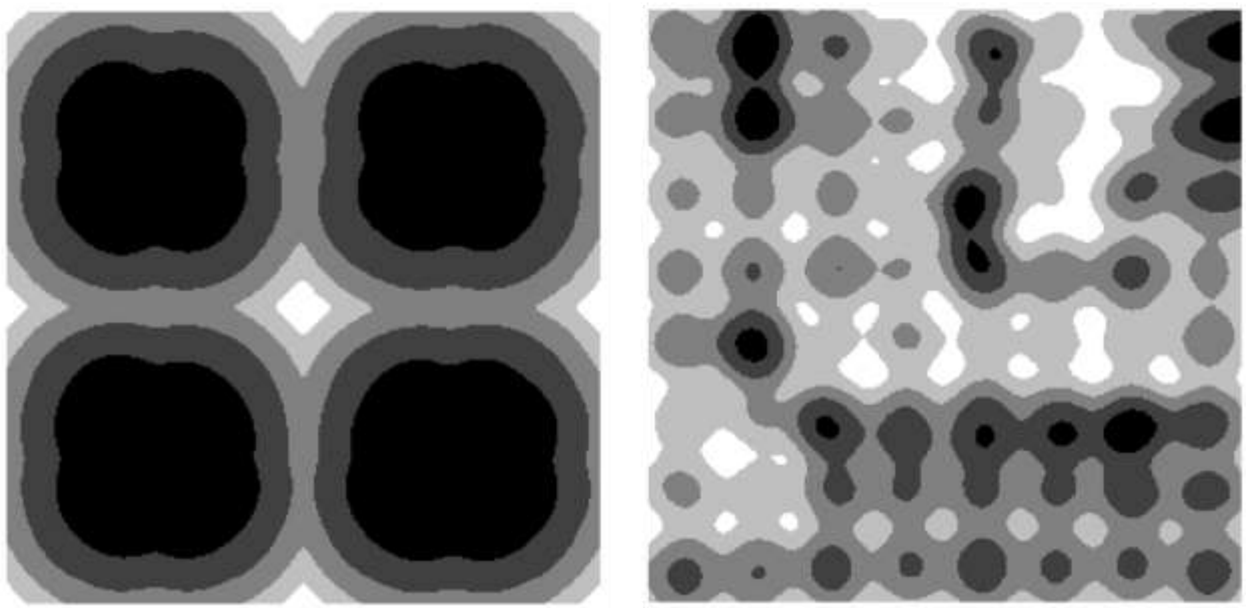

2.0697 – 9.1661 1.9681 – 2.9488

Figure 5.18 Comparison of Spatial Distribution of D Values between Original and Corrected for 10 feet

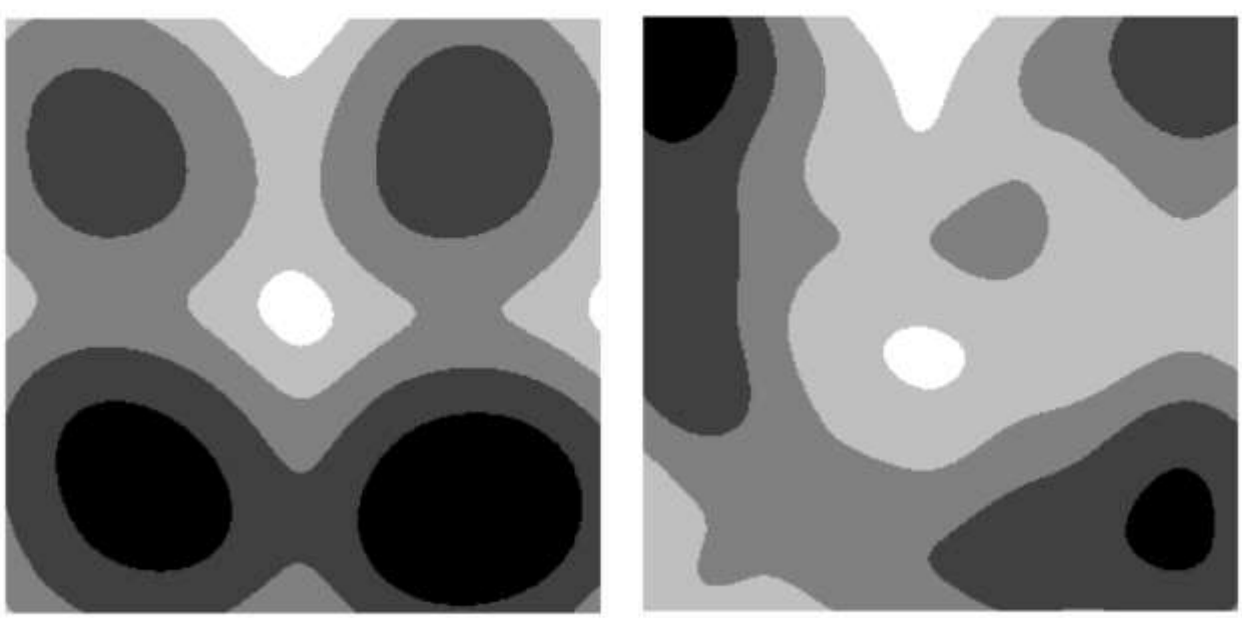

2.0976 – 2.9919 2.2923 – 2.6000

Figure 5.19 Comparison of Spatial Distribution of D Values between Original and Corrected for 30 feet

5.5 Summary

This Chapter focuses on exploring fractal analysis on aerial photograph, a photograph has very fine spatial resolution of 1 foot which is used in this dissertation research. Various analysis has been carried out for calculating the fractal dimension values. Global values are first explored by various methods. Four types of triangular prism methods are used for estimating geometric complexity of two sample images extracted from the original aerial photography. The two samples consist of a water land cover area and a residential dominated area. Among these four methods, the original triangular prism method yields smaller D values for both of the two sample images. The D values of residential area of these four methods are consistently larger than the water area indicating the geometric complexity of residential surface is higher than the complexity of water area. Then the triangular prism methods are compared with the improved differential box counting method. These two methods belong to the same category of fractal approaches in terms of similar manner for computing the quantities. The improved differential box counting method yields larger D values than the other triangular prism methods. Moreover, the Max-difference and the improved differential box counting methods yield the largest R square values indicating a good fit of the regression line to the data points.

Second, the local fractal analysis is carried out on smaller sample images. The Gaussian kernel is used for computing the fractal dimension values for each single pixel. A series of local analysis using the Max-difference method are performed to explore the effect of Gaussian kernel for computing the local fractal dimension values. Several single locations are first examined and the results show that the D values vary according to different places of the image. A built-up area results in a larger D value than the water area, which is correct since the geometric complexity of a built-up area, is higher than a flat water area. In addition to the single location analysis, the local fractal approach is further applied to the entire image for calculating D values for each pixel to generate classification maps for visual representation. A wide range of bandwidths are tested for examining the behavior of the local adaption for the fractal analysis. The results show that, for large bandwidths, the maximum and minimum D values change correctly according to the variation of bandwidths. Also the global D value is within the range of each result of the large bandwidths. However, when the bandwidths become very small, the D values start to change to unexpected number. The regression plot also exhibits a few outliers of dependent variable and some has negative values.

The solution for the small bandwidth is to remove certain number of step sizes in order to remove the outliers for a better fit of the regression line. In this way, the spatial distribution of corrected D values change to a more irregular pattern than the original pattern but still has some unrealistic D values compared to large bandwidth. Chapter Six focuses on exploring the Fourier power spectral density approach for computing both global and local D values. This method is more complex than the previous two methods and the detailed analyzing process is illustrated in Chapter Six.

Chapter Six

Results of Fourier Power Spectral Density Method

6.1 Introduction

The previous chapter examines the results of triangular prism and differential box counting methods for computing fractal dimension values. In general, both of the triangular prism and differential box counting methods belong to the first category method for computing fractal dimension of surface. The comparison between these two methods show different scenarios, however, the use of the same category methods have limited their comparison. Chapter Six is focused on applying the Fourier analysis technique to compute the surface fractal dimension using the same sample images used in Chapter Five. Also, the results of the Fourier method are compared with triangular prism and differential box counting methods for a further and more complete comparison.

As mentioned before, the Fourier analysis method belongs to the second category methods for computing the fractal dimension for surface. The computation procedure of using Fourier analysis for computing a D value involves many more steps than the triangular prism or differential box counting methods. Therefore, this intrinsic complexity has limited its use and applications on landscape analysis using fractal dimension (Sun et al. 2006). It has been previously pointed out that the popular methods used for computing fractal dimension are triangular prism, box counting, variogram and isarithm since all these methods can be easily constructed and accessed through software (Quattrochi et al. 1997). As a sophisticated as well as accurate algorithm, the Fourier spectral approach may need more attention for its use for computing fractal dimension and more importantly, compare with other common fractal methods.

Besides computing a fractal dimension based on a given image, another widely use of the Fourier analysis is to model the natural surfaces with various levels of roughness for constructing 3-D surfaces because many physical processes can be perceived as fractal surfaces (Pentland 1984). Previous studies have used the Fourier function for formulating fractional Brownian surfaces, which possess known D values ranging from 2.1 to 2.9, and the generated surfaces can be used for validating new developed fractal approaches (Pentland 1984, Dubuc et al. 1989). This dissertation does not aim at developing new fractal methods, so the Fourier analysis method is not used for generating fractional Brownian surfaces. Instead, it is worth of comparing the Fourier analysis method with the previously examined methods on the aerial photograph sample images. Chapter Six mainly examines the Fourier spectral approach for computing fractal dimension values which follows the same manner in Chapter Five.

6.2 Fractal Analysis of the Fourier Spectral Approach

This part of the results focuses on analyzing the various possibilities of the Fourier spectral approach for acquiring the average fractal dimension value. Different from the triangular prism method and differential box counting method, there are some variations of the Fourier transform method and the influence of different strategies on the fractal dimension results is analyzed below in this section. The analysis of various procedures of the Fourier spectral approaches for computing global fractal dimension values is crucial because the local D values are built on the results of this section and the computing strategies of the Fourier transform method is selected for computing local D values in the next section.

The test data is as the same as the image of Figure 5.14 in chapter five. A small image is used for computing a global D value using Fourier transform method is because the computation complexity of this particular method has been dramatically increased compared to the previous two methods. The image is not shown here and can be referred to in the last chapter. Based on Turcotte (1997, 88 - 89), the computation of the Fourier transform and the mean power spectral density start from the lower left origin and spread out to the upper right direction. In python script, for reading image, the origin starts from the upper left corner, these two different procedures may result in different results of the computed fractal dimension values. The regression plots are shown in Figure 6.1 for a comparison purpose.

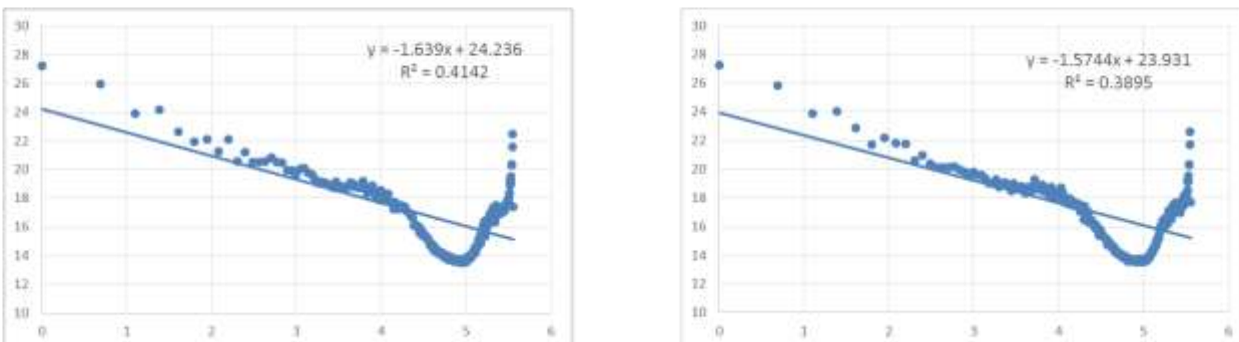

(a) Origin From Upper Left

(b) Origin From Lower Left

Figure 6.1 Regression Plots of Two Origins of Fourier Spectral Approach (horizontal axis: log form of radial wave number; Vertical axis: log form of mean power spectral density)

The first attempted analysis of the Fourier spectral approach is using two different origins of the image. Figure 6.1a uses an origin starting from the upper left corner which is consistent with the python script programming used for this method for the computation while Figure 6.1b uses a different origin starting at the lower left corner which is consistent with the illustration in the literature. The purpose of this comparison is to see whether the change of the origin affects the distribution of the regression points, as the slope and the fractal dimension value are directly influenced by the trend of the fitted line. The D values for these two scenarios are 3.1805 and 3.2128, respectively. Both of these two values excess the upper limits of the theoretical boundary of 3.0. It can be seen from the figure that at the beginning of the radial wave number, the log mean power spectral density does show a decreased trend and the values are distributed in a roughly equal space. Then the points start to become denser than the beginning few points as the radial wave number becomes larger. The overall decreasing trend is still clear until the radial wave number gets to 5 and the there is a sudden increase of the log mean power spectral density which causing the log-log plot lacks of a fractal distribution.

Reexamine Figure 6.1, the regression plot and the slope are closely similar, although the R square values are not high, the change of the origin does not affect the result much. It is acceptable to use the origin at the upper left corner for the Fourier method, the next consideration would be adjusting the radial wave number in order to remove the increasing trend at the tail of the regression line for achieving a linear trend of a fractal distribution.

Recall from the test image used for the first test, the largest value of the radial wave number used is 257 which is as the same as the image size. However, if pay close attention to the relation of computing the radial number, and take the largest position which is 256, the corresponding radial wave number is 362. Therefore, there is a large missing radial wave number and amount of mean power spectral density for the regression. The second test considers using the full extent of radial wave number not only the number of the image size, but the maximum number of the radial wave number according to the image size. Figure 6.2 shows the log-log plot of this test for two different origins. It can be seen from the results that with the 362 regression data points involved, the overall trend for both situations exhibit more than one peaks and bottoms. As the log form of the radial number becomes larger than the first test situation, the power spectral density decreases and then suddenly increases to the values similar to the beginning several values. The reason causing this non-linear trend is that the total number of the radial wave coefficient number. Starting from position (0, 0), as the position index becomes larger, the total amount of the same radial wave number becomes larger. Since the total number of the radial wave coefficient are placed in the denominator position, the mean power spectral density has a great chance being smaller as the radial wave number becomes larger, as shown in both Figure 6.1 and 6.2. However, when the index position gets very large, for example, towards to the upper right corner, the total amount of the same radial wave number does not exhibit the same trend as for the starting positions. For example, for the last position which is 256 by 256, the corresponding radial wave number is 362 and this is the only one number, and the mean power spectral density for 362 would be very large and this is shown in Figure 6.2. The fractal dimension values for test 2 for both scenarios would be non-realistic and are not reported here.

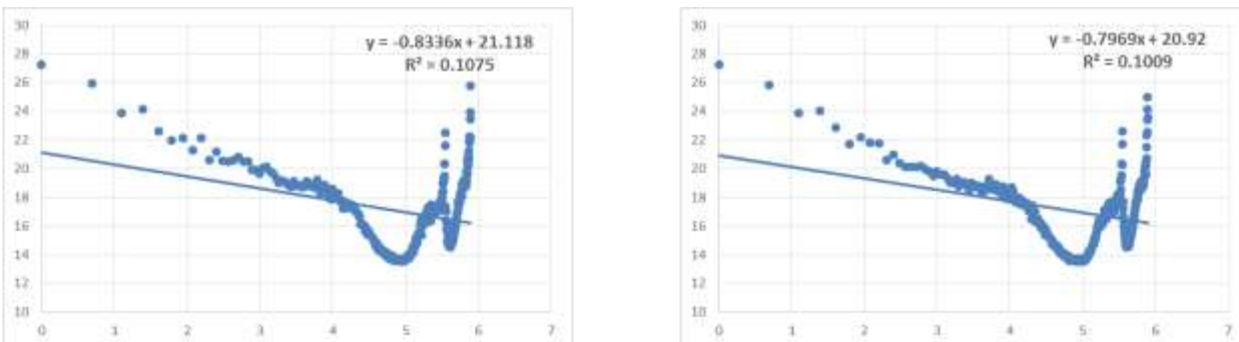

(a) Origin From Upper Left

(b) Origin From Lower Left

Figure 6.2 Regression Plots Using Full Radial Wave Number (horizontal axis: log form of radial wave number; Vertical axis: log form of mean power spectral density)

Instead of using the full radial wave number for the first and second tests, the third test aims at reorganizing the number of radial wave number used for the independent variable for the regression. The procedure of the third test is to combine two radial wave numbers and treat them as a pair and gives them new radial wave numbers. For example, the first pair would be the original radial wave number 0 and 1, combine them and give them a new radial wave number 1. Follow this manner, for the same test image of 257 by 257, the new radial wave number used for regression would start from 1, 3, 5 and until 257, and the total number is 129. This new procedure guarantees that all the mean power spectral density values are included. In addition, for the mean power spectral density values associated with large wave number, the total number increases and this may make the plot of the regression points approaching to a linear trend. Figure 6.3 shows the regression plots using this procedure for acquiring the global fractal dimension values.

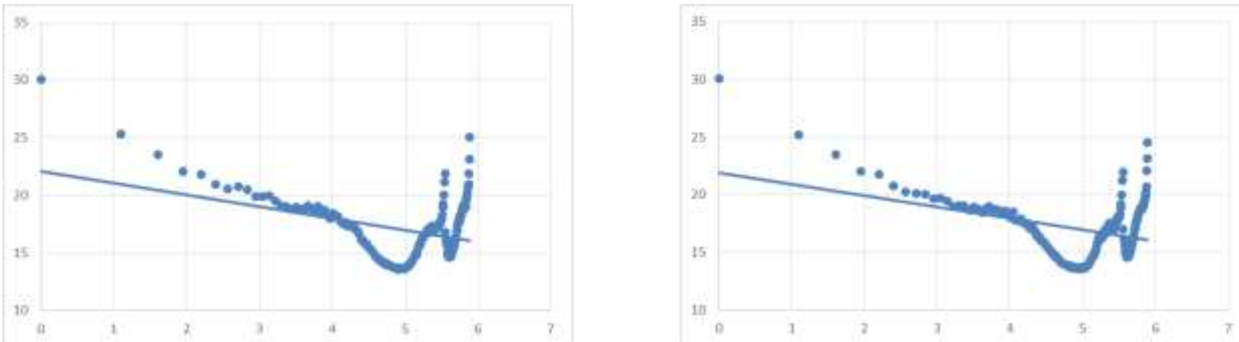

(a) Origin From Upper Left

(b) Origin From Lower Left

Figure 6.3 Regression Plots Using Alternative Sampling of Radial Wave Number (horizontal axis: log form of radial wave number; Vertical axis: log form of mean power spectral density)

With this new procedure of sampling the radial wave number, the regression plots display similar trend with the results of the second attempt, even though the number of regression points decreased. This alternative way of sampling the independent variable, for higher radial wave number, does not decrease the values of the power spectral density. For the beginning of the regression, the quantities of the dependent variable slightly changed, but they are not affected much by this procedure. The equations and the R squared values are not reported for this third attempt.

Based on the previous three tests, using various sampling strategies for the radial wave number, the Fourier transform approach generates different regression trends. The first test has the highest R square value, even though it is only 0.4. All of the tests fail at reporting a realistic global D value because of the nonlinear tendency of the regression. For the power spectral density value, it seems to contain redundant or noisy information as the radial wave number increases in the frequency domain. In other words, the higher radial wave number or frequencies consist of insignificant information for the original image. The first attempt tells us that the important information in the frequency domain is within the radial wave number from beginning to roughly 5 after transforming into a log form. In this way, not all the frequencies have to be included in the regression analysis. In other words, only a subset of all the frequencies should be included in the regression analysis. Furthermore, the starting position is not a factor for the Fourier approach, for each attempt, the paired regression analyses display highly similar results in terms of the equations and the general trend. Therefore, the following analysis concentrates on the starting position located at the upper left of the digital image.

In order to achieve the goal of having only the useful information of power spectral density, some of the large radial wave number need to be removed. Figure 6.4 and 6.5 displays the regression results using two sampling methods. Figure 6.4 uses the sampling method which starts from 1 until half number of the maximum radial coefficient. For this test image, the largest radial coefficient would be 362 and the maximum radial wave number used in the regression is 181. Figure 6.5 uses a different sampling method which starts from 1 until half number of the image size. For both of the cases, the step interval is 1 so this ensures that there are sufficient number of regression points even when the image size is small. It can be seen from the regression plots that the second sampling method results in a more linear trend than the first one. The first regression plot has an increasing tendency at the end for some of the large radial wave number. R square values are 0.9054 and 0.9106, respectively, and these values have been greatly improved from the previous regression results. The fractal dimension values are 2.6143 and 2.6012, respectively. These D values are slightly larger than the results of the same image using triangular prism method and differential box counting method which are 2.4976 and 2.4643.

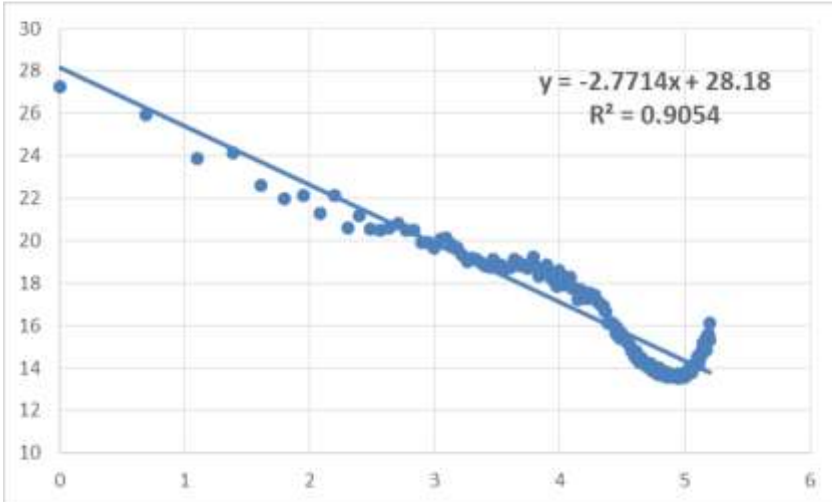

Figure 6.4 Regression Plot Using Half Radial Wave Number of the Maximum Radial Coefficient (horizontal axis: log form of radial wave number; Vertical axis: log form of mean power spectral density)

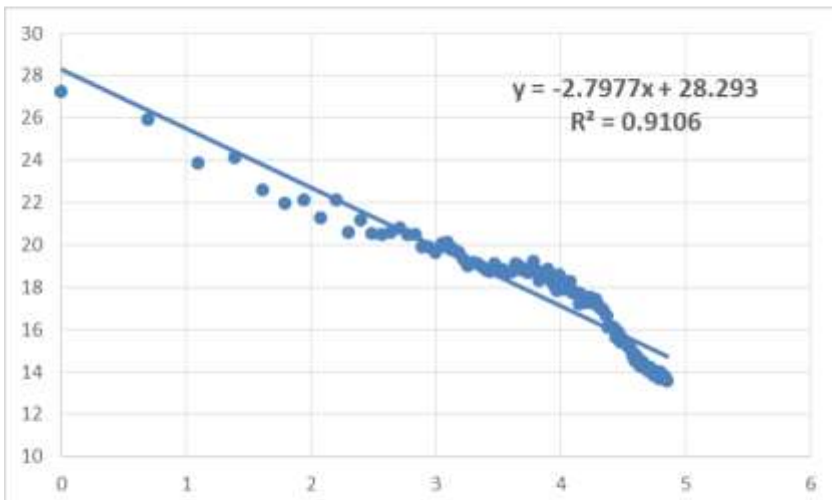

Figure 6.5 Regression Plot Using Half Radial Wave Number of Image Size (horizontal axis: log form of radial wave number; Vertical axis: log form of mean power spectral density)

Based on the previous test, the half number of the image size should be the maximum radial wave number used in the regression analysis. For the sampling issues, there are still some variations can be added to the Fourier approach analysis. Another sampling method which is used by the triangular prism method is a series of geometric steps using power of 2. The advantage of this sampling method is that it can reduce the computation complexity since it only requires several regression points. Figure 6.6 shows the regression results of using this sampling method. The regression points space evenly and look similar to the previous methods. The R square value is again increased from previously 0.91 to 0.97, which is an extremely high value for a regression. However, the slope becomes smaller and the corresponding D value is 2.6905. This D value, close to 2.7, seems not in the same complexity level with 2.5 which is an approximate number of the D values for the previous methods. Moreover, using geometric sampling method, the result D value is larger than using the consecutive sampling method (Figure 6.5).

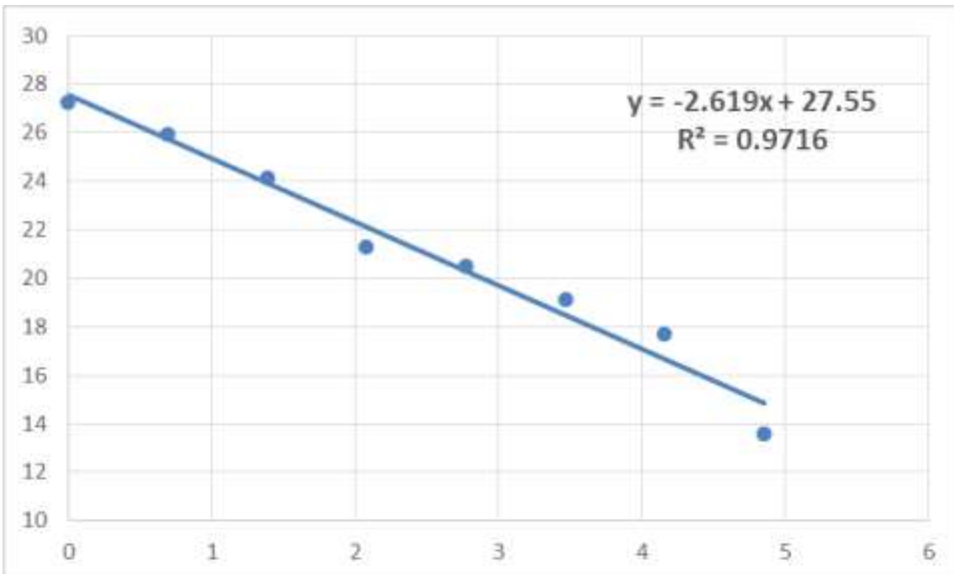

Figure 6.6 Regression Plot Using Geometric Steps (horizontal axis: log form of radial wave number; Vertical axis: log form of mean power spectral density)

Our goal for the results of the Fourier spectral approach is to acquire a fractal dimension with a similar value to the triangular prism and differential box counting method, as well as the R square value should be high for the regression. For all of the previous tests, the first frequency, the power spectral density of the origin has not been employed in the fractal analysis. Based on the previous two attempts, using consecutive and geometric intervals, the following analysis includes the power spectral density associated with the first radial wave number. Since the radial wave number of the origin is 0, the sampling method is adjusted that the radial coefficient plus one is the corresponding independent variable value. Figure 6.7 and 6.8 are the results of the regression analysis using this strategy. The power spectral density associated with the first radial wave number is the largest that can be seen from the following figures. The

R square values are both larger than 0.9, and the slopes are both between -3 to -4. According to the new slopes, the D values are 2.4584 and 2.3595. Because of the incorporation of the first radial wave number, the slopes of the regression line clearly changed and both of the D values become lower than the previous results. Comparing with the result of the other two methods used in previous chapter, the D value of 2.4584 is quite close, that all of these three methods generate approximately the same D values of 2.5 for the same test image. It is noticeable that, for the Fourier spectral approach, the surface complexity information contained in the first half radial wave number are all important for yielding accurate D value.

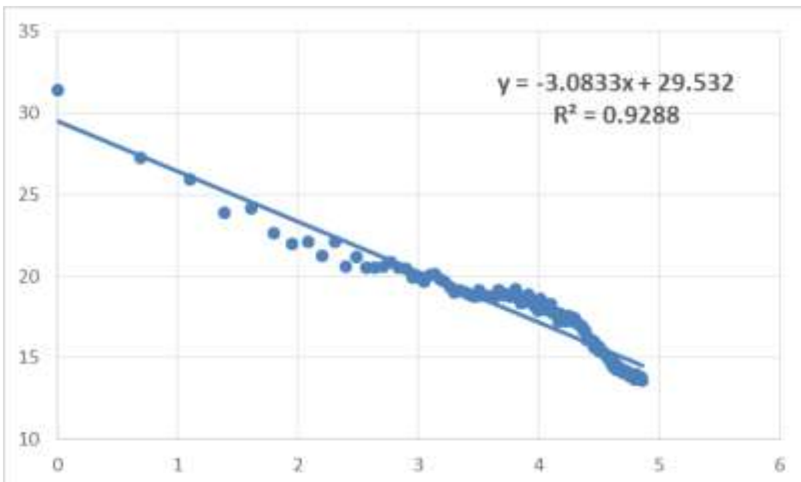

Figure 6.7 Regression Plot Using Consecutive Steps Including Origin Radial Coefficient (horizontal axis: log form of radial wave number; Vertical axis: log form of mean power spectral density)

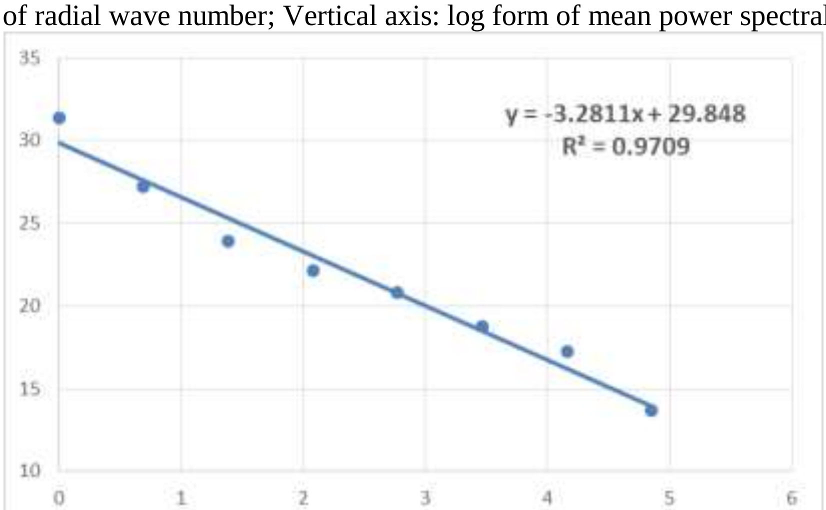

Figure 6.8 Regression Plot Using Geometric Steps Including Origin Radial Coefficient (horizontal axis: log form of radial wave number; Vertical axis: log form of mean power spectral density)

Throughout all the previous testing and comparison of the Fourier spectral approach based on various sampling methods and maximum radial wave number, the strategy utilized for generating the regression plot shown in Figure 6.7 is more preferable to all the other sampling method and will be employed for the following global and local fractal analysis. To further analyze the effectiveness of the Fourier spectral approach for the entire image, a test is carried out using four subsets (Figure 6.9). Each of the subset is extracted from the original aerial photography and the image size is 257 by 257. Four different land covers: water, forest, parking lot and residential areas are selected for this analysis. These four land covers exhibit different surface complexity and the goal is to verify whether the global fractal dimension values resulted from the Fourier spectral approach is comparable to the triangular prism method and the differential box counting method.

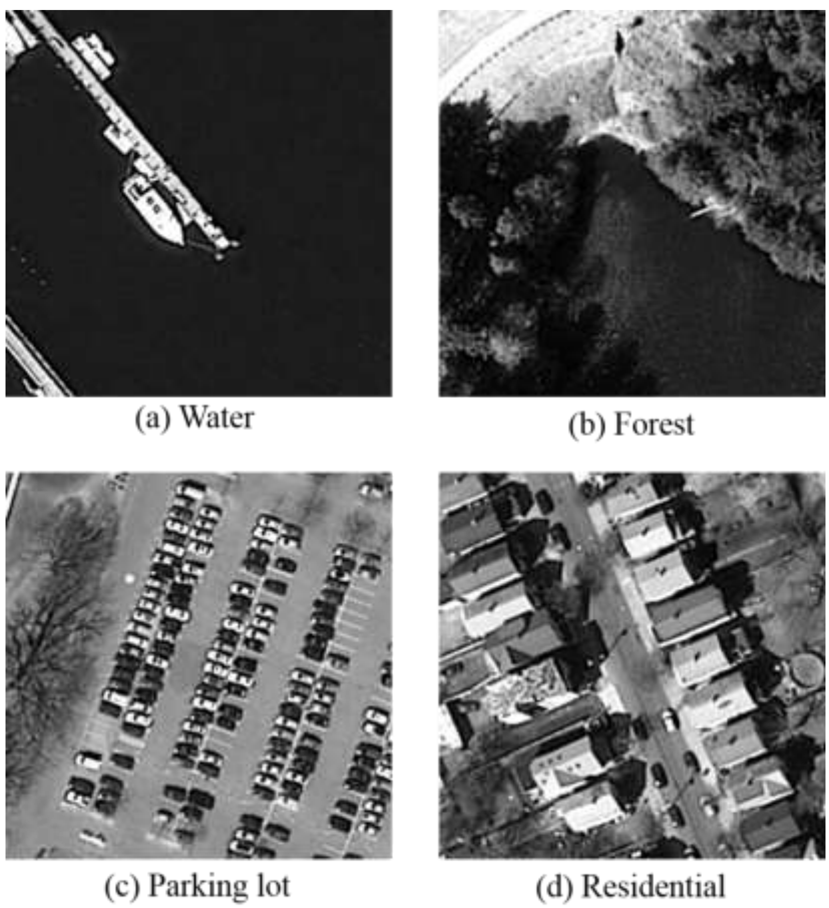

Figure 6.9 Fractal Methods Comparison between All Methods

All the fractal methods are used for computing fractal dimension values for the four subsets. For the Fourier method, both of the two sampling methods: the arithmetic and geometric step sampling methods are included in the analysis. The resultant global D values of each land cover for each method are listed in Table 6.1. Among the methods, the triangular prism and differential box counting method generate similar results, which is consistent with the results from chapter five. It is difficult to recognize the level of the surface complexity based on the visual of the four images. Figure 6.9 (a) exhibits the lowest fractal dimension values for the methods of triangular prism and differential box counting. The Max difference version of the triangular prism method yields the smallest D value for the water body surface. The forest area somehow has slightly larger D values than the water area. The most complex land surfaces are parking lot and residential areas, that both of the triangular prism and differential box counting methods have the largest D values than the water and the forest areas. Parking lot and residential areas have the similar D values, which is as expected that the both of the two land surfaces exhibit regular landscape of objects with relatively high complexity.

As for the Fourier spectral method, the result is quite different from the one acquired in last analysis. In last analysis, the resultant D value of the Fourier spectral method using the arithmetic sampling method is considered to be as the same as to both the Triangular and box counting methods. However, when it comes to this new set of four images, the results of the Fourier method of Figure 6.1 (a) is much larger than the rest methods using both of the arithmetic and geometric sampling methods. It is interesting that Figure 6.1 (a) exhibits very similar image complexity to Figure 5.14 but the results of using Fourier arithmetic step are almost 2.67 compared to 2.46, respectively. For the other three images, the results of using arithmetic sampling method seems comparable to the other two methods. The geometric sampling method produces a similar trend of four D values that the water and parking area show the same surface complexity.

Table 6.1 Global Fractal Dimension of All Methods

	Water	Forest	Parking	Residential
Fourier Arithmetic Step	2.6699	2.5240	2.6433	2.5075
Fourier Geometric Step	2.6002	2.4659	2.6069	2.5637
Triangular	2.4786	2.5413	2.6830	2.6301
Max Triangular	2.3530	2.4988	2.5413	2.5293
Mean Triangular	2.5586	2.5969	2.6556	2.6039
Eight Triangular	2.5167	2.5842	2.6534	2.5962
DBC	2.4334	2.5023	2.5935	2.5860

Overall, both of the arithmetic and geometric sampling methods of the Fourier spectral approach can yield fractal dimension values, which are comparable to the previous two methods. The images, with the similar surface complexity, that the Fourier spectral method yields different D values, may result from the distribution of the DN values of the images, or because there does have difference in surface complexity and the D values reflect it. Next, the local fractal dimension values are computed based on both arithmetic and geometric sampling methods. Because the local analysis always involve the spatial information and the position and recall that, the Fourier spectral method employs two different origins for computing the global D values. Thus, the next analysis utilizes both of the two origins as well as the two sampling methods to report the results of the local fractal dimension of the Fourier spectral method.

6.3 Geographically Weighted Fractal Analysis of the Fourier Spectral Approach

The general way of incorporating the spatial weights for the Fourier spectral approach is based on the position of each radial wave number. Because each radial wave number is associated with a complex coefficient, we treat the position of each radial wave number as the position of each observation. The spatial weights are multiplied to the square of the magnitude of the complex coefficients. Then the procedure is the same as computing the global fractal dimension. Figure 6.10 presents the results of using the arithmetic sampling method for the origins starting at the upper left corner. It is still the same 257 by 257 image used for Triangular prism and differential box counting method for the geographically weighted fractal analysis in Chapter 5. This analysis uses bandwidths of 30 and 70 feet with the Gaussian kernel. Recall that the average D value for this particular sampling method is 2.4584. The range of the fractal dimension values for bandwidths 30 and 70 feet are 2.3425 - 2.5694 and 2.3906 - 2.5124, respectively. It is noted that the average value of 2.4584 is within the range for both of the bandwidths. Furthermore, as the bandwidth becomes larger from 30 to 70, the range becomes narrower, which starts converging to 2.4584. The change of the bandwidth does not seem to dramatically affect the range of the results, which is unlike to the results of the previous methods, for example, the triangular prism method. It is as expected that using this particular method of the Fourier spectral approach, the geographically weighted scheme can be added to the Fourier method. The use of the radial wave number as the observation position seems promising for further exploration between the GW scheme and the Fourier approach. One issue raised here is that the starting position of the Fourier transform seems to be an influencing factor especially for the local analysis.

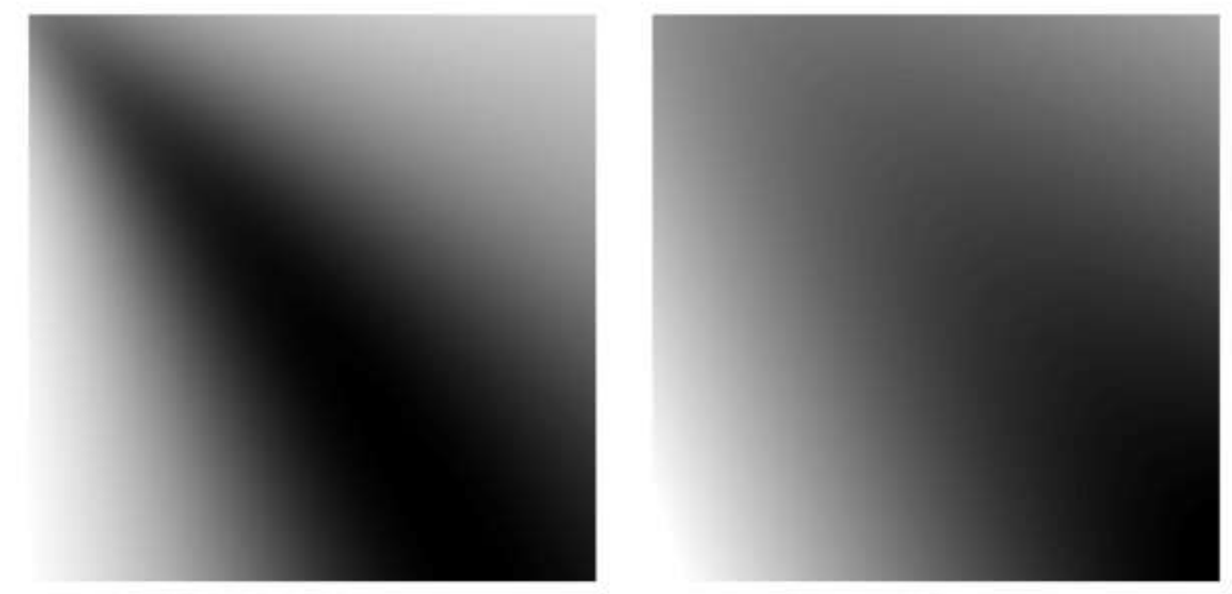

Figure 6.10 Geographically Weighted Fractal Dimension Values for Arithmetic Sampling Method Starting At Upper Left Corner

Figure 6.11 shows the local fractal distribution of the Fourier spectral method using the arithmetic sampling method with the origin starting from the lower left corner. The global D value of using this strategy is 2.4882, which can be treated as the same as the value of 2.4584 result from Figure 6.10. This is consistent with the global analysis of the Fourier spectral method that the position of the origin does not affect the average D value. However, it can be seen from Figure 6.11, that the radial wave number starts from the lower left corner, the distribution of the fractal dimension values flips over to the lower left origin correspondingly. Similar to Figure 6.10, for bandwidth of 30 feet, it clearly shows that the low D values are centered in the diagonal direction. For geographical weighting scheme of bandwidth 30 and 70 feet, the range of the local D values becomes narrower. Both of the ranges enclose the average D value of 2.4882. Compare with the last analysis, for bandwidth 30 feet, the smallest D values are 2.3416 and 2.3425, respectively, the largest D values are 2.5944 and 2.5694. For bandwidth of 70 feet, the smallest D values are 2.4104 and 2.3906; the largest D values are 2.5366 and 2.5124, respectively. The change of the positions of the radial wave number switches the diagonal direction of the distribution of the D values but the pattern stays the same.

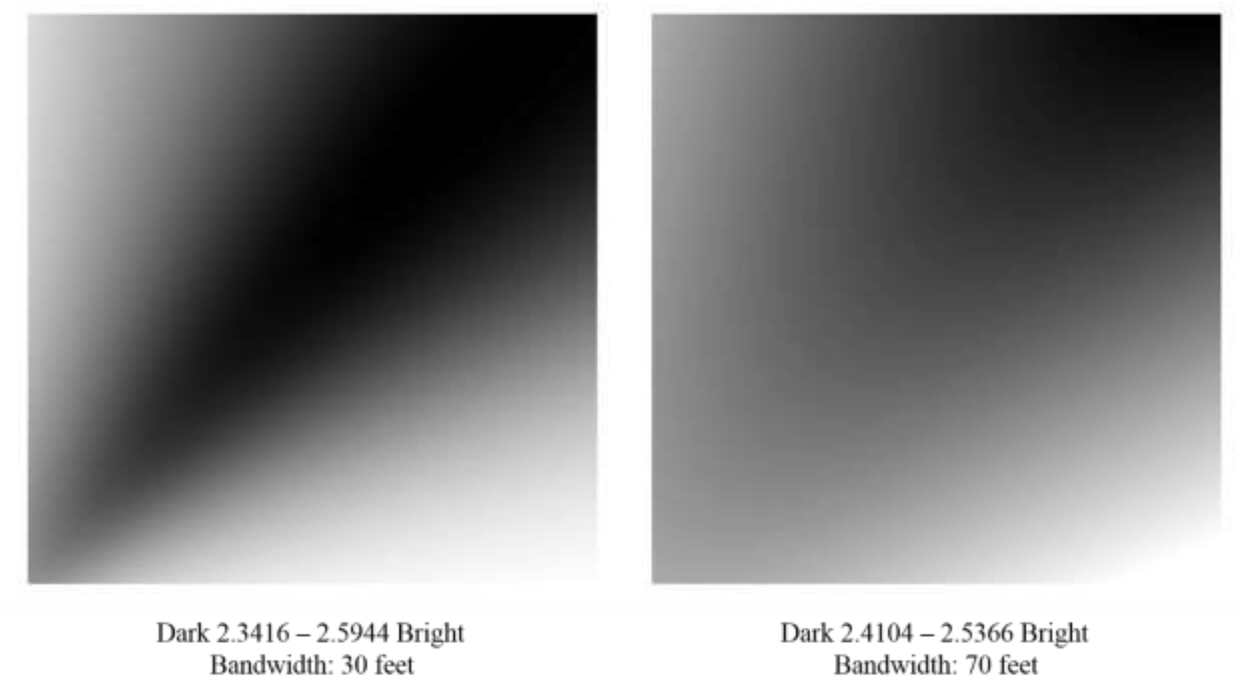

Figure 6.11 Geographically Weighted Fractal Dimension Values for Arithmetic Sampling Method Starting At Lower Left Corner

Figure 6.12 displays the results of the distribution of the local D values of the Fourier spectral method using the geometric sampling based on the lower left corner. The corresponding average D value using the geometric sampling method is 2.6155, which is greater than using the arithmetic sampling method. Similar to the previous local fractal analysis, using the geometric sampling method also obeys the rule of the geographically weighted scheme. However, the resultant D values of using the geometric sampling method may not be as good as using the arithmetic strategy since the computed values are much greater than the D values computed from triangular prism and differential box counting. The pattern of Figure 6.12 is similar to the results that starting from the upper left corner. Regardless to the bandwidth effect, the pattern of using the geometric sampling method does not reflect the surface complexity of the sample image.

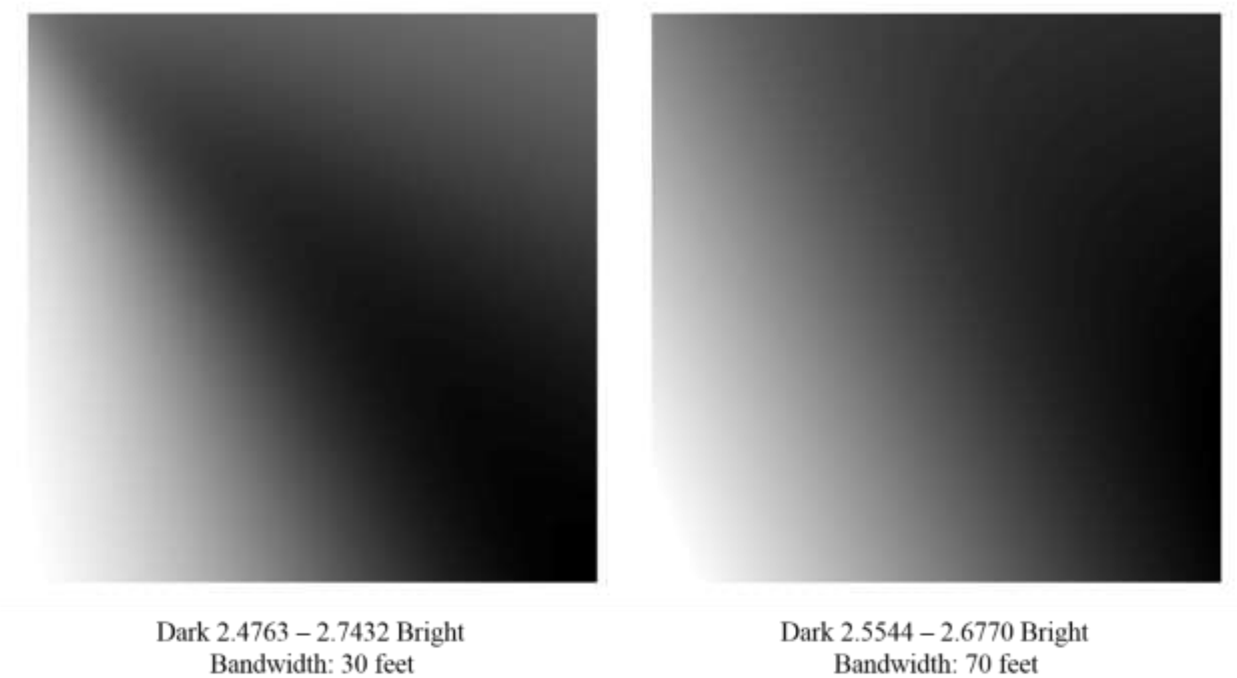

Figure 6.12 Geometrically Weighted Fractal Dimension Values for Geometric Sampling Method Starting At Lower Left Corner

6.4 Summary

Chapter 6 mainly presents the analysis of the Fourier spectral method for computing fractal dimension values. The Fourier spectral method has not drawn much attention to the researchers regarding to the fractal analysis since it is complex in computation. In addition, there are already many other fractal approaches which are easy to implement and can be utilized to analyze the images for characterizing and quantifying the surface complexity. This chapter attempts to compute several fractal dimension values based on the discrete Fourier transform (DFT). The geographically weighted scheme has been incorporated into the Fourier spectral approach for an exploration of the local fractal dimension analysis.

The Fourier spectral approach is first used to analyze the global fractal dimension values. We carried out some initial attempts using various combination of parameters and try to yield the best fit of the Fourier method. The origin of the transformation does not affect the results much. Several regression plots reveal that the R square and the regression equation are very similar for both of the upper and lower starting points. The number of the regression points are another considered parameter. The regression plot show that there are many redundant information if using full number of the radial wave number. These unnecessary information appears with the complex coefficients associated with the large radial wave number which causing a nonlinear distribution of the regression points. All these mean power spectral density values associated with the large radial wave number gradually become large values approaching to the small radial wave number, which makes the regression plots going up and down. At last, the radial wave number decrease to the half number of the image size starting from radial wave number of zero. The global fractal dimension value comes close to the values acquired from the triangular prism and differential box counting method.

Then we carried out a local fractal analysis based on the global result of the Fourier spectral method. The logic of constructing a geographically weighted fractal dimension is similar to the manner used for the previous two methods. Different from the other two methods, which treats the center of each grid window as the observation position, the Fourier spectral method utilizes the existing positions of the radial wave number as the observations. Similarly, for each observation or radial wave number, there are many locations distributed across the image and all of these same values need to be added. The distribution of the geographically weighted fractal dimension values somehow reflects the origin of the Fourier transform. It is encouraging that the scope of the local fractal dimension values become smaller as the bandwidth changes from 30 to 70 feet. However, even though the behavior of the Gaussian kernel function seems to work for the Fourier spectral method, the distribution of the local D values demonstrate a clear pattern, which is consistent with the Fourier transform of the frequency domain instead of the actual surface complexity of the test image.

Chapter 7 continues with the fractal analysis for real remotely sensed images. It utilizes the fractal approaches employed in this dissertation research to carry out an empirical analysis of the fractal characteristics of New York City and Houston. Instead of the analysis of method exploration, Chapter 7 emphasize on the fractal applications for urban areas to reveal the landscape similarity and differences between these two cities.

Chapter Seven

Analysis of Fractal Approaches on Remotely Sensed Images

7.1 **Introduction**

The previous two chapters mainly focused on exploring the fractal methods approaches for characterizing the geometric complexity of the surfaces using the indicator of fractal dimension, which is considered to be an average value for summarizing the whole study area. Then the focus is to develop local fractal dimension values using the geographically weighted scheme. The geographically weighted fractal dimension is acquired using several test images for various bandwidths. Also, the previous chapters compare three fractal methods based on the resultant D values. Chapter 7 continues with the fractal methods and switch from the method exploration to empirical analysis of fractal methods based on remotely sensed images of urban area.

Aerial photograph presents to us a fine spatial resolution that the earth surface can be visualized clearly for various land covers. However, one aspect about aerial photograph is that it can only cover limited earth surface within one photograph and this may restrict the large area analysis of land use and land covers. On the other hand, the aerial photography is suited for fractal method exploration, especially for the local fractal analysis because it has 1 foot spatial resolution and this simplifies the distance calculation for the geographically weighted scheme. However, when it comes to the empirical analysis of the urban area, the remotely sensed images are preferred because with the same size to the aerial photography, the remotely sensed images can cover more grounds than the photography, and the global D value could be a meaningful metric for describing the surface complexity. Therefore, this chapter is designed for using an alternative dataset, the remotely sensed images, to further examine the fractal approaches based on a study area of city settings.

In order to examine whether the fractal methods can effectively describe the geometric complexity of the real earth surface, this chapter uses two urban areas for a comparison purpose to implement this goal. It is not important to examine several single fractal dimension values in a stationary manner, but to compare all these D values of the studied urban area in a dynamic way. This is more meaningful to provide us the intrinsic characteristics of the studied urban surfaces. In this chapter, the surface complexity is mainly studied in a 2D manner and this is the metric for revealing the information whether a city is undergoing a dramatic landscape change.

The morphology of the urban area has been studied using the fractal geometry concept and the quantity of the fractal dimension (Frankhauser 1998). For example, urban sprawling is one of the phenomena, which usually results in an irregular form of urban development. Relate to the focus of this chapter, instead of studying the boundary line of a city, it is desired to examine the surface feature of the various urban areas. Even though studying the surface feature may not describe the horizontal change, it can characterize the vertical change of the studied surface, which is another important fractal information that can be combined with the morphology results for a better understanding of the urban development.

As stated earlier, using fractal tools to examine the texture characteristics of remote sensing images is necessary. For the urban area limited to cities, the remote sensing study becomes to local scale (Liang et al. 2013). The major issue of the urban area is the heterogeneity of the land covers, which challenges the researchers to use the fractal analysis to interpret the structural characteristics of the urban features. Therefore, it is recommended to focus on the overall surface complexity across the spatial domain for urban study. Fractal geometry is a powerful indicator that it can capture the entire variation of the surface complexity as a whole, the summary value examined in the previous chapters, which is appropriate for urban land use measurement. Many urban areas have been studied using wide range of the fractal methods to understand the fractal characteristics based on different perspectives (Table 7.1). In the table, for the method column, some of the studies use the common software package, which is mentioned previously known as ICAMS for computing the fractal dimension values. This software provides the ability to compute the texture features of the surface using the three commonly used fractal algorithms: Triangular prism, isarithm and variogram methods. These three methods are replaced by ICAMS in the table.

Table 7.1 Image Complexity of Various Urban Areas

Indianapolis, IN	Liang et al. 2013	ICAMS software
Fuzhou, China	Luan et al. 2012	Triangular prism Fractal Brownian Motion Differential Box Counting Multi-fractal
Baton Rouge, LA	Myint 2003	ICAMS software
Los Angeles, CA	Qiu et al. 1999	Isarithm Triangular prism
Huntsville, AL	Emerson et al. 1999	Isarithm
Lake Charles, LA	Lam 1990	Isarithm Variogram
Atlanta, GA	Lam 2004 Emerson et al. 2007	Triangular prism Triangular prism

Most of these studied urban areas are U.S. cities. Among them, Atlanta, GA has been studied twice by different scholars and both of them used the triangular prism method. Almost every study utilized the ICAMS software package for computing the fractal dimension values. These studies used either the three methods programmed into the software or only one or two methods. Besides the fractal methods, these studies also employed several other spatial statistical metrics such as Moran's I, to compare with the resultant surface D values. It can be seen from the table that the triangular prism method is the most popular one used for computing D values for the urban area. The following analysis examines the New York City and Houston, which have not been studied before in the domain of fractal analysis. Furthermore, the selected methods also examine the scale and the temporal aspects of the fractal property.

7.2 Landscapes of New York City and Houston

New York City is located in the northeastern region of the United States and it is the most popular city in the country. It is considered as the most famous world's city with many leading fields. Among all these outstanding categories, New York City is best known for its central place of the world's finance and politics with the Wall Street and the United Nation. New York City has an estimated population of 8,537,000 in 2016 and it is ranked number 1 in United States. The population spreads out in a land area of roughly 784 km^2. New York City is settled in 1624 and consolidated in 1898 with a development of approximately 400 years.

Houston is the most popular city in the state of Texas and a major city in the United States. It has a population of 2,303 million in 2016 and it is the fourth largest city in the nation. Houston is situated in southern United States and it is the largest city in this region. It has a total area of 1,730 km^2 ,which is larger than New York City, which has a total area of 1,213 km^2. Houston has massive land area with less population than New York City, which make Houston not a dense city. Houston is incorporated in 1837 with development of approximately 180 years. Houston has a broad economy industry and it is famous for its NASA's Johnson Space Center. Houston is the center of the Texas Medical center, which is the world's largest institute for health and research. As an important city in southern U.S., Houston has the number of the Fortune 500 headquarters more than any other U.S. cities except New York City.

New York City has many different landscape features made by nature and human beings. People recognizes New York City as a coastal city because it is located in the mouth of the Hudson River, which naturally extends to the Atlantic Ocean. This natural location provides New York City great opportunities for trading business and it has grown as a trading city since then. The city consists of three islands: Long Island, Manhattan and Staten Island. Because of its densely populated characterization, New York City is undergoing scare land use situations. Among the total area of 1,213 km^2, 429.53 km^2 is water area, which is one third of the total area. The most famous green area in the city is the central park in Manhattan borough. New York City has been substantially intervened by human being for urban development. The Manhattan area is the main place, which was altered significantly for several decades. The land reclamation primarily happened along the shore and waterfront and an example is the Battery Park City during 1980s. The financial district Manhattan has become the city symbol attracting visitors. Many high-rise buildings such as Empire State Building, MetLife tower are concentrated in Manhattan. Some of the skyscrapers are recognized as the tallest buildings in the world.

Houston has a total area of 1,700 km^2 where only 58 km^2 area are covered by water. Compared to New York City, which has a total area 430 km^2 of water, Houston is mainly covered by massive land area. Most of Houston city is located in the gulf coastal plain. Because of its southern location, Houston is filled with various forest and grassland. The highest point of Houston is roughly 38 m in elevation. There are four major bayous in the city, which are Buffalo Bayou, Houston Ship Channel, White Oak Bayou and Brays Bayou. The topography of Houston city is flat, which makes the city tend to draw flood easily. Houston has developed five business districts throughout the city and this makes Houston the third largest skyline in the United States after New York and Chicago.

7.3 **Fractal Analysis of Scale Effect**

As mentioned earlier, scale effect is an important aspect of the fractal analysis. As for the remote sensing images, the surface complexity is different from the real fractals, which means the fractal results of using the regular remote sensing images may not reflect the property of the scale independence of the fractals. In fact, when the scale changes, the purpose of using fractal method is to compute several fractal dimension to observe the trend of the D values. For remotely sensed images, within the range of the selected spatial resolutions, it is desired to observe some of the D values forming a curvy trend instead of some equal values. For different bands of the remote sensed images, it may have contrasting behavior of the D values, which may reveal some information for band selection when dealing with specific land cover types. This section intends to examine the scale effect using the test images (Figure 7.1). The test images use the New York City as an example for scale exploration.

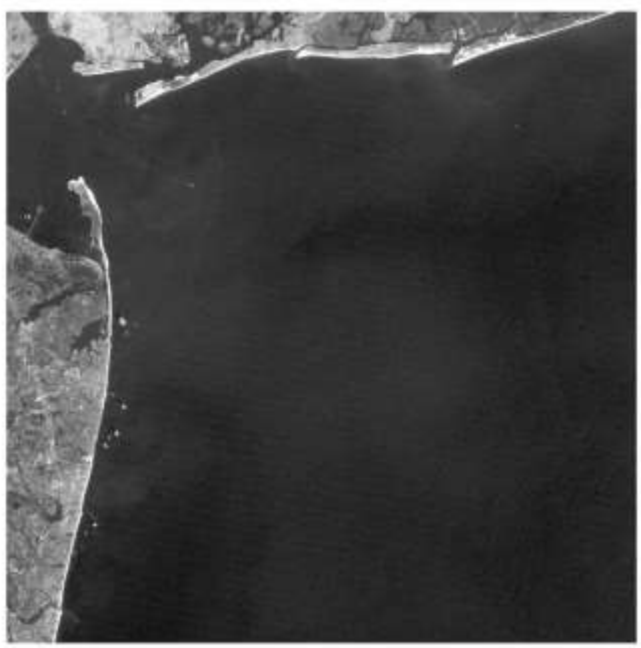

Figure 7.1 Green Band of Coastal Area of Landsat Image

Figure 7.1 displays a test image subset from New York City image acquired by Landsat at 2010. It shows the single green band with an image size of 2049 by 2049. The majority of the image is water body. The overall surface complexity should be low. To simulate the scale effect on fractal dimension values, the spatial resolution needs to be changed for computing a series of fractal dimension values. The original spatial resolution is 30m. Because of the computing complexity of the Fourier transform method, it is not considered for this analysis. Instead, the triangular prism, Max-difference and the differential box counting methods are employed for this analysis. To be consistent with the method, the used spatial resolutions are 30m, 60m, 120m and 240m. Figure 7.2 presents the results of the change of the fractal dimension values using these three methods. Three methods demonstrate different behaviors of the fractal dimension values against spatial resolution. Triangular prism and its Max-difference version has the similar trend of D values according to the change of the spatial resolution. The triangular prism method has the lowest D values for all the four spatial resolutions. Among them, the lowest D value is 2.0667 with a spatial resolution of 30m. The Max-difference method shows slightly larger D values than its original method across the four scales. From scale of 30m to 240m, both of the methods yield constantly increasing D values. For resolution of 240m, they have very similar D values of 2.1872 and 2.2077.

On the other hand, the differential box counting method presents a different trend compared to the other two methods. For scale of 30m, the DBC method has a D value of 2.3872 which is much larger than the result of triangular prism method. The differential box counting method seems a scale-independent method that it yields four fractal dimension values which are 2.3872, 2.3771, 2.3722 and 2.3314. These four values are quite the same in fractal perspective. Instead of increasing its D values, the DBC produces a steady trend against the spatial resolution change. For the resolution of 240m, the D values of the three methods tend to converge to the same value. For test image similar to Figure7.1, the scale effect may not obvious because the majority of the image has the similar low DN values. With a low surface complexity contrast, the resampling technique may not significantly change the DN number and also the its distribution.

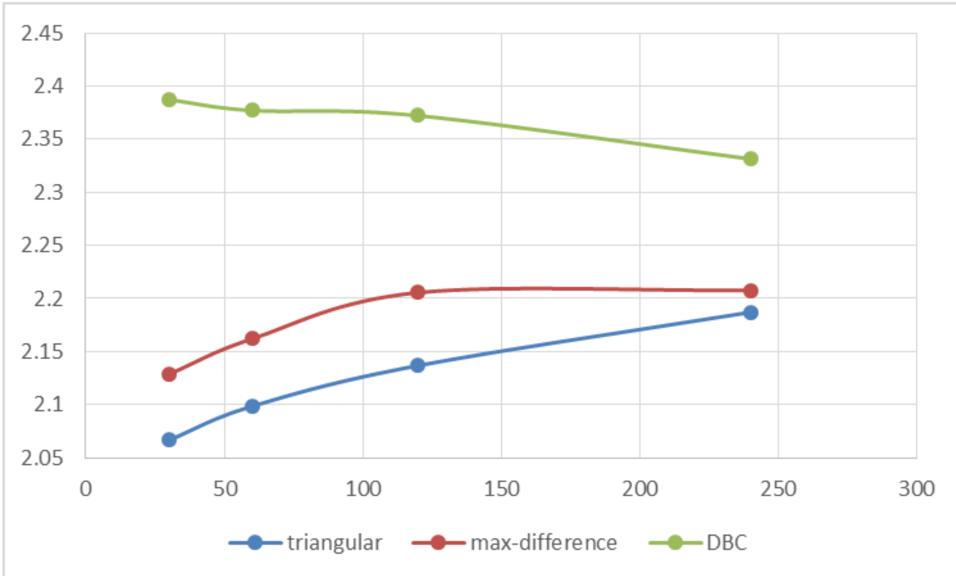

Figure 7.2 Fractal Dimension Values of Scale Effect of Coastal Area of Green Band (horizontal axis: spatial resolution of remote sensing image; Vertical axis: D value)

Figure 7.3 displays the same test image using the red band, its pixel DN values ranging from 13 to 228. Compare to the same area of the green band (Figure 7.1), it has the similar digital number distribution, that the green band has a pixel DN values ranging from 18 to 171. Follow the same manner, the same three methods are used for the scale analysis based on the red band. Figure 7.4 presents the results of the fractal dimension values change against the spatial resolution for 30m, 60m, 120m and 240m. The trend of all the three methods is similar compared to the results of using green band. Triangular prism method has a lowest value of 2.0925 at spatial resolution of 30m, compared to 2.0667 of the green band. The other three values of triangular prism method also has the similar D values to the green band for each of the spatial resolutions. The resultant D values of 60m resolution are 2.1334 and 2.0985, 120m of 2.1814 and 2.1369, 240m of 2.2412 and 2.1872, for red and green band. The general D value of using the triangular prism method of both two images is 2.20, which should be a correct value characterizing a coastal area with a large area of consistent water body. For both of Max-difference and differential box counting methods, they also yield comparable D values between each spatial resolution for green and red bands.

Figure 7.3 Red Band of Coastal Area of Landsat Image

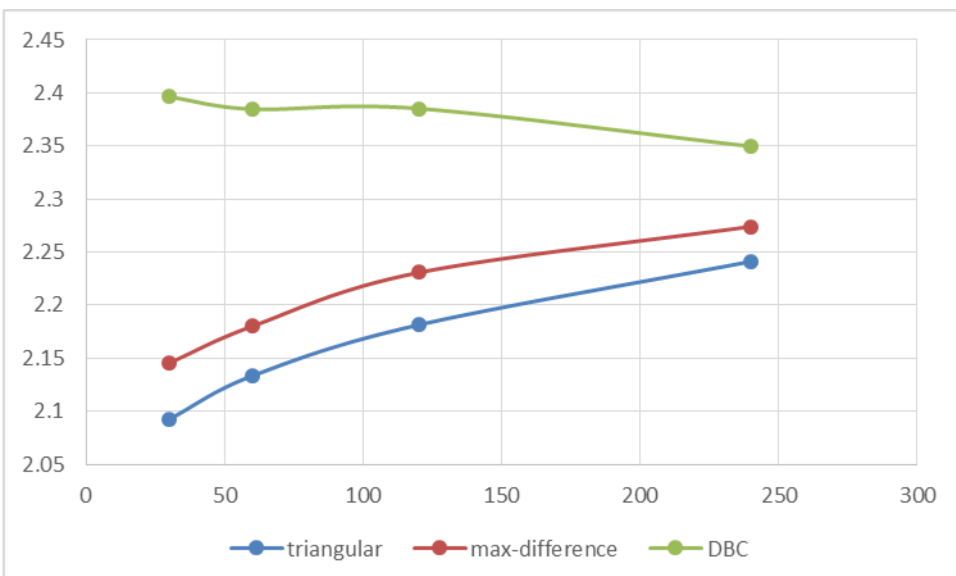

Figure 7.4 Fractal Dimension Values of Scale Effect of Coastal Area of Red Band (horizontal axis: spatial resolution of remote sensing image; Vertical axis: D value)

The coastal area has a low D value in general, for both of red and green bands, and the change of spatial resolution does not produce significant variation for any of the three methods. It is necessary to test a completely different land cover based on the same manner. The goal is to examine whether the change of spatial resolution can significantly affect the trend of the D values, if possible, for any of the methods. Figure 7.5 shows a test image covered not only water, but with many other land covers. Because of the resolution, it is hard to distinguish the land cover of majority. However, the selection criteria is to choose combination of bright and dark surfaces appearing intermitted. The image is again in green band with a size of 2049 by 2049. This image displays a much smaller body of water compared with the previous image. Figure 7.6 is the corresponding result of using this test image. The general trend of each of the three methods keeps constant that the fractal dimension values of triangular prism and max-difference methods are gradually increasing, and the differential box counting method yields steady D values. Each method has larger D values than its coastal test image for each corresponding spatial resolution. However, the results of the non-water area are not too large indicating the surface complexity of the non-water area is not high. The trends of Max-difference method and differential box counting method intersect at the large spatial resolution and Max-difference method produces the largest D value at spatial resolution of 240m.

Figure 7.5 Green Band of Non-water Area of Landsat Image

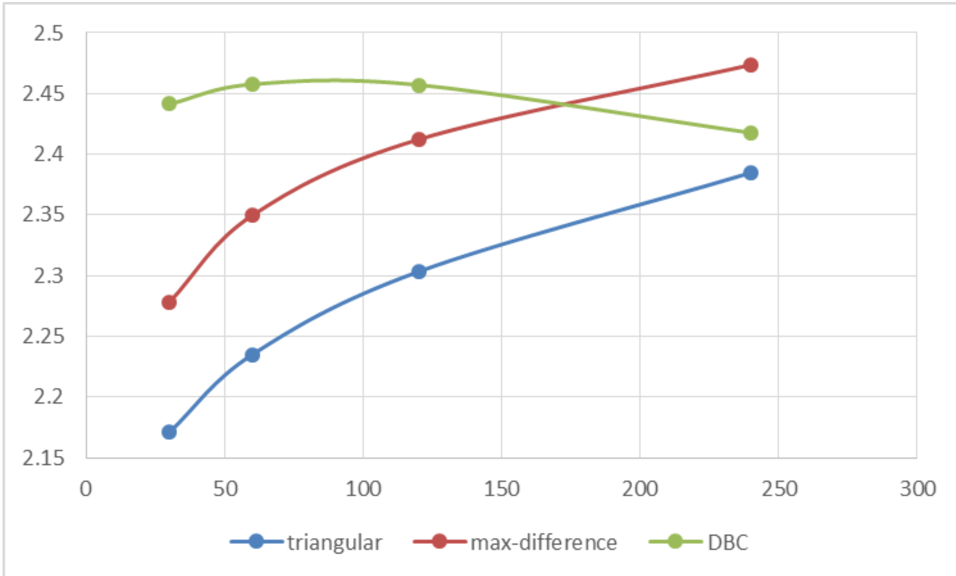

Figure 7.6 Fractal Dimension Values of Scale Effect of Non-water Area of Green Band (horizontal axis: spatial resolution of remote sensing image; Vertical axis: D value)

Figure 7.7 is the non-water area of red band corresponding to Figure 7.5. The range of the DN value is 13 to 255 compared to 20 to 211 of the green band. Figure 7.8 is the trend of the D values of using the red band. Different from green band, the results of the max-difference method intersects with the differential box counting method at 120m spatial resolution. Max-difference method seems increase its fractal dimension values quite fast according to scale change. Surprisingly, for spatial resolution of 240m, the differential box counting method yields the smallest D values and the max-difference method has the largest D value. Again, the triangular prism method constantly yields the smallest D values for small spatial resolutions. For resolution of 30m, all of the three methods compute larger D values than the green band image. Similar to the coastal test image, the results between green and red are not different for this more complex surface landscape area.

Figure 7.7 Red Band of Non-water Area of Landsat Image

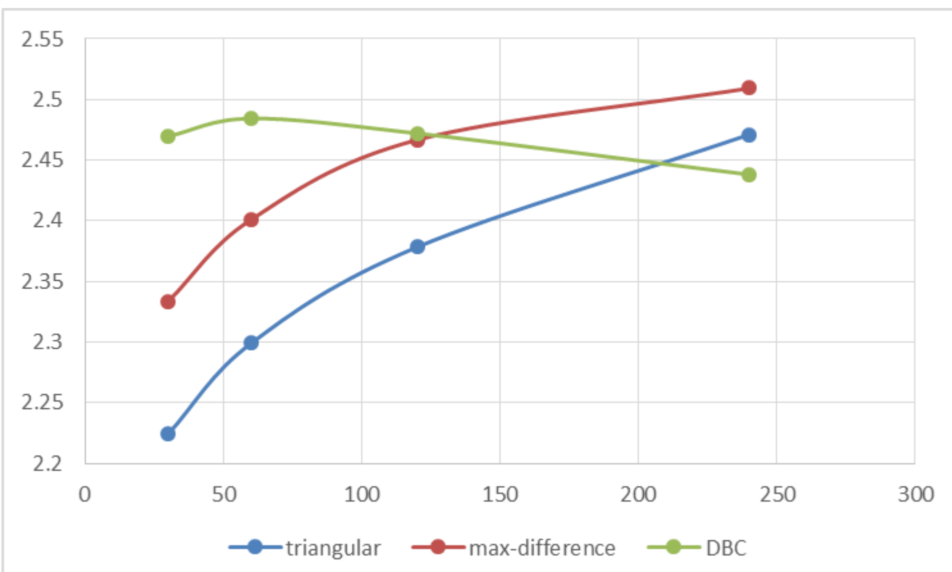

Figure 7.8 Fractal Dimension Values of Scale Effect of Non-water Area of Red Band (horizontal axis: spatial resolution of remote sensing image; Vertical axis: D value)

7.4 Time Series Analysis of New York and Houston

Besides scale analysis, another important analysis of fractal geometry for surface features is to compare landscape characterization between two cities located in different regions, as well as the surface landscape change between different periods. As mentioned earlier, New York City and Houston, two cities located in different regions in U.S., are considered for a time series analysis. For choosing the image representing the city area, the core location of the city is used for the basis, and then urban area is decided using the core location as a center and spread out to a certain image size. For a better distinction within cities for the surface characterization, a 16-year period is considered, that is year of 2000 and 2016. The years in between are not considered since short time periods may not affect the land cover change, and not change the fractal dimension values too much.

Figure 7.9 shows a study area from New York City, New York in two images of year 2000 and 2016 using their DN values in red band. The study area is defined by 513 by 513 pixels with a pixel size of 30m. The study area mainly covers the Manhattan Island at its center for the New York City metropolitan area. In general, a 16-year period may not have much significant urban development. Based on the visual comparison, some development occurred at the upper left region of the image.

Again, the same methods used in scale analysis are employed for the time series analysis. Each of the methods compute the two entire images for two global D values. The results of the D values for each method are shown in Table 7.2. From the table, we can see that the entire fractal dimension values are very similar. Specifically, for year 2000, the triangular prism method yields a D value of 2.4487. The other two methods also yield similar D values, which are 2.4545 and 2.4820. All these three values are under 2.5, which may indicate a medium surface complexity for year 2000. For year of 2016, triangular prism method again computes the smallest D value of 2.4101. Differential box counting method always have the largest D values among the three methods for both two periods.

For these two dates, the D values do not increase much, which means that the Manhattan area does not undergo much land cover changes. This corresponds to the visual examination of these two images. Furthermore, even though the DN values change across the study area, the fractal method is a useful tool to characterize the general surface complexity with some stable quantitative results.

New York City: 2000

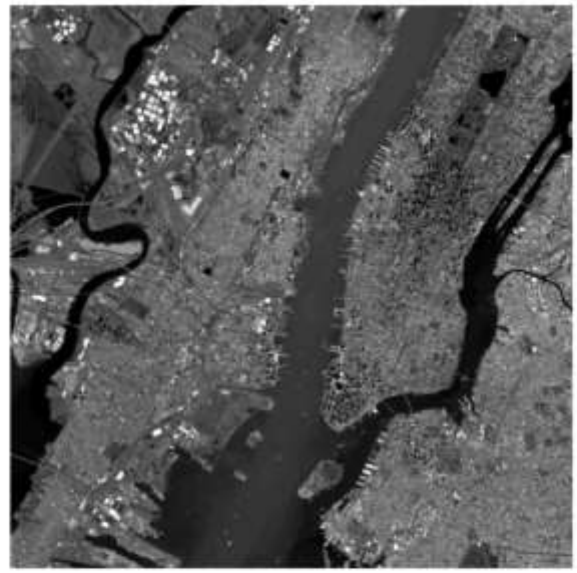

New York City: 2016

Figure 7.9 Images of New York City for Year 2000 and 2016

Table 7.2 Fractal Dimension Values of New York City for Year 2000 and 2016

	2000	2016
Triangular prism	2.4487	2.4101
Max-difference	2.4545	2.4418
Differential box counting	2.4820	2.4553

Figure 7.10 shows the study area from Houston, Texas in two dates of year of 2000 and 2016. The properties of the images of Houston are consistent with New York. This study area of the Houston metropolitan area is different from the New York City area. Figure 7.10 shows many roads systems and their branches, which appears more fractal than New York City. The fractal dimension values of Houston

is shown in Table 7.3. For year of 2000, all of the three methods yield very similar fractal dimension values, which is around 2.60. Similarly, for year of 2016, the three methods have approximately a general D value of 2.50. Compare between the methods between the two dates, there is no extreme D values among the methods, which suggest that the selection methods are comparable, especially between triangular prism method and differential box counting method.

For the two dates of the study area of Houston, the average D values are 2.60 and 2.50 for year 2000 and 2016, respectively. Based on the D values, this is not a dramatic change for a 16-year period. Examine these two images visually, there is a clear land cover change at the lower right region. Some roads can be seen at the lower right part of year of 2016, which is not appeared in the image of year 2000.

For the study areas of New York City and Houston, the fractal dimension values are similar for these two entire regions. For year of 2000, the average D value is between 2.45 to 2.48 for New York City, and between 2.57 to 2.59 for Houston. Based on the D values, the surface complexity of Houston is more irregular than New York City. It corresponds to the visual inspection of the images of year 2000 for both study areas that Houston seems more fractal and irregular with intersected road systems and land patches than New York City, which is dominated by some water and islands with less color contrast of the land cover. For year 2016, the average D value of the three methods of New York City is 2.43 compared to a summary D value of 2.50 of Houston. These two values are closely similar that indicates the same surface complexity of these two cities for year 2016.

Figure 7.10 Images of Houston for Year 2000 and 2016

Table 7.3 Fractal Dimension Values of Houston for Year 2000 and 2016

	2000	2016
Triangular prism	2.5735	2.4852
Max-difference	2.5711	2.5021
Differential box counting	2.5894	2.5107

7.5 Summary

This chapter focuses on providing an empirical analysis using fractal methods. The analysis mainly consists of two parts: scale effect of remote sensing images and time series of city area. The fractal methods comparison is another main topic for the empirical analysis. To examine the scale effect, the original test image is 2049 by 2049 size in order to have enough regression points for coarser spatial resolution. Two various land cover types: coastal and noncoastal are used for a better distinction of the surface complexity. All of the three methods yield larger D values of noncoastal area than the coastal area. It is consistent with the surface complexity of the land cover itself. Moreover, each of the land cover has two images with two bands: red and green for a band comparison using the fractal methods. The results show that the band does not affect D values much for each land cover types. Among the methods, the differential box counting method has the largest D values and the triangular prism method has the lowest D values. For scale effect, changing from 30m to 240m, the D values stay stable for each of the methods.

For time series analysis, New York City and Houston located in different regions in the country. Year of 2000 and 2016 are used for time series analysis. The results show that the study area of Houston has a more irregular landscape than the study area of New York City. This corresponds to the visual inspection of the two images of the study areas that the image of Houston displays more land patches and color contrast. Between two dates, for both of the cities, the D values slightly changes, which indicates that both of the cities have not developed much in the study area during 2000 and 2016.

CHAPTER EIGHT

Summary and Conclusions

8.1 Summary

This research dissertation is a method exploration research focusing on fractals. There are various fractal techniques, which have been developed for measuring natural phenomena with different shapes and properties. The geographic phenomena are appropriate earth objects for studying the fractal characterizations. The surface feature is an important category for measuring its complexity, which also relates to land cover and land use study. Besides the global fractal dimension values, there is a lack of algorithms for computing local fractal dimension values for small study neighborhoods.

The main goal of this dissertation research is to develop several algorithms for computing local fractal dimension values. The more common way of computing the local D values are using moving window based on the original fractal techniques. In this manner, the single D value is separated into several D values for small regions, which is defined by the size of the moving window. Moving window has the advantage of easily adjusting the size of the study area. It can also be easily applied to any fractal methods with little modifications. Another local form of computing D values is to compute four quadrants of an entire image. This way computes four local D values in four directions and can be compared with the global value. The computation complexity of this method is relatively low because only a few regions need to be computed. It is similar to moving window that it only uses four moving window to cover the entire image. Even though it is local D values, it still covers a large area and variations of surface complexity may still exist. This research dissertation employed the geographically weighted scheme to develop methods for computing GW fractal dimensions. By using GW scheme, it localize the global D value into each single pixel. In other words, each pixel of the entire image can have its corresponding D value. This could be the smallest neighborhood for having a D value. Using GW scheme, each place of the image can result in a fractal dimension value, but the computation complexity would be high if a large image is used.

First, the GW scheme is tested with two widely used fractal methods: the triangular prism and differential box counting method. The triangular prism methods and its three versions: Max-difference, Mean-difference and Eight-pixel are also included in the analysis. The differential box counting method used is the improved version of the original one. There are two basic rules for GW scheme to follow for any GW quantities. One is that the global value should be within the full range of the local values; the second is that the range of the results should change the opposite direction against the bandwidth. The results of GW fractal dimension values using triangular prism and differential box counting methods are promising in general. However, there is an issue with the small bandwidth for fractal methods. For the test image of size 257 by 257, a bandwidth below 50 could cause the fractal dimension values significantly out of the theoretical range of surface feature. For method comparison, the fractal distributions are similar and the local D values can somehow reflect the surface complexity of the test image.

Second, the Fourier technique applies to the same test image for computing global and local fractal dimension values. The Fourier technique belongs to a different category of the fractal methods compared to the previous two methods. The Fourier technique method require much more computation time for a global value than the previous used method. The global fractal dimension values of Fourier method are different from the other two methods. This could caused by the algorithm of the Fourier spectral method itself. For local fractal analysis, the numerical values seems follow the rules of the geographical weighting scheme while the distribution is not similar to the other methods. The local distribution of the Fourier technique seems correspond to the frequency domain image of the Fourier transform. Lastly, three methods are selected for an empirical analysis. As shown in chapter 7, each of the three methods yields stable D values for various land cover types in different spectral bands. This result may suggest that the image surface is self-similar within the selected spatial resolutions. For the selected study areas of New York and Houston, Houston has a larger D values than New York. This could possibly indicate the complexity difference for the chosen study area. A 16-year period analysis suggests that there are slight changes for both cities.

8.2 Future research

Future research should continue with the development of the methods for computing the local fractal dimension values. Especially for the GW scheme, the issue of small bandwidth needs to be resolved. For Fourier spectral method, the distribution of the GW fractal dimension values needs to be investigated deeper in order to be consistent with the surface complexity of various land covers. Some other kernel functions could be considered to compare with the Gaussian kernel. Furthermore, the pixel-based fractal dimension values could be compared with moving window technique.

The GW based local fractal dimension should be considered with other quantity values for some other applications. It can be incorporated into some regression models for better land cover classification. Only use fractal dimension value is not sufficient, several social information such as population size, geometric property of land cover, economic factors et al can be related to fractal dimension values for better characterizing the urban landscape and urban development.

References

Anagnostakis, M. J., et al. "Natural radioactivity mapping of Greek surface soils." *Environment International* 22 (1996): 3-8.

Anas, Alex, Richard Arnott, and Kenneth A. Small. "Urban spatial structure."*Journal of economic literature* (1998): 1426-1464.

Andrle, Robert. "THE WEST COAST OF BRITAIN: STATISTICAL SELF-SIMILARITY VS. CHARACTERISTIC SCALES IN THE LANDSCAPE." *Earth surface processes and landforms* 21.10 (1996): 955-962.

Anselin, Luc. "Local indicators of spatial association-LISA." *Geographical analysis* 27.2 (1995): 93-115.

Anselin, Luc, and Arthur Getis. "Spatial statistical analysis and geographic information systems." *Perspectives on spatial data analysis*. Springer Berlin Heidelberg, 2010. 35-47.

Antes, James R., and Kang-tsung Chang. "An empirical analysis of the design principles for quantitative and qualitative area symbols." *Cartography and Geographic Information Systems* 17.4 (1990): 271-277.

Arthur Robinson, H. "Elements of cartography." (1958).

Assuncao, Renato M., and Edna A. Reis. "A new proposal to adjust Moran's I for population density." *Statistics in medicine* 18.16 (1999): 2147-2162.

Barredo, José I., et al. "Modelling dynamic spatial processes: simulation of urban future scenarios through cellular automata." *Landscape and urban planning* 64.3 (2003): 145-160.

Batty, Michael, and P. A. Longley. "The fractal simulation of urban structure." *Environment and Planning a* 18.9 (1986): 1143-1179.

Batty, Michael, and P. A. Longley. "The morphology of urban land use."*Environment and Planning B: Planning and Design* 15.4 (1988): 461-488.

Batty, Michael. "Cities as fractals: simulating growth and form." *Fractals and chaos*. Springer New York, 1991. 43-69.

Batty, Michael, and Paul A. Longley. *Fractal cities: a geometry of form and function*. Academic Press, 1994.

Batty, Michael, Yichun Xie, and Zhanli Sun. "Modeling urban dynamics through GIS-based cellular automata." *Computers, environment and urban systems*23.3 (1999): 205-233.

Benguigui, Lucien, et al. "When and where is a city fractal?." *Environment and Planning B* 27.4 (2000): 507-520.

Benguigui, Lucien, Daniel Czamanski, and Maria Marinov. "City growth as a leap-frogging process: an application to the Tel-Aviv Metropolis." *Urban studies*38.10 (2001): 1819-1839.

Benz, Ursula C., et al. "Multi-resolution, object-oriented fuzzy analysis of remote sensing data for GIS-ready information." *ISPRS Journal of photogrammetry and remote sensing* 58.3 (2004): 239-258.

Berentsen, William H., and Robert G. Cromley. "Regional Income Inequalities among EU NUTS 2 Regions, 1995 and 2010: Perspectives from a Geographically Weighted Approach." (2013): 45-60.

Berke, Olaf. "Choropleth mapping of regional count data of Echinococcus multilocularis among red foxes in Lower Saxony, Germany." *Preventive Veterinary Medicine* 52.2 (2001): 119-131.

Berthon, Simon, and Andrew Robinson. *The shape of the world*. Rand McNally & Company, 1991.

Bitter, Christopher, Gordon F. Mulligan, and Sandy Dall'erba. "Incorporating spatial variation in housing attribute prices: a comparison of geographically weighted regression and the spatial expansion method." *Journal of Geographical Systems* 9.1 (2007): 7-27.

Boots, Barry, and Atsuyuki Okabe. "Local statistical spatial analysis: Inventory and prospect." *International Journal of Geographical Information Science* 21.4 (2007): 355-375.

Breheny, M. J., *Sustainable Development and Urban Form*. London: Pion Ed, 1992.

Brewer, Cynthia A. "Color use guidelines for mapping and visualization."*Visualization in modern cartography* 2 (1994): 123-148.

Brewer, Cynthia A., and Linda Pickle. "Evaluation of methods for classifying epidemiological data on choropleth maps in series." *Annals of the Association of American Geographers* 92.4 (2002): 662-681.

Brunsdon, Chris, Stewart Fotheringham, and Martin Charlton. "Geographically weighted regression." *Journal of the Royal Statistical Society: Series D (The Statistician)* 47.3 (1998): 431-443.

Brunsdon, Chris, J. McClatchey, and D. J. Unwin. "Spatial variations in the average rainfall–altitude relationship in Great Britain: an approach using geographically weighted regression." *International Journal of Climatology*21.4 (2001): 455-466.

Brunsdon, Chris, A. S. Fotheringham, and Martin Charlton. "Geographically weighted summary statistics—a framework for localised exploratory data analysis." *Computers, Environment and Urban Systems* 26.6 (2002): 501-524.

Brunsdon, Chris, and Martin Charlton. "Local trend statistics for directional data—A moving window approach." *Computers, environment and urban systems*30.2 (2006): 130-142.

Bucci, Ovidio M., and Giorgio Franceschetti. "On the spatial bandwidth of scattered fields." *Antennas and Propagation, IEEE Transactions on* 35.12 (1987): 1445-1455.

Buczkowski, Stéphane, et al. "The modified box-counting method: analysis of some characteristic parameters." *Pattern Recognition* 31.4 (1998): 411-418.

Burrough, P. A. "Multiscale sources of spatial variation in soil. I. The application of fractal concepts to nested levels of soil variation." *Journal of soil science* 34.3 (1983): 577-597.

Campbell, James B. *Introduction to remote sensing*. CRC Press, 2002.

Campbell, Scott. "Green cities, growing cities, just cities?: Urban planning and the contradictions of sustainable development." *Journal of the American Planning Association* 62.3 (1996): 296-312.

Chang, Kang-tsung. *Introduction to geographic information systems*. Boston: McGraw-Hill Higher Education, 2015.

Chang, S. Grace, Bin Yu, and Martin Vetterli. "Spatially adaptive wavelet thresholding with context modeling for image denoising." *Image Processing, IEEE Transactions on* 9.9 (2000): 1522-1531.

Chen, Yanguang. "A new model of urban population density indicating latent fractal structure." *International Journal of Urban Sustainable Development* 1.1-2 (2010): 89-110.

Chen, Yanguang. "Exploring the fractal parameters of urban growth and form with wave-spectrum analysis." *Discrete Dynamics in Nature and Society* 2010 (2010).

Chen, Yanguang. "Fractal dimension evolution and spatial replacement dynamics of urban growth." *Chaos, Solitons & Fractals* 45.2 (2012): 115-124.

Cheng, Qiuming. "Multifractality and spatial statistics." *Computers & Geosciences* 25.9 (1999): 949-961.

Chica-Olmo, M., and F. Abarca-Hernandez. "Computing geostatistical image texture for remotely sensed data classification." *Computers & Geosciences*26.4 (2000): 373-383.

Cho, S., et al. "Estimating effects of an urban growth boundary on land development." *Journal of Agricultural and Applied Economics* 38.2 (2006): 287.

Clarke, Keith C. "Computation of the fractal dimension of topographic surfaces using the triangular prism surface area method." *Computers & Geosciences*12.5 (1986): 713-722.

Clark, N. N. "Three techniques for implementing digital fractal analysis of particle shape." *Powder Technology* 46.1 (1986): 45-52.

Cliff, Andrew D., and Keith Ord. "Spatial autocorrelation: a review of existing and new measures with applications." *Economic Geography* (1970): 269-292.

Cromley, E. K., and R. G. Cromley. "An analysis of alternative classification schemes for medical atlas mapping." *European Journal of Cancer* 32.9 (1996): 1551-1559.

Cromley, Robert G. "Classed versus unclassed choropleth maps: A question of how many classes." *Cartographica* 32.4 (1995): 15.

Cromley, Robert G., and Dean M. Hanink. "Focal location quotients: specification and applications." *Geographical Analysis* 44.4 (2012): 398-410.

Cromley, Robert G., Dean M. Hanink, and Jie Lin. "Developing Choropleth Maps of Parameter Results for Quantile Regression." *Cartographica: The International Journal for Geographic Information and Geovisualization* 48.3 (2013): 177-188.

Cromley, Robert G., and Dean M. Hanink. "Visualizing robust geographically weighted parameter estimates." *Cartography and Geographic Information Science* 41.1 (2014): 100-110.

Cromley, Robert G., Dean M. Hanink, and George C. Bentley. "Geographically weighted colocation quotients: specification and application." *The Professional Geographer* 66.1 (2014): 138-148.

Cromley, Robert G., Shuowei Zhang, and Natalia Vorotyntseva. "A concentration-based approach to data classification for choropleth mapping."*International Journal of Geographical Information Science* 29.10 (2015): 1845-1863.

David, Martin. "Automatic neighborhood identification from population surfaces [J]." *Computers, Environment and Urban Systems* 22.2 (1998): 107r120.

De Jong, S. M., and P. A. Burrough. "A fractal approach to the classification of Mediterranean vegetation types in remotely sensed images." *Photogrammetric Engineering and Remote Sensing* 61.8 (1995): 1041-1053.

De Keersmaecker, Marie-Laurence, Pierre Frankhauser, and Isabelle Thomas. "Using fractal dimensions for characterizing intra-urban diversity: the example of Brussels." *Geographical analysis* 35.4 (2003): 310-328.

Dent, Borden D. "Cartography-thematic map design." (1999).

Diamantini, Corrado, and Bruno Zanon. "Planning the urban sustainable development The case of the plan for the province of Trento, Italy."*Environmental impact assessment review* 20.3 (2000): 299-310.

Dixon, O. M. "Methods and progress in choropleth mapping of population density." *The Cartographic Journal* 9.1 (1972): 19-29.

Dong, Pinliang. "Lacunarity for spatial heterogeneity measurement in GIS."*Geographic information sciences* 6.1 (2000): 20-26.

Dray, Stéphane, Pierre Legendre, and Pedro R. Peres-Neto. "Spatial modelling: a comprehensive framework for principal coordinate analysis of neighbour matrices (PCNM)." *ecological modelling* 196.3 (2006): 483-493.

Dubuc, B., et al. "Evaluating the fractal dimension of surfaces." Proceedings of the Royal Society of London A: Mathematical, Physical and Engineering Sciences. Vol. 425. No. 1868. The Royal Society, 1989.

Emerson, Charles W., N. Siu-Ngan Lam, and D. A. Ouattrochi. "Multi-scale fractal analysis of image texture and patterns." *Photogrammetric Engineering and Remote Sensing* 65 (1999): 51-62.

Emerson, Charles W., Nina Siu-Ngan Lam, and Dale A. Quattrochi. "A comparison of local variance, fractal dimension, and Moran's I as aids to multispectral image classification." *International Journal of Remote Sensing*26.8 (2005): 1575-1588.

Falconer, Kenneth J. "The Hausdorff dimension of self-affine fractals." *Math. Proc. Camb. Phil. Soc*. Vol. 103. No. 3. 1988.

Falconer, Kenneth. *Fractal geometry: mathematical foundations and applications*. John Wiley & Sons, 2004.

F Dormann, Carsten, et al. "Methods to account for spatial autocorrelation in the analysis of species distributional data: a review." *Ecography* 30.5 (2007): 609-628.

Feitosa, Flávia F., et al. "Global and local spatial indices of urban segregation." *International Journal of Geographical Information Science* 21.3 (2007): 299-323.

Feng, Jian, and Yanguang Chen. "Spatiotemporal evolution of urban form and land-use structure in Hangzhou, China: evidence from fractals." *Environment and planning B: Planning and design* 37.5 (2010): 838-856.

Fortin, Marie-Josée, Pierre Drapeau, and Pierre Legendre. "Spatial autocorrelation and sampling design in plant ecology." *Vegetatio* 83.1-2 (1989): 209-222.

Fotheringham, A. Stewart. "Trends in quantitative methods III: stressing the visual." *Progress in Human Geography* 23.4 (1999): 597-606.

Fotheringham, A. Stewart. "“The problem of spatial autocorrelation” and local spatial statistics." *Geographical analysis* 41.4 (2009): 398-403.

Fotheringham, A. Stewart, and Chris Brunsdon. "Local forms of spatial analysis." *Geographical Analysis* 31.4 (1999): 340-358.

Fotheringham, A. Stewart, Chris Brunsdon, and Martin Charlton. *Geographically weighted regression: the analysis of spatially varying relationships*. John Wiley & Sons, 2003.

Fotheringham, Stewart, Martin Charlton, and Chris Brunsdon. "Geographically weighted regression: a natural evolution of the expansion method for spatial data analysis." *Environment and planning A* 30.11 (1998): 1905-1927.

Fractal Applications. *Fractal Foundation Online Course*. Fractal Foundation, 2003. Web. 10 Sept. 2015. <http://fractalfoundation.org/OFC/OFC-12-3.html>.

Fractal Dimension. *Fractal Foundation Online Course*. Fractal Foundation, 2003. Web. 24 Sept. 2015. <http://fractalfoundation.org/OFC/OFC-10-5.html>.

Frankhauser, Pierre. "The fractal approach. A new tool for the spatial analysis of urban agglomerations." *Population* 10.1 (1998): 205-240.

Frankhauser, Pierre. "Comparing the morphology of urban patterns in Europe–a fractal approach." *European Cities–Insights on outskirts, Report COST Action*10 (2004): 79-105.

Frankhauser, Pierre, et al. "A new concept for managing urban sprawl based on a fractal approach and link with public transport." Colloque" Building the urban future and Transit Oriented Development". 2012.

Frenkel, Amnon, and Maya Ashkenazi. "Measuring urban sprawl: how can we deal with it?." *ENVIRONMENT AND PLANNING B PLANNING AND DESIGN*35.1 (2008): 56.

Gatrell, Anthony C., et al. "Spatial point pattern analysis and its application in geographical epidemiology." *Transactions of the Institute of British geographers* (1996): 256-274.

Getis, Arthur. "Interaction modeling using second-order analysis."*Environment and Planning A* 16.2 (1984): 173-183.

Getis, Arthur, and Janet Franklin. "Second-order neighborhood analysis of mapped point patterns." *Ecology* (1987): 473-477.

Getis, Arthur, and Jared Aldstadt. "Constructing the spatial weights matrix using a local statistic." *Perspectives on spatial data analysis*. Springer Berlin Heidelberg, 2010. 147-163.

Getis, Arthur, and J. Keith Ord. "The analysis of spatial association by use of distance statistics." *Geographical analysis* 24.3 (1992): 189-206.

Goodchild, Michael F. "The fractional Brownian process as a terrain simulation model." *Modeling and Simulation* 13.113 (1982): 3-1137.

Goodchild, Michael F., and David M. Mark. "The fractal nature of geographic phenomena." *Annals of the Association of American Geographers* 77.2 (1987): 265-278.

Goodchild, Michael F., and Robert P. Haining. "GIS and spatial data analysis: Converging perspectives." *Papers in Regional Science* 83.1 (2004): 363-385.

Goovaerts, Pierre, and Geoffrey M. Jacquez. "Detection of temporal changes in the spatial distribution of cancer rates using local Moran’s I and geostatistically simulated spatial neutral models." *Journal of Geographical Systems* 7.1 (2005): 137-159.

Greene, Richard P., and James B. Pick. *Exploring the urban community: A GIS approach*. Pearson Higher Ed, 2011.

Guo, Luo, Zhihai Ma, and Lianjun Zhang. "Comparison of bandwidth selection in application of geographically weighted regression: a case study."*Canadian Journal of Forest Research* 38.9 (2008): 2526-2534.

Haase, Peter. "Spatial pattern analysis in ecology based on Ripley's K-function: introduction and methods of edge correction." *Journal of vegetation science*(1995): 575-582.

Haralick, Robert M., Karthikeyan Shanmugam, and Its' Hak Dinstein. "Textural features for image classification." *Systems, Man and Cybernetics, IEEE Transactions on* 6 (1973): 610-621.

Harris, Paul, Martin Charlton, and A. Stewart Fotheringham. "Moving window kriging with geographically weighted variograms." *Stochastic Environmental Research and Risk Assessment* 24.8 (2010): 1193-1209.

Harris, Paul, and Chris Brunsdon. "Exploring spatial variation and spatial relationships in a freshwater acidification critical load data set for Great Britain using geographically weighted summary statistics." *Computers & Geosciences*36.1 (2010): 54-70.

Herold, Martin, Joseph Scepan, and Keith C. Clarke. "The use of remote sensing and landscape metrics to describe structures and changes in urban land uses." *Environment and Planning A* 34.8 (2002): 1443-1458.

Huang, Jingnan, X. X. Lu, and Jefferey M. Sellers. "A global comparative analysis of urban form: Applying spatial metrics and remote sensing."*Landscape and urban planning* 82.4 (2007): 184-197.

Huang, Yefang, and Yee Leung. "Analysing regional industrialisation in Jiangsu province using geographically weighted regression." *Journal of Geographical Systems* 4.2 (2002): 233-249.

Hubert, P., et al. "Multifractals and extreme rainfall events." *Geophysical Research Letters* 20.10 (1993): 931-934.

Hudson, Richard R. "A new statistic for detecting genetic differentiation."*Genetics* 155.4 (2000): 2011-2014.

Jacquez, Geoffrey M. "Spatial cluster analysis." *The handbook of geographic information science* 395 (2008): 416.

Jong, P. de, C. Sprenger, and F. Van Veen. "On extreme values of Moran's I and Geary's c." *Geographical Analysis* 16.1 (1984): 17-24.

Karperien, A. ""Box Counting"" *"Box Counting"* FracLac for ImageJ, 1999-2013. Web. 24 Sept. 2015. <http://rsbweb.nih.gov/ij/plugins/fraclac/FLHelp/BoxCounting.htm>.

Keeble, Lewis B. *Principles and practice of town and country planning*. Estates Gazette, 1969.

Klinkenberg, Brian. "A review of methods used to determine the fractal dimension of linear features." *Mathematical Geology* 26.1 (1994): 23-46.

Klinkenberg, B., and M. F. Goodchild. "The fractal properties of topography: a comparison of methods." *Earth Surface Processes and Landforms* 17.3 (1992): 217-234.

LAM, NINAS. "Description and measurement of Landsat TM images using fractals." *Photogrammetric engineering and remote sensing* 56.2 (1990): 187-195.

Lam, Nina Siu-Ngan, et al. "An evaluation of fractal methods for characterizing image complexity." *Cartography and Geographic Information Science* 29.1 (2002): 25-35.

Lam, Nina Siu Ngan, and Lee De Cola. *Fractals in geography*. Blackburn Press, 2002.

Lam, Nina Siu-Ngan. "Fractals and scale in environmental assessment and monitoring." *Scale and geographic inquiry: Nature, society, and method* (2004): 23-40.

Lee, C-K., et al. "Fractal analysis of temporal variation of air pollutant concentration by box counting." *Environmental Modelling & Software* 18.3 (2003): 243-251.

Lee, Jong-Sen. "Digital image smoothing and the sigma filter." *Computer Vision, Graphics, and Image Processing* 24.2 (1983): 255-269.

Le Corbusier. *The city of to-morrow and its planning*. Courier Corporation, 1987.

Legendre, Pierre. "Spatial autocorrelation: trouble or new paradigm?." *Ecology*74.6 (1993): 1659-1673.

LeSage, James P. "A family of geographically weighted regression models."*Advances in spatial econometrics*. Springer Berlin Heidelberg, 2004. 241-264.

Li, Feng, et al. "Measurement indicators and an evaluation approach for assessing urban sustainable development: A case study for China's Jining City." *Landscape and Urban Planning* 90.3 (2009): 134-142.

Li, Hongfei, Catherine A. Calder, and Noel Cressie. "Beyond Moran's I: testing for spatial dependence based on the spatial autoregressive model."*Geographical Analysis* 39.4 (2007): 357-375.

Li, Jian, Qian Du, and Caixin Sun. "An improved box-counting method for image fractal dimension estimation." *Pattern Recognition* 42.11 (2009): 2460-2469.

Liang, Bingqing, Qihao Weng, and Xiaohua Tong. "An evaluation of fractal characteristics of urban landscape in Indianapolis, USA, using multi-sensor satellite images." *International journal of remote sensing* 34.3 (2013): 804-823.

Liu, Song-tao. "An improved differential box-counting approach to compute fractal dimension of gray-level image." *Information Science and Engineering, 2008. ISISE'08. International Symposium on*. Vol. 1. IEEE, 2008.

Lloyd, Chris, Ian Shuttleworth, and David McNair. "Measuring local segregation in Northern Ireland." *International Population Geography Conference, University of St. Andrews, August*. 2004.

Lloyd, Christopher D. *Local models for spatial analysis*. CRC Press, 2010.

Longley, Paul A., and Victor Mesev. "On the measurement and generalization of urban form." *Environment and Planning A* 32.3 (2000): 473-488.

Lovejoy, S., and B. B. Mandelbrot. "Fractal properties of rain, and a fractal model." *Tellus, Series A-Dynamic Meteorology and Oceanography* 37 (1985): 209-232.

Lovejoy, S., and D. Schertzer. "Scale invariance, symmetries, fractals, and stochastic simulations of atmospheric phenomena." *Bulletin of the American meteorological society* 67.1 (1986): 21-32.

Lovejoy, S., D. Schertzer, and P. Ladoy. "Fractal characterization of inhomogeneous geophysical measuring networks." (1986): 43-44.

Luan, Haijun, et al. "Comparison of methods of fractal texture extraction for high-resolution remotely sensed images." *Earth Observation and Remote Sensing Applications (EORSA), 2012 Second International Workshop on*. IEEE, 2012.

Makse, Hernán A., Shlomo Havlin, and H. Eugene Stanley. "Modelling urban growth patterns." *Nature* 377.6550 (1995): 608-612.

Mandelbrot, Benoıt B. "How long is the coast of Britain." *Science* 156.3775 (1967): 636-638.

Mandelbrot, Benoit B., and James R. Wallis. "Noah, Joseph, and operational hydrology." *Water resources research* 4.5 (1968): 909-918.

Mandelbrot, Benoit B. "Fractals." (1977).

Mandelbrot, Benoit B. *The fractal geometry of nature*. Vol. 173. Macmillan, 1983.

Marghany, Maged, Arthur P. Cracknell, and Mazlan Hashim. "Comparison between radarsat-1 SAR different data modes for oil spill detection by a fractal box counting algorithm." *International Journal of Digital Earth* 2.3 (2009): 237-256.

Masson, V. "Urban surface modeling and the meso-scale impact of cities."*Theoretical and Applied Climatology* 84.1-3 (2006): 35-45.

Tso, B., and P. M. Mather. "Classification Methods for Remotely Sensed Data. 2001." *London and New York: Taylor & Francis* 332 (2001).

Matthews, Stephen A., and Tse-Chuan Yang. "Mapping the results of local statistics: Using geographically weighted regression." *Demographic research*26 (2012): 151.

McMullen, Curt. "The Hausdorff dimension of general Sierpiński carpets."*Nagoya Mathematical Journal* 96 (1984): 1-9.

Mennis, Jeremy. "Mapping the results of geographically weighted regression." *The Cartographic Journal* 43.2 (2006): 171-179.

Mennis, Jeremy L., and Lisa Jordan. "The distribution of environmental equity: Exploring spatial nonstationarity in multivariate models of air toxic releases." *Annals of the Association of American Geographers* 95.2 (2005): 249-268.

Mukherjee, Kriti, et al. "Comparative performance of fractal based and conventional methods for dimensionality reduction of hyperspectral data."*Optics and Lasers in Engineering* 55 (2014): 267-274.

Myint, S. W. "Fractal approaches in texture analysis and classification of remotely sensed data: Comparisons with spatial autocorrelation techniques and simple descriptive statistics." *International Journal of Remote Sensing* 24.9 (2003): 1925-1947.

Myint, Soe W., Victor Mesev, and Nina Lam. "Urban textural analysis from remote sensor data: Lacunarity measurements based on the differential box counting method." *Geographical Analysis* 38.4 (2006): 371-390.

Nader, Manal R., Bachir Abi Salloum, and Nadim Karam. "Environment and sustainable development indicators in Lebanon: a practical municipal level approach." *Ecological indicators* 8.5 (2008): 771-777.

Oden, Neal. "Adjusting Moran's I for population density." *Statistics in medicine*14.1 (1995): 17-26.

Olsson, Jonas, Janusz Niemczynowicz, and Ronny Berndtsson. "Fractal analysis of high-resolution rainfall time series." *Journal of Geophysical Research Atmospheres* 982 (1993): 23265-23274.

Openshaw, Stan, and Peter J. Taylor. "A million or so correlation coefficients: three experiments on the modifiable areal unit problem." *Statistical applications in the spatial sciences* 21 (1979): 127-144.

Orey, Steven. "Gaussian sample functions and the Hausdorff dimension of level crossings." *Zeitschrift für Wahrscheinlichkeitstheorie und verwandte Gebiete* 15.3 (1970): 249-256.

O'Sullivan, David, and David Unwin. *Geographic information analysis*. John Wiley & Sons, 2014.

Palmer, Michael W. "Fractal geometry: a tool for describing spatial patterns of plant communities." *Vegetatio* 75.1-2 (1988): 91-102.

Peitgen, Heinz-Otto, and Peter H. Richter. "Frontiers of chaos." *Frontiers of Chaos: Computer Graphics Face Complex Dynamics* (1985): 61-91.

Pentland, Alex P. "Fractal-based description of natural scenes." IEEE transactions on pattern analysis and machine intelligence 6 (1984): 661-674.

Ping, J. L., et al. "Exploring spatial dependence of cotton yield using global and local autocorrelation statistics." *Field Crops Research* 89.2 (2004): 219-236.

Pinkse, Joris, and Margaret E. Slade. "Contracting in space: An application of spatial statistics to discrete-choice models." *Journal of Econometrics* 85.1 (1998): 125-154.

Potvin, François, Barry Boots, and Alastair Dempster. "Comparison among three approaches to evaluate winter habitat selection by white-tailed deer on Anticosti Island using occurrences from an aerial survey and forest vegetation maps." *Canadian journal of zoology* 81.10 (2003): 1662-1670.

Poulsen, Erika, and Leslie W. Kennedy. "Using dasymetric mapping for spatially aggregated crime data." *Journal of Quantitative Criminology* 20.3 (2004): 243-262.

Qiu, H. L., et al. "Fractal characterization of hyperspectral imagery."*Photogrammetric Engineering and Remote Sensing* 65.1 (1999): 63-71.

Quattrochi, D. A., et al. "Image characterization and modeling system (ICAMS): a geographic information system for the characterization and modeling of multiscale remote sensing data." *Scale in Remote Sensing and GIS* (1997): 295-307.

Reardon, Sean F., and David O'Sullivan. "Measures of spatial segregation."*Sociological methodology* 34.1 (2004): 121-162.

Repetti, Alexandre, and Gilles Desthieux. "A Relational Indicatorset Model for urban land-use planning and management: Methodological approach and application in two case studies." *Landscape and Urban Planning* 77.1 (2006): 196-215.

Reps, John William. *The making of urban America: A history of city planning in the United States*. Princeton University Press, 1965.

Ridd, Merrill K. "Exploring a VIS (vegetation-impervious surface-soil) model for urban ecosystem analysis through remote sensing: comparative anatomy for cities†." *International journal of remote sensing* 16.12 (1995): 2165-2185.

Rigon, Riccardo, Ignacio Rodriguez-Iturbe, and Andrea Rinaldo. "Feasible optimality implies Hack's law." *Water resources research* 34.11 (1998): 3181-3189.

Rogerson, Peter A. "The Detection of Clusters Using a Spatial Version of the Chi-Square Goodness-of-Fit Statistic." *Geographical Analysis* 31.2 (1999): 130-147.

Rogerson, Peter, and Ikuho Yamada. *Statistical detection and surveillance of geographic clusters*. CRC Press, 2008.

Roy, Andrg G., Ginette Gravel, and Cline Gauthier. "Measuring the dimension of surfaces: A review and appraisal of different methods." *Proceedings of the 8th International Symposium on Computer-Assisted Cartography (Auto-Carto 8)*. 1987.

Sarkar, Nirupam, and B. B. Chaudhuri. "An efficient differential box-counting approach to compute fractal dimension of image." *Systems, Man and Cybernetics, IEEE Transactions on* 24.1 (1994): 115-120.

Schell, Lawrence M., and Stanley J. Ulijaszek. *Urbanism, health and human biology in industrialised countries*. Vol. 40. Cambridge University Press, 1999.

Schleicher, Dierk. "Hausdorff dimension, its properties, and its surprises." *The American Mathematical Monthly* (2007): 509-528.

Sémécurbe, François, Cécile Tannier, and Stéphane Roux. "Spatial distribution of human population in France: exploring the MAUP using multifractal analysis." Analysis 48.3: 292-313.

Shen, Guoqiang. "Fractal dimension and fractal growth of urbanized areas."*International Journal of Geographical Information Science* 16.5 (2002): 419-437.

Sun, W., et al. "Fractal analysis of remotely sensed images: A review of methods and applications." *International Journal of Remote Sensing* 27.22 (2006): 4963-4990.

Sun, Wanxiao. "Three new implementations of the triangular prism method for computing the fractal dimension of remote sensing images." *Photogrammetric Engineering & Remote Sensing* 72.4 (2006): 373-382.

Sun, Youshun, et al. "Adaptive moving window method for 3D P-velocity tomography and its application in China." *Bulletin of the Seismological Society of America* 94.2 (2004): 740-746.

Tannier, Cécile. "Optimal Urban Forms and Sustainable Cities: Reflections Arising from the Study of the Fractal City." Espaces et sociétés 3 (2009): 153-171.

Tannier, Cécile. "About fractal models in urban geography and planning: refuting the aesthetics and the universal norm." (2018).

Tannier, Cécile, and Denise Pumain. "Fractals in urban geography: a theoretical outline and an empirical example." *Cybergeo: European Journal of Geography*(2005).

Tannier, Cécile, et al. "A Fractal Approach to Identifying Urban Boundaries. 城市边界识别的分形方法." *Geographical Analysis* 43.2 (2011): 211-227.

Tannier, Cécile, and Isabelle Thomas. "Defining and characterizing urban boundaries: A fractal analysis of theoretical cities and Belgian cities." Computers, Environment and Urban Systems 41 (2013): 234-248.

Tannier, Cécile, and Isabelle Thomas. "Urban boundaries: a fractal analysis on theoretical and empirical cities." 17th European Colloqium on Quantitative and Theoretical Geography (ECQTG). 2011.

Tannier, Cécile, Jean-Christophe Foltête, and Xavier Girardet. "Assessing the capacity of different urban forms to preserve the connectivity of ecological habitats." Landscape and urban planning 105.1-2 (2012): 128-139.

Terzi, Fatih, and H. Serdar Kaya. "Analyzing urban sprawl patterns through fractal geometry: The case of Istanbul metropolitan area." (2008).

Theera-Umpon, Nipon. "Fractal dimension estimation using modified differential box-counting and its application to MSTAR target classification." (2002).

Thomas, I. L., et al. "Textural enhancement of a circular geological feature."*Photogrammetric engineering and remote sensing* 47 (1981): 89-91.

Thomas, Isabelle, Pierre Frankhauser, and Christophe Biernacki. "The morphology of built-up landscapes in Wallonia (Belgium): A classification using fractal indices." *Landscape and urban planning* 84.2 (2008): 99-115.

Thomas, Isabelle, Cécile Tannier, and Pierre Frankhauser. "Is there a link between fractal dimensions and other indicators of the built-up environment at a regional level." Cybergeo: Revue européenne de géographie/European journal of geography 413 (2008): 24.

Tobler, Waldo R. "A computer movie simulating urban growth in the Detroit region." *Economic geography* (1970): 234-240.

Tobler, Waldo. "Resolution, resampling, and all that." *Building databases for global science* 12 (1988): 9-137.

Townshend, John RG. *The spatial resolving power of earth resources satellites: a review*. NASA, Goddard Space Flight Center, 1980.

Tsai, Pui-Jen, et al. "Spatial autocorrelation analysis of health care hotspots in Taiwan in 2006." *BMC Public Health* 9.1 (2009): 464.

Tufte, Edward R., and P. R. Graves-Morris. *The visual display of quantitative information*. Vol. 2. No. 9. Cheshire, CT: Graphics press, 1983.

Turcotte, Donald L. *Fractals and chaos in geology and geophysics*. Cambridge university press, 1997

Tzeng, Yu-Chang, Kuo-Tai Fan, and Kun-Shan Chen. "A parallel differential box-counting algorithm applied to hyperspectral image classification."*Geoscience and Remote Sensing Letters, IEEE* 9.2 (2012): 272-276.

University of Warwick. "Lectures of fractals and dimension theory." PDF file. 28 Sept. 2015. < https://homepages.warwick.ac.uk/~masdbl/dimension-total.pdf>.

Unwin, David J. "GIS, spatial analysis and spatial statistics." *Progress in Human Geography* 20.4 (1996): 540-551.

Unwin, Antony, and David Unwin. "Spatial data analysis with local statistics."*Journal of the Royal Statistical Society: Series D (The Statistician)* 47.3 (1998): 415-421.

Vance, James E. *The continuing city: urban morphology in Western civilization*. JHU Press, 1990.

Voss, Richard F. "Characterization and measurement of random fractals."*Physica Scripta* 1986.T13 (1986): 27.

Waldhör, Thomas. "The spatial autocorrelation coefficient Moran's I under heteroscedasticity." *Statistics in Medicine* 15.7-9 (1996): 887-892.

Weng, Qihao. "Fractal analysis of satellite-detected urban heat island effect."*Photogrammetric engineering & remote sensing* 69.5 (2003): 555-566.

Wentz, Elizabeth A. "A shape definition for geographic applications based on edge, elongation, and perforation." *Geographical Analysis* 32.2 (2000): 95-112.

White, Roger, and Guy Engelen. "Cellular automata and fractal urban form: a cellular modelling approach to the evolution of urban land-use patterns."*Environment and planning A* 25.8 (1993): 1175-1199.

White, Roger, et al. "Developing an urban land use simulator for European cities." *Proceedings of the Fifth EC GIS Workshop: GIS of Tomorrow. European Commission Joint Research Centre: S*. 2000.

Wong, D. W. S., and A. S. Fotheringham. "Urban systems as examples of bounded chaos: Exploring the relationship between fractal dimension, rank-size, and rural-to-urban migration." *Geografiska Annaler. Series B. Human Geography* (1990): 89-99.

Woodcock, Curtis E., and Alan H. Strahler. "The factor of scale in remote sensing." *Remote sensing of Environment* 21.3 (1987): 311-332.

Wu, Changshan, and Alan T. Murray. "Estimating impervious surface distribution by spectral mixture analysis." *Remote sensing of Environment* 84.4 (2003): 493-505.

Wu, Fulong. "A linguistic cellular automata simulation approach for sustainable land development in a fast growing region." *Computers, Environment and Urban Systems* 20.6 (1996): 367-387.

Wulder, M., and B. Boots. "Local spatial autocorrelation characteristics of remotely sensed imagery assessed with the Getis statistic." *International Journal of Remote Sensing* 19.11 (1998): 2223-2231.

Yamada, Ikuho, and Jean-Claude Thill. "Local indicators of network-constrained clusters in spatial point patterns." *Geographical Analysis* 39.3 (2007): 268-292.

Zhang, Chaosheng, et al. "Use of local Moran's I and GIS to identify pollution hotspots of Pb in urban soils of Galway, Ireland." *Science of the Total Environment* 398.1 (2008): 212-221.